Modéliser la variation antigénique dans le paludisme

Inayat Bhardwaj

THÈSE POUR OBTENIR LE GRADE DE DOCTEUR DE L'UNIVERSITÉ DE MONTPELLIER

En Mathématiques et modélisation

École doctorale I2S

Unité de recherche UMR5294

Modelling Antigenic Variation in Malaria

Présentée par Inayat BHARDWAJ

le 27 mars 2024

Sous la direction de Ovidiu RADULESCU
et Antoine CLAESSENS

Devant le jury composé de

Michael WHITE, Professor,Department of Global Health, Institut Pasteur, Paris, France	**Rapporteur**
Anna BACHMANN, Research Group Leader, Bernhard Nocht Institute for Tropical Medicine, Hamburg, Germany	**Rapportrice**
Ramses DJIDJOU-DEMASSE, CR, HDR, Institut de Recherche pour le Développement (IRD), France	**Examinateur**
Ovidiu Radulescu, Professor, LPHI, Universite de Montpellier, France	**Directeur**
Antoine Claessens CR, HDR, Universite de Montpellier, France	**invité**, **Co-Directeur**

UNIVERSITÉ DE MONTPELLIER

List of Figures

List of Tables

Contents

DECLARATION

I declare that the experimental work carried out in this dissertation (in Chapter 02) was not performed by me. The experiments related to *var* gene expression *in vivo* and *in vitro* were carried out by Prince Nyarko, a fellow PhD student (at the time), collaborating on the same project.

The microarray data for the CHMI study was generated and kindly shared by the team of Mark Travassos, at the University of Maryland, USA.

Acknowledgements

To begin with, I would like to thank my supervisors, Ovidiu Radulescu and Antoine Claessens, for allowing me to work on this exciting project for the past three years. I am immensely grateful to Ovidiu Radulescu for the unwavering rigour and creativity he brings to science. His meticulous attention to detail and out-of-the-box approaches have motivated me to pursue interdisciplinary projects independently and develop my ideas. Thank you for always giving the last push and helping whenever needed.

I also extend my heartfelt thanks to Antoine Claessens for his continuous guidance throughout my PhD. His enthusiasm and dedication to malaria research have been a constant source of inspiration, and I am genuinely thankful for his support, not just for the project alone. He has always gone out of his way to host the GATAC team, and I will always be grateful for that. Thank you for keeping us going, from team meetings to GATAC outings.

I would also like to thank Dr Mark Travassos, for extremely helpful discussions related to my work.

Next, I would like to acknowledge the support I have had from both my teams, and I have learned a lot from all members, present and past. Camille, Marion, and Maria, I am especially indebted to you for your help navigating the French system's twists and turns. I would have been completely lost without you.

Maria, thank you for being my office mate and first friend in the city. I am glad to have discovered our shared love for all things related to food and travel. Thanks for inspiring me to do things 'my way.'

Rachel and Sarah, thank you for your help and feedback on my work and for your fresh perspective. Next, I'd like to thank Dr. Pawan Kumar in the Systems Biology team for being the 'nicest' colleague. To more coffee-fueled discussions! Special thanks to Prince Nyarko for his dedicated work on our collaborative project. I thank Marc, Camiile, Mathieu, Balotin, and Sophia in the GATAC Team for all our chit-chats about 'varology' or not.

I'd also like to thank my family for being my ultimate cheerleaders and for their eternal optimism that keeps me motivated. They have kept me from the crazies and continue to do so from afar. The countless hardships they have gone through to raise me only keep me grounded, and I hope to live up to their expectations.

To my friends, in the lab and elsewhere, for always being there for me irrespective of being far away. And finally, thank you, Ojaswi Gupta, for turning your world around for me.

Abstract

High transmission endemic areas pose a substantial challenge to *falciparum* malaria management and elimination due to the vast reservoir of chronic asymptomatic infections that sustain transmission. *P. falciparum* 's worldwide burden is now concentrated only in fifteen high transmission endemic countries, primarily in Sub-Saharan Africa. Hidden reservoirs of chronic asymptomatic infections are attributed not only to the high transmission rates in endemic regions, but also from non sterile specific immunity to *P. falciparum* that exhibits antigenic variation, which is facilitated by several multi-copy gene families.

In the case of *falciparum* malaria infections, the most studied multigene family responsible for mediating antigenic variation, is known as *var* and it encodes Plasmodium falciparum erythrocyte membrane protein 1 (PfEMP1), which is the major target of host immunity during the blood stage infection and has been linked to protection against severe disease and parasite clearance. Each parasite genome contains about 60 copies of *var* genes that undergo mutually exclusive expression. In highly endemic areas, each parasite isolate will typically contains a unique set of *var* gene sequences. This diversity in the number of antigenic variants mounts to huge pressure on the hosts' immune system and enables the parasite to establish long infections as hosts might not have encountered most of the variants from the repertoire during previous infections. However, the frequency of *var* switching and

the immunogenicity of each expressed PfEMP1 remain unclear.

In this thesis, we aimed to exploit theoretical approaches to gain insights into the switching rates of *var* variants in different environments: within the host and subsequently *in vitro* after infection. To this end, we took advantage of a Controlled Human Malaria Infection (CHMI) study with 19 adult African volunteers in The Gambia to gain insight into the effect of naturally acquired immunity on the expressed *var* gene repertoire during early phase of an infection. Our results revealed a significant association between the diversity of var expression, as measured by entropy, and infection outcomes.

Individuals with low immunity exhibited higher *var* entropy profiles, increased parasitemia, and reduced recognition of PfEMP1 domains compared to those with high immunity. Furthermore, we quantified the probability of *var* gene switching *in vitro* and turnover *in vivo* for the first time. This allowed us to estimate both intrinsic switching and negative-selection effects, indicating rapid turnover/switching probabilities of 69% - 97% and 7% - 57% per generation, *in vivo* and *in vitro*, respectively. *Var* (PfEMP1) expression triggered time-dependent humoral immune responses in low immunity individuals. Surprisingly, many PfEMP1 domains failed to elicit an antibody response. Our study suggests that intrinsic *var* switching serves to reset and maintain a diverse *var* repertoire. The high *var* switching rates, along with potentially weak PfEMP1 immunogenicity, appear to confer advantages for parasite survival during CHMI.

In the second part of the thesis, antigenic variation in malaria is then mathematically and numerically investigated in more detail using a model accounting for antigenic diversity to explore parasite persistence under the effects of host immunity. To this end, we derived inspiration from an existing viral antigenic variation framework, and characterise the infection both analyticallly and numerically, given some mild constraints.

We analytically and numerically showed the effects on antigenic variation on elongation of infection, and the dependence on the variant pool, which revealed that infection length is a linear correlate of the number of variants present in a population.

Using stochastic implementation of a theoretical model, we also show that at the early stages of infection, antigenic variants can be equally likely to occur, and can sustain the pressure mounted by the immune system even with switching rates incorporated using the deterministic analogue of Markov Processes. Switching rates of the order $10^{-}1$ were found to be sufficient for successfully establishing infection, under a constant immune response. Analytically, we provide stability criteria for the existence of stable solutions of the parasite population subjected to switching. On analysing the deterministic model with switching rates originating from a generator process, we found that the infection was characterised by overlapping peaks corresponding to multiple variants, and decreased in amplitude over time.

Résumé

Les zones d'endémie à transmission élevée posent un défi substantiel à la gestion et à l'élimination du paludisme à *Plasmodium falciparum* en raison du vaste réservoir d'infections chroniques asymptomatiques. La plupart des zones d'endémie à transmission élevée se situent en Afrique subsaharienne. Le réservoir d'infections chroniques asymptomatiques est attribué non seulement aux taux élevés de transmission dans les régions endémiques, mais aussi à l'immunité spécifique non stérile à *P. falciparum* qui présente une variation antigénique, facilitée par plusieurs familles de gènes multicopies.

Dans le cas des infections palustres à *P. falciparum*, la famille de gènes responsable de la variation antigénique est connue sous le nom de textit{var}, codant pour PfEMP1, qui est la cible principale de l'immunité de l'hôte lors de l'infection à stade sanguin et a été liée à la protection contre les formes graves de la maladie. Chaque génome parasitaire contient environ $\tilde{6}0$ copies de gènes *var* qui subissent une expression mutuellement exclusive. Dans les zones fortement endémiques, chaque isolat parasitaire contiendra généralement un ensemble unique de séquences de gènes *var*. Cette diversité dans le nombre de variants antigéniques exerce une énorme pression sur le système immunitaire de l'hôte et permet au parasite d'établir de longues infections car l'hôte pourrait ne pas avoir rencontré la plupart des variants du répertoire lors d'infections précédentes. Cependant, la fréquence de la commutation des gènes *var* et l'immunogénicité de chaque PfEMP1 exprimée restent incertaines.

Dans cette thèse, nous avons cherché à exploiter des approches théoriques pour comprendre les taux de commutation des variants *var* dans différents environnements : à l'intérieur de l'hôte et ensuite *var* après l'infection. À cette fin, nous avons tiré parti d'une étude d'infection palustre contrôlée chez l'homme avec 19 volontaires adultes africains en Gambie pour comprendre l'effet de l'immunité naturellement acquise sur le répertoire génétique *var* exprimé au cours des premières phases d'une infection. Nos résultats ont révélé une association significative entre la diversité de l'expression des gènes *var*, mesurée par l'entropie, et les résultats de l'infection. Les individus à faible immunité présentaient des profils d'entropie *var* plus élevés, une parasitémie accrue et une reconnaissance réduite des domaines PfEMP1 par rapport à ceux avec une forte immunité. De plus, nous avons quantifié pour la première fois la probabilité de commutation des gènes *var in vitro* et le renouvellement *in vivo*. Cela nous a permis d'estimer à la fois les effets de commutation intrinsèque et de sélection négative, indiquant des probabilités rapides de renouvellement/commutation de 69 % à 97 % et de 7 % à 57 % par génération, *in vivo* et *in vitro*, respectivement. L'expression de *var* (PfEMP1) a déclenché des réponses immunitaires humorales chez les individus à faible immunité. De manière surprenante, de nombreux domaines PfEMP1 n'ont pas réussi à susciter de réponse anticorps. Notre étude suggère que la commutation intrinsèque des gènes *var* sert à réinitialiser et à maintenir un répertoire *var* diversifié. Les taux élevés de commutation des *var*, ainsi que l'immunogénicité potentiellement faible de PfEMP1, semblent conférer des avantages à la survie du parasite lors de l'infection palustre contrôlée chez l'homme.

Dans la deuxième partie de la thèse, la variation antigénique dans le paludisme est ensuite examinée de manière plus détaillée sur le plan mathématique et numérique à l'aide d'un modèle tenant compte de la diversité antigénique pour explorer la persistance du parasite sous l'effet de l'immunité de l'hôte. À cette fin, nous nous sommes inspirés d'un cadre existant de variation antigénique virale et caractérisons l'infection à la fois de manière analytique et numérique, en tenant compte de certaines contraintes.

Nous avons montré analytiquement et numériquement les effets de la variation antigénique sur l'allongement de l'infection, ainsi que la dépendance vis-à-vis du pool de variants, ce qui a révélé que la durée de l'infection est une corrélation linéaire du nombre de variants présents dans une population. En utilisant une mise en œuvre stochastique d'un modèle théorique, nous avons également montré qu'aux premiers

stades de l'infection, les variants antigéniques peuvent être tout aussi susceptibles de se produire et peuvent maintenir la pression exercée par le système immunitaire même avec l'incorporation de taux de commutation utilisant l'analogie déterministe des processus de Markov. Des taux de commutation de l'ordre de 10^{-1} se sont révélés suffisants pour établir avec succès une infection, sous une réponse immunitaire constante. Analytiquement, nous fournissons des critères de stabilité pour l'existence de solutions stables de la population parasitaire soumise à la commutation. En analysant le modèle déterministe avec des taux de commutation provenant d'un processus générateur, nous avons constaté que l'infection était caractérisée par des pics chevauchants correspondant à plusieurs variants, et diminuait en amplitude au fil du temps.

CHAPTER 1

Introduction

1.1 Biological motivation

Mammalian hosts often function as reservoirs for various organisms and provide an environment conducive to the survival, replication, and transmission of several infectious agents. One of the deadliest microorganisms that cause acute as well as chronic infections in humans is the protozoan apicomplexan parasite of the genus *Plasmodium* that causes malaria. The single-celled pathogen propagates itself in a complicated, multi-stage life cycle with quite a range of hosts, ranging from insects to vertebrates, including mice, birds, non-human primates, and humans. [Paul et al., 2003; Schuster, 2002]. There are several species of *Plasmodium* that affect humans, namely: *P. falciparum, P. vivax, P. ovale wallickeri, P. ovale curtisi, P. malariae* [Mayxay et al., 2004; Antinori et al., 2012] and sometimes *P. knowlesi* [Ahmed and Cox-Singh, 2015; Singh and Daneshvar, 2013; Cox-Singh and Singh, 2008] that accounts for most of the zoonotic malaria infections in humans.

Out of all *Plasmodium* species affecting humans, *P. falciparum* is the deadliest and most prevalent [Snow et al., 2017]. Approximately 80 % of the worldwide incidence of malaria is concentrated in 15 countries, predominantly situated in Sub-Saharan

Africa, with India being the exception. Severe malaria caused by *P. falciparum* is also the primary cause of half a million malaria deaths that occur each year [World Health Organization et al., 2023]. *P. falciparum* infections also exist in the absence of clinical symptoms and are frequently described as asymptomatic or afebrile [Galatas et al., 2018]. However, they are as much of a public health concern in Sub-Saharan Africa as clinical infections, as they are often chronic and serve as parasite reservoirs for transmission.

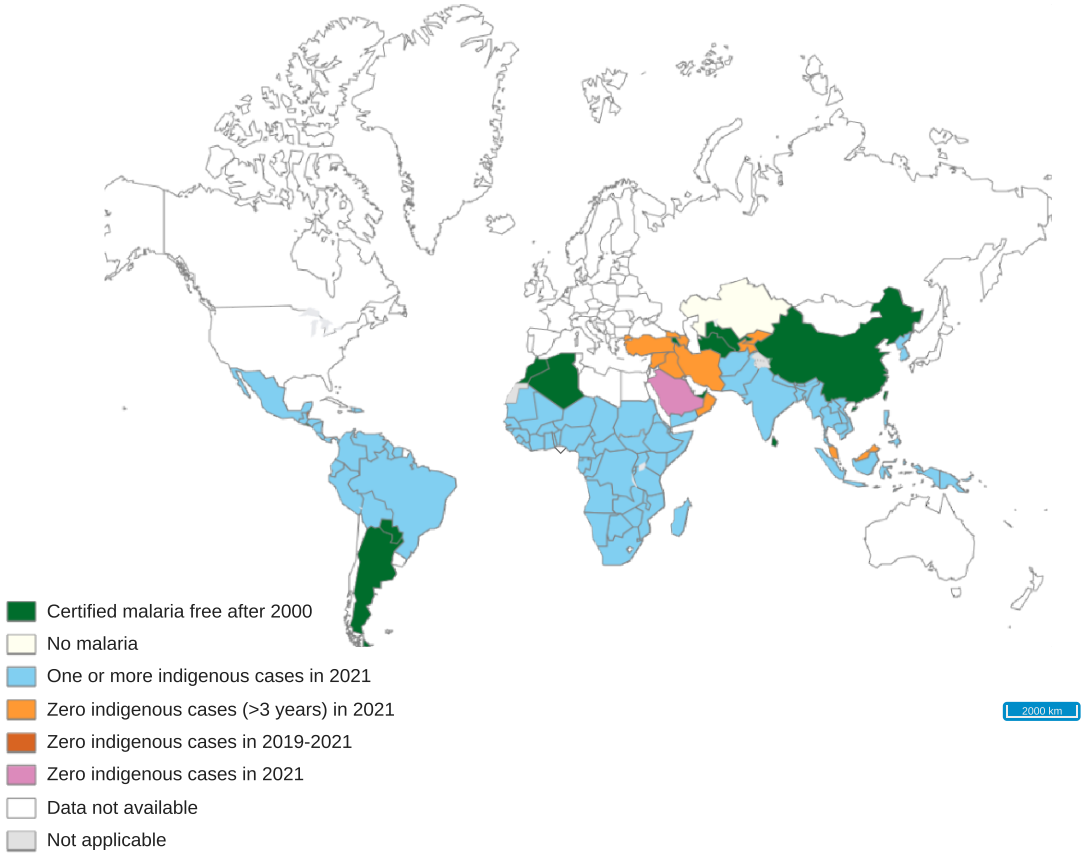

Figure 1.1: **World Population at risk of Malaria**: The map represents the overall risk of malaria in different regions across the world, as updated in 2021. Modified from the World Malaria Report, 2023 [World Health Organization et al., 2023].

1.1.1 Clinical presentation of malaria and diagnosis

In human hosts, the clinical symptoms of malaria are linked to the asexual blood stages of the parasite's life cycle. First infections with *falciparum* irrespective of host age, are usually symptomatic and occur with a wide range of clinical symptoms such as cyclic fever, chills, diarrhea, and vomiting [Oakley et al., 2011; Hafalla et al., 2011; Bartoloni and Zammarchi, 2012]. Fever waves typically characteristic of clinical malaria are linked to the bursting of red blood cells during the parasite's intraerythrocytic cycle. Around 0.5% of all cases of mild infections escalate to severe malaria, which is marked by the presentation of anemia, acute renal failure, coma and even death [Bartoloni and Zammarchi, 2012].

Even though malaria infections can present a wide range of symptoms, diagnosing malaria clinically is challenging because of the non-specificity of the symptoms.
Malaria symptoms can often considerably overlap with other common and potentially severe illnesses, such as viral or bacterial infections and different febrile diseases. Upon presentation of symptoms, malaria diagnosis is most commonly made using a variety of techniques. These include microscopic diagnosis by staining thin and thick peripheral blood smears [Ngasala et al., 2008], which is the most traditional and widely used method for diagnosis. Other concentration techniques include the quantitative buffy coat method [Tangpukdee et al., 2009], rapid diagnostic tests, and more sensitive molecular diagnostic methods like PCR [Holland and Kiechle, 2005].

1.1.2 P *falciparum* life cycle

A malaria infection with *falciparum* in humans is initiated when sporozoites are injected by an infected female Anopheles mosquito during a blood meal [Ezema et al., 2023]. Mature sporozoites enter the bloodstream and pass through it until they reach the liver after the initial inoculation within 20–30 minutes, beginning the pre-erythrocytic stage of the parasite life cycle. The sporozoites cross several hepatocytes before finally invading one of these cells. While in the liver, the parasite divides and develops into a schizont containing thousands of merozoites, in a process known as exoerythrocytic schizogony, with no clinical manifestation. The schizonts

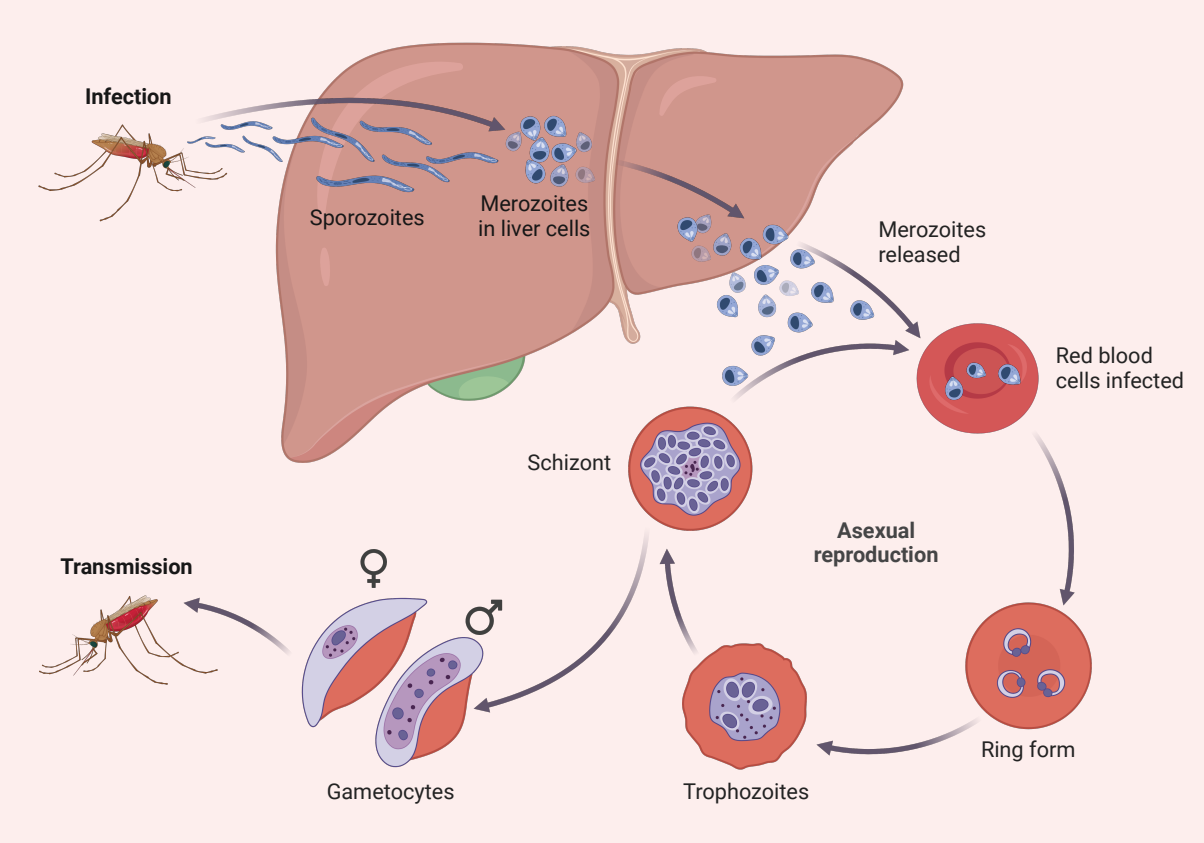

Figure 1.2: ***P. falciparum* life cycle in the human host** Image adapted from Biorender's disease mechanisms library [BioRender, n.d.], content from [Meibalan and Marti, 2017]

burst open within a span of 5 to 15 days (typically 7 days), releasing approximately 10,000 to 30,000 merozoites. The asexual erythrocytic cycle commences with merozoites penetrating red blood cells (RBCs). Initially, the merozoite, cloaked with merozoite surface protein (MSP-1), adheres to a RBC. Subsequently, it adjusts its position, anchoring itself to the RBC via its apical end, facilitated by apical membrane antigen 1 (AMA-1). As invasion progresses, a distinct membrane invagination, known as the parasitophorous vacuole, forms, eventually encapsulating the parasite within the erythrocyte. The infected red blood cell (iRBC) is subject to massive modifications induced by the developing parasite, that stiffen the RBC. Multiple cycles of DNA replication occur and, after about 48hours, newly generated merozoites burst and infect more erythrocytes. Some parasites at this stage differentiate into male and female gametocytes, a necessary step for transmission

[White et al., 2013; Maier et al., 2019].

During a mosquito bite, late-stage gametocytes enter the mosquito blood meal. Once in the mosquito's midgut, male gametocytes exflagellate to produce eight motile gametes. The fertilisation of a female gamete results in an ookinete, with the first stages of meiosis beginning immediately. The motile ookinete migrates from the lumen of the midgut to the basal lamina, where it forms an oocyst. A large amount of replication occurs to produce about 2000–8000 haploid nuclei. The oocyst then bursts, releasing sporozoites that migrate to the mosquito salivary gland, ready to re-initiate yet another transmission cycle.

1.1.3 Malaria pathogenesis

Fatality resulting from malaria is broadly attributed to the parasite's ability to alter the surface of infected red blood cells (iRBCs), inducing adhesion to the microvasculature. This unique trait enables the parasite to spend over half of its asexual life sequestered within microvessels, thereby evading circulation. This sequestration is a hallmark of *falciparum* malaria compared to other malaria types [Craig et al., 2012]. The adhesion of iRBCs can occur with diverse cellular components such as endothelial cells, platelets, and uninfected red blood cells [Fairhurst and Wellems, 2006; Kraemer and Smith, 2006; Smith et al., 2013].

While "hidden" within an infected red blood cell (iRBC) during the first 20 hours (called the ring stage), at the trophozoite stage, the parasite exposes itself to host immunity by exporting antigens to the iRBC's surface. *P. falciparum* 's cytoadherence and sequestration are understood to be evolutionary responses that hinder the splenic transit of infected erythrocytes, allowing parasites to avoid filtration and elimination from the bloodstream [Sherman et al., 2003].

Among the severe forms of the disease, cerebral malaria coupled with high parasitic loads stands out due to iRBC sequestration in the brain's microvasculature [Aikawa, 1988; MacPherson et al., 1985], disrupting the blood-brain barrier eventually leading to brain hypoxia, coma, and even death. In spite of several decades of research, little is known about the etiology of CM or the reason why some individuals are predisposed to the condition [Dunst et al., 2017]. It is still unknown if sequestration of red blood

cells (iRBCs) infected with *P. falciparum* is directly or exclusively responsible for the clinical condition, despite the fact that it is correlated with severe disease. This process of sequestration is facilitated by parasite-variant surface antigens (VSA) displayed on the iRBC membrane [Wahlgren et al., 2017; Kyes et al., 2001; Urban and Roberts, 2002; Deitsch and Hviid, 2004]. These surface antigens are also the major targets of host immunity [Chattopadhyay et al., 2003; Chan et al., 2012].

In the case of *P. falciparum* , multiple families of VSAs have been identified, with the multicopy gene families *var* being the most extensively studied (Table1.1.3, see also next section) whereas little is known about the *rif* and *stevor* genes, and other subtelomeric multigene families are only theoretically described [Wahlgren et al., 2017]. The manifestation of cerebral malaria is associated with the expression of a subset of proteins encoded by the *var* genes that bind to the endothelial protein C receptor (EPCR) and to a lesser extent intercellular adhesion molecule 1 (ICAM-1) [Jensen et al., 2004, 2020; Avril et al., 2012; Claessens et al., 2012]. The proteins encoded by *rif* and *stevor* families are also potentially involved in immune evasion mechanisms (see Table 1.1.3).

Table 1.1: Multigene families encoding variant surface antigens in *P. falciparum*. Modified and adapted from [Wahlgren et al., 2017]

	var	***rif***	***stevor***
Protein Encoded	PfEMP1	RIFIN	STEVOR
Approximate Copy Number	60	150	30
Chromosomal Location	Subtelomeric & internal clusters	Subtelomeric & internal clusters	Subtelomeric & internal clusters
Function	Cytoadherence, Immune evasion	Immune evasion	Rosetting

1.2 Immunity to Malaria

Casualties related to malaria predominantly occur children under the age of five, irrespective of the intensity of transmission, making *P. falciparum* the major cause of child mortality caused by infectious diseases worldwide [Schumacher and Spinelli, 2012; Stone et al., 2015; Khagayi et al., 2019; Snow et al., 2004]. Additionally, the peak

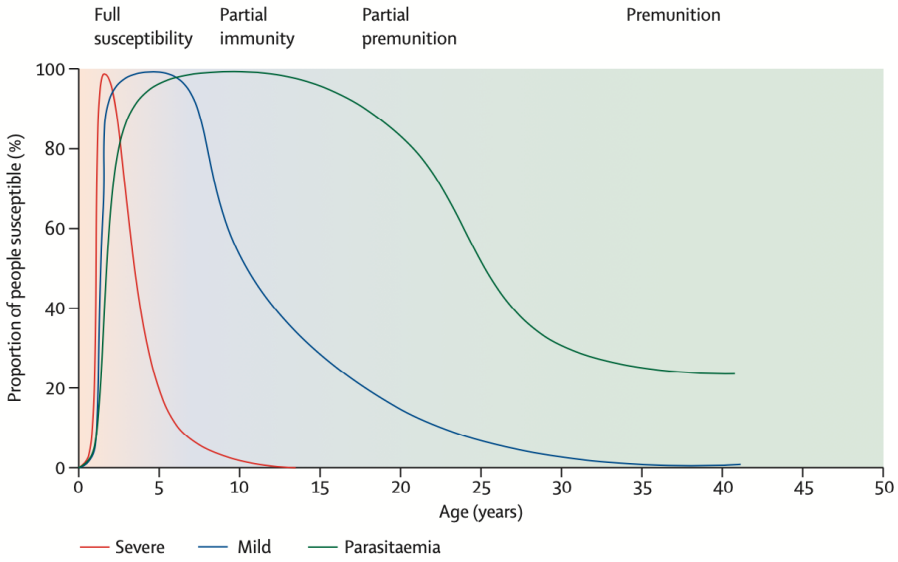

Figure 1.3: **Relation between age and malaria severity in an area of moderate transmission intensity**. With repeated exposure, protection is acquired, first against severe malaria, then against illness with malaria, and, much more slowly, against microscopy-detectable parasitemia. Figure taken directly from [White et al., 2013]

age of clinical malaria incidence lowers as transmission intensity increases. In contrast, in endemic areas with lower transmission, clinical malaria is observed in both adults and children and is evenly distributed across age [Postels and Birbeck, 2013]. These age-related patterns of severity highlight the importance of understanding the processes underlying naturally acquired immunity to malaria[Carneiro et al., 2010; Okiro et al., 2009; Cowman et al., 2016].
In areas with high transmission, adults develop clinical immunity due to continuous exposure Barua et al. [2019], Dodoo et al. [2001], Barry and Hansen [2016], Gonzales et al. [2020], Bousema et al. [2006], which is associated with a decrease in the incidence of severe symptoms in these areas. During the initial few months after birth, infants are shielded from severe malaria by maternal IgGs specific to VSAs

[Staalsoe et al., 2004]. However, until the age of five years, children are at high risk of severe complications. Over time, individuals gradually develop clinical immunity to the parasite, typically experiencing uncomplicated malaria [McGregor, 1974] or even remaining asymptomatic throughout the infection. In fact, despite the heavy burden of malaria, the majority of all *P. falciparum* infections in highly endemic countries are asymptomatic [Galatas et al., 2016]. Nevertheless, the immune responses against *P. falciparum* antigens dwindle in the absence of exposure.

1.2.1 Malaria immunity against sporozoite stages

Sporozoites injected through the bite of an infected *Anopheles* mosquito leave the dermis, then use their gliding motility to reach the liver within an hour. However, some sporozoites deviate into lymph nodes instead of blood vessels, where dendritic cells (DCs) engulf them, priming CD8+ T cells to counter liver stage parasite infection [Hassert et al., 2023]. The parasite-triggered host immune response will elicit antibodies that may neutralize proteins crucial for hepatocyte entry, facilitate opsonic phagocytosis, and instigate Natural Killer T-cells to mediate parasite lysis. The primary antigen target on sporozoites, conferring immunity, has been identified as circumsporozoite protein (CSP). This antigen is the basis of the only WHO-approved vaccine against malaria. However, the current very high prevalence of *P. falciparum* asymptomatic blood-stage infection in endemic countries indicates that even repeated exposure to infectious mosquito bites is insufficient to elicit a sterile immunity against sporozoites [Hassert et al., 2023].

1.2.2 Malaria immunity against intra-erythrocytic stages

During the erythrocytic stage of malaria infection, the host immune system launches a robust response driven by the release of inflammatory cytokines upon detecting the invading parasite [Ezema et al., 2023]. IFNγ emerges as a significant cytokine elicited in response to asexual iRBC, fueling phagocytic activity by dendritic cells (DCs) and monocytes, thereby enhancing antigen presentation and cytokine secretion. Key inflammatory cytokines include TNF α and IL-12, which trigger the production of reactive oxygen and nitrogen species by macrophages to eliminate the parasite. Subsequently, IL-10 secretion counterbalances the initial pro-inflammatory response,

contributing to immune regulation. To summarize a complex cell-mediated response (reviewed in [Butler et al., 2013]), Neutrophils, arriving early at the site of infection, deploy reactive oxygen species and neutrophil extracellular traps to ensnare the parasite. The adaptive immune response starts with DCs presenting antigens and releasing inflammatory cytokines. NK cells and macrophages are first activated through cytokines stimulation and play a role in the defense against erythrocytic stage infection. This ongoing interplay underscores the complex dynamics in malaria pathogenesis and immune evasion strategies employed by the parasite. Of particular interest, it was recently shown that Rifin, the largest family of VSA, binds to leucocyte immunoglobulin-like receptor B1 (LILRB1) and inhibits the activation of LILRB1-expressing immune cells [Saito et al., 2017].

1.2.3 Malaria immunity: humoral response and naturally acquired immunity to malaria

Millions of people who are consistently exposed to *P. falciparum* infection develop naturally acquired immunity (NAI) to *falciparum* malaria, preventing severe sickness and death. Until now, there has been no clear understanding of the rate at which immunity is acquired in endemic regions. The importance of acquired immunity to malaria was demonstrated as early as the 1960s, when the passive transfer of purified immunoglobulin G (IgG) from malaria immune individuals reduced parasitaemia in non-immune children by 99% within four days [Cohen et al., 1961] highlighting the importance of antibodies in symptomatic malaria protection. Further research revealed that these purified IgG inhibited parasite growth *in vitro* [Cohen et al., 1969].

In endemic areas, after the age of peak clinical infection, the number of clinical malaria attacks each year falls considerably, as does the risk of death. Severe illness is quite infrequent after adolescence, but mild clinical episodes are still common, and the cumulative incidence of parasitemia can even reach 100% in some cases[Owusu-Agyei et al., 2001]. However, it is hypothesised that clinical (anti-disease) and anti-parasite immunity develop at separate rates. For example, clinical cases of malaria appear to arise primarily in people who emigrate from malaria-endemic areas and are not re-exposed for at least 3-5 years [Struik and Riley, 2004]

Epidemiological observations in endemic populations have also previously revealed that naturally acquired immunity to malarial disease takes years of repeated exposure to *Plasmodium* and is often age-related Aponte et al. [2007], Baird et al. [1991] and tends to be antigen-specific [Akpogheneta et al., 2008; Bull et al., 1998; Hviid, 2005]. Field investigations have shown that *P. falciparum* specific antibodies are inefficiently developed and short-lived, especially in children [Cavanagh et al., 1998, 2004; Kinyanjui et al., 2004]. It has also been shown that children and young adults in areas with high seasonal transmission experience delayed formation of memory B cells specific to *P. falciparum* , despite repeated parasite infection [Weiss et al., 2010]. Research in lower transmission settings also indicates that it is the breadth of circulating B memory cells against *P. falciparum* , and not the magnitude that is associated with age [Nogaro et al., 2011], hinting that acquired malarial immunity might indeed be defective. Although antigenic polymorphism is likely to contribute to the relatively slower development of protective immunity, there is also strong evidence that malaria infection modifies the host immune response [Hviid and Jensen, 2015]. In contrast, in areas with stable transmission more stable IgG responses towards *P. falciparum* are associated with increasing age [Akpogheneta et al., 2008; Wipasa et al., 2010]. Additionally, B cell memory in young infants appears to be protective [Jahnmatz et al., 2022], develops and maintains throughout time, even in the absence of ongoing infection [Ndungu et al., 2012].

Antibodies interact with merozoites, inducing complement-mediated lysis and opsonic phagocytosis, which prevents their invasion of erythrocytes. Additionally, they bind to the surface of infected erythrocytes, triggering complement activation and facilitating phagocytosis by circulating monocytes and macrophages.
Furthermore, these antibodies impede infected erythrocyte sequestration by binding to cytoadhesion molecules involved in rosetting or adhesion. The primary target of these antibodies is the PfEMP1 surface protein, making them key targets of naturally acquired immunity [Chan et al., 2014, 2012; Travassos et al., 2018]. The critical role of anti-parasitic antibodies is prominently illustrated in placental malaria. Pregnant women in endemic areas are particularly at risk of developing placental malaria [Dorman and Shulman, 2000] , involving iRBC sequestration in the placenta, which can result in infant mortality due to low birth weight [Uneke, 2007; Sharma and Shukla, 2017]. The cytoadherence is mediated by an unusually semi-conserved

PfEMP1, named VAR2CSA, that binds to Chondroitin Sulfate A (CSA), a glycosaminoglycan in the placenta. Consequently, pregnant women are particularly susceptible to placental malaria due to their lack of prior exposure to VAR2CSA. Then, with successive pregnancies and *P. falciparum* infections, women progressively develop antibodies against VAR2CSA and an effective adaptive response [Mahamar et al., 2023]. A VAR2CSA-derived placental malaria is currently being tested [Gamain et al., 2021].

1.3 Antigenic Variation in *P. falciparum*

Over the course of evolution, mammals have developed sophisticated immune systems to combat pathogens. This has driven infectious agents to co-evolve and respond with complex mechanisms to invade the hosts' immune systems. To achieve this, infectious organisms deploy various strategies to prolong their survival within the host. One of the most well-characterised strategies to ensure this is **antigenic variation**. The strategy involves changes in the variant surface molecules presented to the host, reducing the pathogen's clearance and establishing long-term infection within the host. Some antigenic variation systems involve the activation and silencing of genes that encode molecules that interact with the infected host's immune system. This mechanism is called phase variation and regulates the expression of genes in an "on-off" manner[Van Der Woude and Bäumler, 2004].

In the case of more complex pathogens, antigenic variation is mediated by hypervariable, multicopy gene families, and each copy only encodes a unique surface protein. Each gene can be silenced or activated during the infection, but there is a tight mechanism of regulation that ensures that only one of these genes is expressed at a given time, leading to mutually exclusive expression [Deitsch et al., 2009]. Multiple protozoan parasite species including *Trypanosoma brucei*, *Babesia bovis*, *Giardia lamblia* and *P. falciparum* exhibit programmed antigenic variation through regulated expression of hypervariable genes, depicted in Figure 1.6. The adaptive immune system of an infected host usually selects against the initial surface antigen, which is not longer effective on the subsequent variants, and hence the infection persists. Viruses also exhibit antigenic variation, but it is achieved by either fast

accumulation of mutations so that initial immune responses are rendered useless, or through recombination of antigens of multiple infecting genotypes [Barbour and Restrepo, 2000].

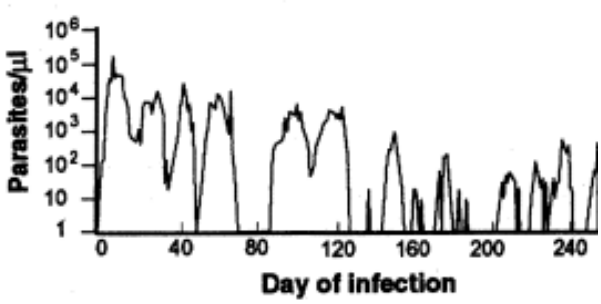

Figure 1.4: Waves of parasitemia observed during a single *P. falciparum* infection, characterized by recurrent peaks. Image source: [Miller et al., 1994].

The earliest evidence of antigenic variation in *Plasmodium* species came through observations of recurring infections in non-human hosts [Cox, 1959; Brown et al., 1966]. Eventually, antigenic variation in *P. falciparum* infections in human hosts was first described in 1994, wherein within a single infection, recurrent peaks and troughs of parasitemia were observed [Miller et al., 1994; Pasloske and Howard, 1994], Figure 1.4.

1.3.1 PfEMP1 Structure & Diversity

PfEMP1 proteins, encoded by the *var* multi-gene family, play a crucial role in this mechanism in *P. falciparum* [Baruch et al., 1995]. The *var* gene family is present in all species within the *Laverania* subgenus of *Plasmodium* [Larremore et al., 2015; Otto et al., 2019]. *Laverania* species primarily infect African great apes, with *P. falciparum* being the only species capable of infecting humans. During an infection with *P. falciparum* , at the parasite's ring stage , only one *var* is transcribed, resulting in a single PfEMP1 variant appearing on the parasite's surface in the trophozoite or schizont stage [Scherf et al., 1998] (see section below). However, it has been shown recently that the expression of *var* genes is not restricted to the intra-erythrocytic stages, it also occurs during the mosquito stages and PfEMP1 are displayed on the

surface of sporozoites [Gómez-Díaz et al., 2017; Zanghì et al., 2018]. PfEMP1 in this stage has been suggested to play a role in hepatocyte invasion [Zanghì et al., 2018].

P. falciparum genomes include around 60 *var* genes with two exons that encode PfEMP1 proteins [Scherf et al., 1998; Chen et al., 1998]. Within and between repertoires, PfEMP1s exhibit significant levels of diversity. The first exon of *var* gene is the longest and encodes extracellular domains, starting with a NTS domain (60 amino acids). Then the typical PfEMP1 is made up of 2-10 Duffy-binding-like (DBL) and cysteine-rich interdomain regions (CIDRs) domains. The DBL and CIDR domains are organized into seven $\alpha, \beta, \gamma, \delta, \epsilon, x$ and three α, β, γ primary sequence classes, respectively, with numerous subdivisions. The exon I encodes the short transmembrane domain and exon II encodes the acidic intracellular terminal segment (ATS) [Bull and Abdi, 2016]. The DBL-CIDR combination in a particular type of PfEMP1 protein exists non-randomly, ordered as specific sequences known as domain cassettes [Rask et al., 2010].

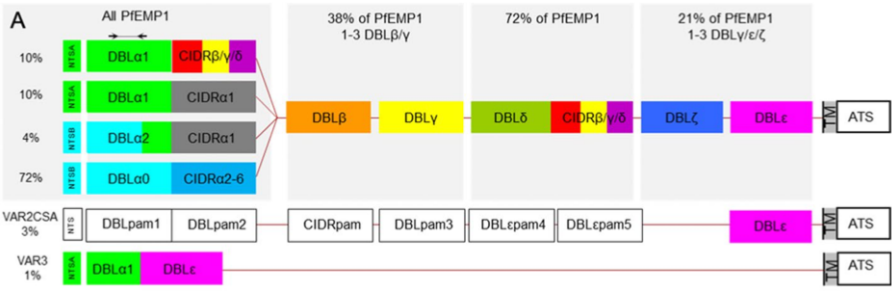

Figure 1.5: PfEMP1 structure: PfEMP1 proteins comprise several domains: N-terminal segment (NTS), DBL, CIDR, transmembrane (TM), and acidic terminal segment (ATS). Figure taken directly from [Mackenzie et al., 2022].

Although *var* genes are substantially sequentially diverse, they can be classified into groups A (10 variants in the 3D7 *Pf* strain), B (22 variants), C (13 variants), and E based on a conserved upstream (Ups) flanking sequence, chromosomal position, and orientation [Kraemer and Smith, 2003], Figure 1.5. Group A (UpsA) genes are located near the subtelomeres, Group B includes both subtelomeric and within

internal clusters, Group C genes are solely within these internal clusters. Group E is a special case, with 1 or 2 copies of *var2csa*, with their expression associated with placental malaria (see above) and putatively a coordinator role in the *var* transcription switching process [Zhang et al., 2022]. Additionally, *var* genes undergo more frequent mitotic recombination than the rest of the parasite genome to maintain antigenic diversity [Taylor et al., 2000; Bopp et al., 2013; Freitas-Junior et al., 2000].

1.3.2 Mutually Exclusive Expression of the *var* Family

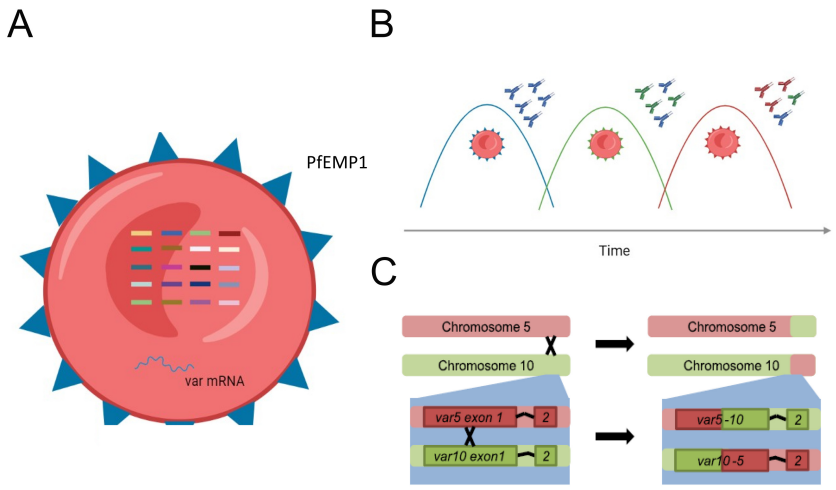

Figure 1.6: Antigenic Variation in *P. falciparum* : A) There is only one *var* expressed per infected cell at the ring stages. Within a population of parasites, a number of variants can be expressed, & B) the *var* gene variants undergo transcriptional switching, which leads to recrudescence because acquisition of specific antibodies is hypothesized to clear parasites expressing a certain variant until the next variant expands in the population. C) In addition, *var* genes can recombine and give rise to 'chimeric' *var* genes. Figure modified and adapted from [Nyarko and Claessens, 2021].

In addition to already-existing sequence diversity across parasite populations, mutually exclusive expression, and recombination to diversify, PfEMP1 variants also exhibit transcriptional switching over time, changing expression from one cycle to the next. Although the mechanism of transcriptional switches in *var* genes is unknown,

current understanding suggests that *var* genes differ in activation and transition rates based on their chromosomal location as well as Ups type [Guizetti and Scherf, 2013]. Understanding how infections persist over time and how parasites infect partially immune hosts requires identifying these factors and their correlations. Most investigations on *var* gene switching dynamics have focused on parasite cultures, as the distribution of PfEMP1 variants *in vivo* is influenced by host variables and immunological pressure, in addition to antigenic variation. The first study to document switching of PfEMP1 proteins [Roberts et al., 1992] discovered that an initially isogenic clone rapidly switched to different antigenic types.

This selective expression is mediated by mechanisms involving epigenetic regulation, as well as specific DNA fragments and RNA transcripts that activate or silence the *var* gene [Deitsch and Dzikowski, 2017]. Histone markers are differentially enriched in different flanking regions. The majority of *var* genes are suppressed in a heterochromatin environment marked by histone 3 lysine 9 trimethylation (H3K9me3), which is bound by heterochromatin protein 1 (HP1) [Lopez-Rubio et al., 2009]. The active *var* gene lacks H3K9me3 and has a euchromatic structure with promoter enrichment of H2A.Z and H2B.Z, as well as histone acetylations such as H3K9ac and H3K27ac [Tang et al., 2020]. Transcriptionally active genes exhibit di- and trimethylation of histone H3K4, while silent genes exhibit trimethylation of H3K9 and H3K36 [Chookajorn et al., 2007; Lopez-Rubio et al., 2007; Flueck et al., 2009] Jiang et al. [2013]. A recent study has shown *var2csa* as an important node for maintaining the *var* switching network *in vitro* [Zhang et al., 2022]. Several factors contribute to the default silencing of *var* genes, but no specific regulator of mutually exclusive activation or switching factors has been identified [Dzikowski et al., 2006].

1.4 Controlled Human Malaria Infection Studies

In the early 1900s, deliberate malaria infection through inoculation with infected blood was employed as a treatment (malariatherapy) for neurosyphilis in Europe and the United States [Chernin, 1984; Austin et al., 1992; Snounou and Pérignon, 2013] before the advent of Penicillin. Later, In the 1990s, it was also tested as a potential therapy for HIV infection which is rather disputed [Nierengarten, 2003]. The utility

of Controlled Human Malaria Infection (CHMI) studies as a method for evaluating prospective antimalarial medications was identified as early as the 1940s, when they were used to examine antimalarial efficacy in healthy, non-immune males via *Plasmodium* -infected blood or mosquitoes. Nowadays, CHMI studies a well-controlled and safe framework to conduct *in vivo* assessments of the efficacy of malaria [Abuelazm et al., 2024] vaccines. They are carried out through sporozoite inoculation via mosquito bite or by injecting sporozoites or *Plasmodium* -infected RBC directly. Based on specific criteria in each CHMI study, antimalarials are administered upon the diagnosis of infection. Infections are routinely treated at a preset blood-stage parasite density (measured by PCR) or when individuals test positive by microscopy.

Previously, only the NF54 isolate of *P. falciparum* was routinely used for CHMI studies. The NF54 isolate was obtained from a Dutch patient who lived near Schiphol Airport in Amsterdam and had never left the country. This airport malaria case was most likely caused by an infected mosquito imported from Africa. 3D7 was then cloned from NF54. Now, other genetically and geographically different strains, such as 7G8 from Brazil, NF166.C8 from Guinea, and NF135.C10 from Cambodia, have become accessible for heterologous CHMI studies. These strains reflect their geographic origin and vary in genome structure and immunogenic potential. In 1984, 7G8 was cloned from the IMTM22 isolate and chosen for its capacity to produce microgametes, exflagellate, and infect *Anopheles freeborni*, resulting in oocysts and sporozoite formation that can be used for CHMI challenges. Table 1.2 highlights a non-exhaustive list of recent CHMI studies that examine host-pathogen interactions. For a better understanding of infection outcomes in these studies, semi-immune individuals were sometimes classified into 'controllers' and 'non-controllers', depending on their ability to control the induced CHMI infection. Amongst these studies, of particular interest is a study by Wichers-Misterek *et al* just reported the first CHMI study to analyse *var* gene transcription from a non-NF54/3D7 strain, specifically the 7G8 clone[Wichers-Misterek et al., 2023].

Table 1.2: Summary of CHMI Studies evaluating host-pathogen interactions

Study	**Immune Status**	**Inoculation Method**	**Study Site**	**Detection Method**
[Wang et al., 2009]	Naïve (n=1)	Mosquito bite	Nijmegen	qPCR
[Bachmann et al., 2016]	Naïve (n=18)	Intradermal Sporozoite Injection (PfPZ=2500) (n=3), Intravenous Sporozoite Injection (IV) (PfPZ=800) (n=5), Intravenous Sporozoite Injection (IV) (PfPZ=3200) (n=9)	Tübingen/ Barcelona	Thick Blood Smear
[Bachmann et al., 2019]	Naïve (n=18), Non-Controllers (n=6), Controllers (n=5), Clearers (n=6)	Intradermal Sporozoite Injection (PfPZ=2500) (n=3), Intravenous Sporozoite Injection (IV) (PfPZ=3200) (n=15)	Gabon	qPCR & or Thick Blood Smear
[Hoo et al., 2019]	Naïve (n=13)	Intradermal Sporozoite Injection (PfPZ=2500) (n=3), Intravenous Sporozoite Injection (IV) (PfPZ=800) (n=3), Intravenous Sporozoite Injection (IV) (PfPZ=3200) (n=7)	Tübingen	Thick Blood Smear
[Achan et al., 2020]	Non-Controllers (n=16), Controllers (n=2)	Intravenous Sporozoite Injection (IV) (PfPZ=3200) (n=15)	Gambia	qPCR

Study	Immune Status	Inoculation Method	Study Site	Detection Method
[Milne et al., 2021]	Naïve (n=19)	Mosquito bite (n=5), Blood Challenge (No. of parasites=690) (n=14)	London	Thick Blood Smear and/or qPCR
[Pickford et al., 2021], follow up from a previous CHMI study	Naive (n=4)	Intravenous Sporozoite Injection (IV) (PfPZ=3200) (n=3), Intra-muscular Injection (IM) (PfPZ=2500) (n=1)	Barcelona	Thick Blood Smear
[Wichers-Misterek et al., 2023]	Naïve(n=11), enrolled in PfSPZ-CVac and PfSPZ Vaccine Trials	Intravenous Sporozoite Injection (IV) (PfPZ=800) (n=2), Intravenous Sporozoite Injection (IV) (PfPZ=1600) (n=1), Intravenous Sporozoite Injection (IV) (PfPZ=3200) (n=8) with 7G8 *Pf* strain	Tübingen	Thick Blood Smear and/or qPCR

Changes in the expression of VSAs play a significant part in the adaptation process of parasites, affecting their antigenic and functional features. However, we have still not been able to fully characterise expression of these genes in human circulation and its impact on transmission phases. To probe into this particular aspect of the parasites' virulence, CHMI studies serve as excellent tools to fully trace an infection with malaria. Using CHMI data, significant differences in the transcription of VSAs, especially *var* genes have been found to be associated with infection outcome in naive and semi-immune individuals. Previous studies have found that parasites transcribe a wide range of genes in naive hosts, with group B variants being the most

commonly expressed and no significant changes between volunteers with similar immune-status [Bachmann et al., 2016, 2019; Milne et al., 2021]. The CHMI study with the 7G8 clone also reported broad activation of mainly B-type subtelomeric located *var* genes, however, surprisingly, a single UpsC *var* gene dominated the *var* transcription repertoire both *in vitro* and *in vivo*. To what extent 7G8 is representative of other *P. falciparum* strains is unclear, but this important result highlights the need to replicate findings on multiple strains [Wichers-Misterek et al., 2023]. In addition to parasite related characteristics, CHMIs have proven useful in understanding the host-intrinsic factors controlling *var* expression and turnover as the volunteers are often infected with the genetically identical parasites. Moreover, time series data from CHMI infections provide the unique opportunity to model *var* switching rates *in vivo* , which has only been theoretically described before using *in vitro* experimental datasets [Recker et al., 2011; Noble and Recker, 2012; Horrocks et al., 2004].

1.5 Mathematical Modelling of Malaria

The mathematical modelling of infectious diseases traces its origins to 1766, with Daniel Bernoulli's study of smallpox in England. In this study, Bernoulli constructed a mathematical model to assess the mortality caused by smallpox in England, which accounted for one in every fourteen deaths during that period. The model demonstrated that immunisation against the virus would enhance life expectancy at birth by around three years. The model was later improved by incorporating parameters that were age-dependent.

However, mathematical approaches to understanding infections were not developed rigorously until 1911, when Ronald Ross established the field of contemporary mathematical epidemiology. In this seminal work, Ross addressed the mechanistic *a priori* modelling technique employing a set of equations to simulate the discrete-time dynamics of malaria through mosquito-borne disease transmission [Smith et al., 2012]. Since this breakthrough, mathematical modelling approaches have consistently improved our understanding of transmission, epidemiology, ecology, evolution and host-parasite interactions pertaining to infectious diseases. In recent times, it has made even more sense to investigate realistic infectious disease models to

predict and control outbreaks and minimise disease burden due to epidemics [Ciotti et al., 2020].
To serve this purpose, mathematical models of infectious diseases focus on both within-host dynamics that are significant to our understanding of the biology of the disease and between-host models that have impact on our understanding of infectious diseases at the population level [Enderle, 2012; Brauer, 2008; Sattenspiel, 1990; Sattenspiel and Lloyd, 2009].

1.5.1 Within-Host Modelling Approaches

Despite substantial work, modelling to understand the within-host dynamics of malaria infections has received far less attention from modellers than viral diseases. Most mathematical models for studying intra-host dynamics with the human host incorporate recovery rates from infectious compartments as constants, which can undermine the importance of including factors such as heterogeneity in symptomatic period and discrete latency. One of the most widely used modelling approaches to infectious disease dynamics is Ordinary Differential Equations (ODEs) [Ciupe and Heffernan, 2017]. Depending on the context and the infection being studied, the basic model of pathogen dynamics includes certain fundamental aspects of disease dynamics in the host. These include and are not limited to, the cells that the pathogen infects, the existence of the pathogen in the host (i.e., which organs of the body pathogen targets), the time-scale of the infection of the host, i.e., persistent or acute infections, the pathogen's life-cycle and its interactions with the immune system. In the case of malaria, qualitatively, within-host models are similar to the viral dynamics model, and the latter has been also extensively documented and well-studied theoretically. These similarities make it lucrative to study the two systems theoretically for mathematical modelling and bring new insights to malaria research. The standard framework of within-host models of HIV and malaria infections within the host are depicted in Figure 1.7 [Khoury et al., 2018].

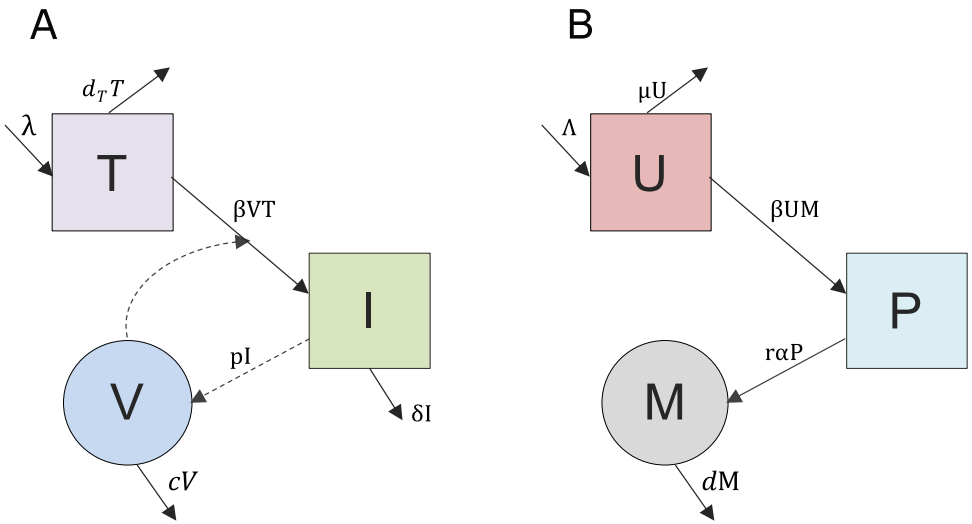

Figure 1.7: Model schematic and mathematical formulation depicting similarities between viral and parasitic infection dynamics. Figure modified from: [Khoury et al., 2018]

Model A:

$$\frac{dT}{dt} = \lambda - d_T T - \beta VT \tag{1.1}$$

$$\frac{dI}{dt} = \beta TV - \delta I \tag{1.2}$$

$$\frac{dV}{dt} = pI - cV \tag{1.3}$$

Model B:

$$\frac{dU}{dt} = \Lambda - \mu U - \beta UP \tag{1.4}$$

$$\frac{dP}{dt} = \beta UP - \alpha P \tag{1.5}$$

$$\frac{dM}{dt} = r\alpha P - dM \tag{1.6}$$

Model A) represents the typical form of HIV infection ODE model [Perelson, 2002]. Target CD4+ T cells (T) are generated at rate λ and perish at the natural death rate (d_T). T cell infection is determined by the availability of T cells, the amount of free virus (V), and the infectivity (β). Infected cells (I) are lost at rate δ. Similarly, the conventional model of Plasmodium infection (Model B) describes the dynamics of uninfected red blood cells (RBCs) U, infected red blood cells (iRBCs) P, and merozoites M. Uninfected RBCs are generated at a rate Λ and destroyed at a rate μ. When a merozoite infects an RBC, it produces infected RBCs at a rate dependent on the availability of uninfected RBCs, merozoites, and infectivity, denoted by β. infected RBCs rupture at a rate of α, resulting in r merozoites. Merozoites are also lost at a rate d. [Anderson et al., 1989]

Even though these two mathematical models are very similar (Figure 1.7), the key difference in the model formulation stems from the fact that while viral production of HIV is directly proportional to the infected cell number, because viral replication does not cause cell mortality. However, the production of merozoites during the blood stages is strictly dependent on the rupture of mature merozoites (Figure 1.7). This inconsistency was first highlighted by [Saul, 1998], highlighting that defining the quantity of merozoites produced per infected cell as r resulted in a significant overestimation of the growth rate of infected cells. Even though the model accurately captures the idea that r merozoites are formed at the end of a iRBC's life cycle, it does not describe the differences in lifespans of iRBCs. This complexity has been addressed in mathematical *falciparum* growth models by modelling merozoite production proportionally to infected iRBCs. Additionally, ODE based models also fail to capture the $\tilde{2}$ day parasite life-cycle (asexual stage) within the human host, which results in the release of merozoites and leads to the periodic fevers in the host. Despite the complications with modelling the *P. falciparum* blood-stage life-cycle, we can still infer infection characteristics, like the growth rate. The *falciparum* growth rate *in vivo* is considered analogous to the growth rate of a viral infection, i.e exponentially growth per time, in the case of *falciparum* this growth rate is modelled as the Parasite Multiplication Rate (PMR), per cycle, which is estimated as the fold-increase in the number of parasites per 48h cycle.

The PMR, which measures the growth rate of the parasite population within its host, serves as a proxy to link parasite dynamics to clinical outcomes [Kingston et al., 2017; Chotivanich et al., 2000]. The PMR *in vivo* can be treated as a within-host analogue of the reproduction number R_0 at a population scale [Chotivanich et al., 2000; Wockner et al., 2020]. The PMR can be incorporated as a parameter to evaluate disease severity and within-host dynamics of parasite growth under selection [Gnangnon et al., 2021; Georgiadou et al., 2019]. The PMR in early infection in previously unexposed people has been estimated to range between 8 and 17 for *P. falciparum* [Dietz et al., 2006; Wockner et al., 2020; Douglas et al., 2013]. Mathematically, the PMR corresponds to the average number of progeny produced by a single iRBC, therefore it takes into account the likelihood that some iRBCs will not survive to produce merozoites and that not all merozoites produced will successfully infect RBCs.

1.5.2 Modelling Antigenic Variation

Antigenic variation exhibited by malaria parasites is subject to the action of immune pressure, and the parasite population in early stages of infection should be able to not expose its entire repertoire, yet develop enough diversity to escape the immune pressure to sustain long term infections. Mathematical models of antigenic variation were applied to *Trypanosoma brucei*, another protozoan parasite that exhibits antigenic variation facilitate immune escape [Turner, 1997]. The first models incorporating antigenic variation found that infection growth rates alone did not result in the ordered development of antigenic variants in infections. An alternate model that involved the brief expression of two antigens per pathogen and differential vulnerability to immune responses was proposed early on [Agur et al., 1989]. While this model mimicked ordered expression, it lacked experimental evidence of the same. It was eventually shown that intrinsic gene activation rates, not the previously active gene, can explain the ordered antigenic variation observed during acute *T. brucei* infection [Lythgoe et al., 2007; Gjini et al., 2010]. Antigenic variation at later stages in *trypanosome* infections is sustained by generation of variants by DNA rearrangement in addition to switching. In the case of *falciparum* infections its hard to envision a *var* gene switching network capable of ensuring the sequential dominance of 60 PfEMP1 variants during an infection, especially in endemic regions where hosts can have immunity against some variants from the *var* pool. The persistence of chronic infections in malaria has also been attributed to antigenic variation [Nyarko and Claessens, 2021]. Different mathematical studies have investigated the outcomes of antigenic variation - estimation of switching rates, bias and order of switching, but it is imperative to note that antigenic variation generated by these models relies on the number of variants expressed at the beginning of infection, and chronic infections are favoured if this number is restricted.

However, it has been shown that in chronic infections, during the low-transmission season in endemic areas, there exist antibodies against a variety of surface antigens [Collins et al., 2022; Rono et al., 2013]. Even after accounting for differences in exposure, this association holds true, suggesting that antibodies expressed during asymptomatic infections could be cross-reactive and short-lived Warimwe et al. [2013]. Stochastic discrete models, including differential growth rates , have been

used to simulate chronic *P. falciparum* infections with clinically relevant dynamics [Paget-McNicol et al., 2002; Molineaux et al., 2001]. The model developed by [Molineaux et al., 2001] was the first model to distinguish between different types of immune responses to infection into three components: innate, variant specific, and cross-reactive adaptive response. Alternatively, [Recker et al., 2004] proposed a deterministic ODE based model that incorporated each PfEMP1 as a combination of a single major epitope that causes a long-lasting immune response, and several minor epitopes that cause temporary, cross-reactive responses. The authors successfully replicated their findings using only these assumptions . In the presence of cross-reactive immune responses, some variants are suppressed and cannot provoke a variant-specific immune response for clearance. Later, with the decline in cross-reactive immunity leads to proliferation by variants that were previously suppressed.

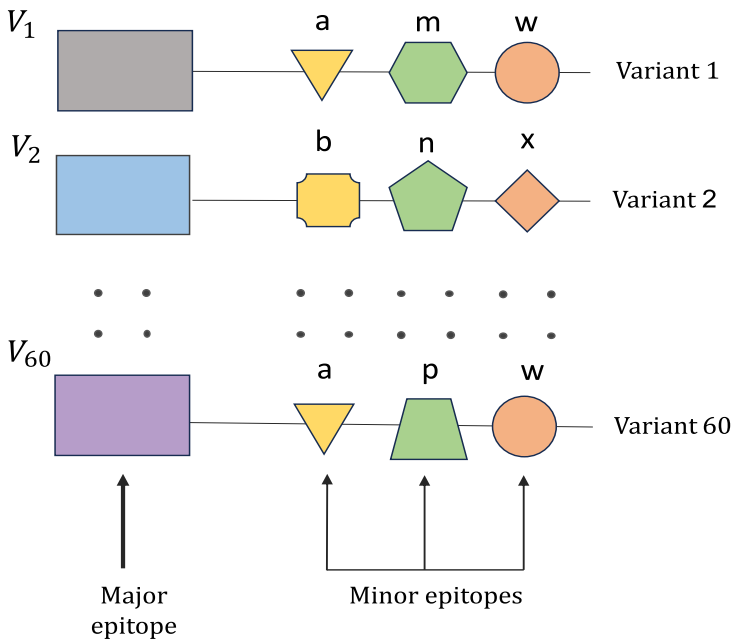

Figure 1.8: Multiple Epitope Model: The mathematical model incorporates multiple minor variants (shared) and one major variant (unique) per antigenic variant in each parasite.

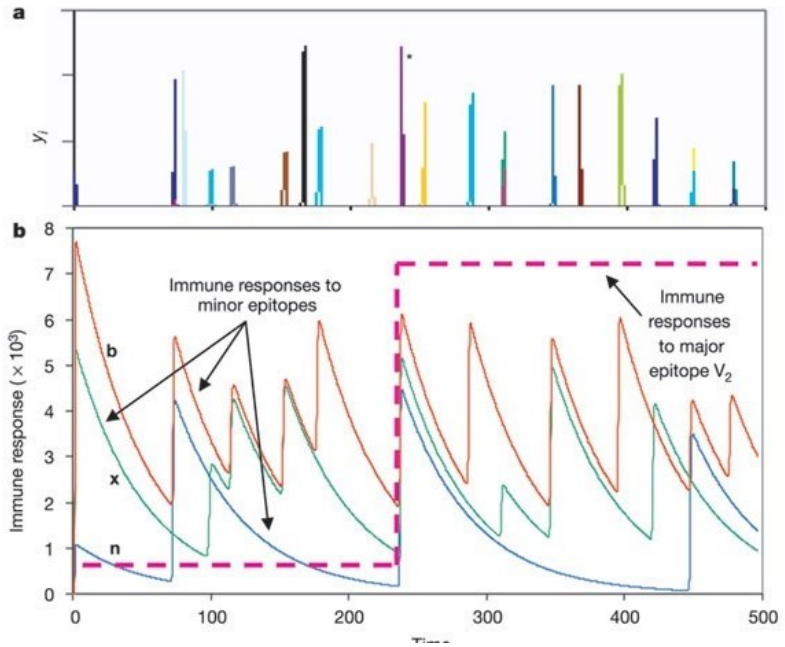

Figure 1.9: Infection dynamics in the model proposed by [Recker et al., 2004]: A) Different antigenic variants appear sequentially during the course of infection, and previously expressed variants can re-appear owing to waning cross-reactive responses during a single infection. B) The cross reactive responses are triggered by minor epitopes and decline due to lack of exposure once a variant has been expressed (solid lines). The specific immune response (dotted line) once activated, does not decay for each expressed variant during the infection. Figure directly sourced from [Recker et al., 2004].

Although this model managed to recreate long term infection dynamics (Figure 1.9), the model was unable to replicate early infection dynamics because it is limited by the time required to stimulate cross-reactive immune responses. The authors had proposed that antigenic variation contributes to the initial conditions by expressing a distribution of variants in the early stages of infection. There are several discrete intra-host models that incorporate antigenic variation in malaria and are described in Table 1.3. Eventually, in a computational model with cross-immunity, it was demonstrated that the optimal antigenic switching network comprised of "source" antigenic variants (nodes) that could converge to "sink" variants in the parasite population [Recker et al., 2011] and this could explain the presumably ordered expression of *var* variants in a chronic infection. Additionally, several studies have attempted to resolve *in vitro* switching rates and therefore postulating the switching

rates of *var* genes *in vivo* .

The first study to estimate switching rates *in vitro* [Roberts et al., 1992], predicted a switching rate of 2.4% which has been consistently quoted. This estimate was based on an exponentiated decay model and other models estimating switching *in vitro* have followed the same method with varying results [Peters et al., 2002, 2007]. Using *in vitro* time series data that it was also shown that *var* genes located in central sections of chromosomes have considerably lower "off" rates compared to those in subtelomeric loci [Frank et al., 2007] and the sharp drop in transcription of Group A genes in laboratory cultures of *P. falciparum* can be explained using these observations [Gatton and Cheng, 2004; Peters et al., 2002]. These studies were aimed at mainly estimating the rates at which *var* genes are turned "off" in a clonal population, and hence take into consideration only the expressed genes, and not the general architecture of the *var* gene network.

Several other models have demonstrated that higher switching rates might not be sustainable for the parasite's persistence in the human host, as exposure of the *var* repertoire would risk immune selection rapidly Childs and Buckee [2015], Eckhoff [2012] and are described in Table 1.3. The idea of structured switching network *in vitro* was further developed using time series data [Noble and Recker, 2012], which implied that *in vitro* , *var* genes switch in a network structure defined by a "single-many-single" structure, with several transient *var* genes being expressed. Recently, an experimental study further elaborated that the conserved *var* gene, *var2csa*, might be a transient *var* gene necessary to sustain the switching network Zhang et al. [2022]. In their *in vitro* experiments, the authors found that inhibiting the expression of *var2csa* disrupted the switching network, emphasising the importance of transient nodes for facilitating intrinsic switching. It has since been demonstrated that the switching *in vitro* follows a structured pattern, highlighted in eqn 1.7, where v_i is a given variant transcript at given time t with a parameter that described the switch bias (probability) from one variant i to j modelled by β_{ji} and an independent "off" rate per gene, w_i. This model's main advantage over others is the inclusion of off-rates independently to switching-probabilities between genes.

$$v_i^t = (1 - \omega_i)v_i^{t-1} + \sum_j \omega_j \beta_{ji} v_j^{t-1} \tag{1.7}$$

In addition to switching mediated antigenic variation, it has also been demonstrated that infections with multiple strains lead to an extended duration of infection, even if the infections are initiated around the same time period [Rek et al., 2022; Nassir et al., 2005]. Deterministic models can also give rise to heterogeneity in duration of infection length, peak parasitemia etc. owing to small pertubations. In one such model described in [Childs and Buckee, 2015], g_i is the growth rate for a particular variant i, and I, Γ_{VS},Γ_{CR} are the effective innate, variant-specific, and cross-reactive immune responses and M is the general adaptive response (eqn 1.8). Recombination within the *var* gene repertoire of *P. falciparum* has a severe effect on strain diversity and the process of acquiring immunity against clinical malaria. The model described by [Childs and Buckee, 2015] attempts to capture the effect of recombination on infection persistence under immune pressure.

$$p_i(t+1) = g_i(t+1)I(t+1)\Gamma_{VS_i}(t+1)\Gamma_{CR_i}(t+1)M(t+1) \tag{1.8}$$

Some of the mechanistic within hosts models described in 1.3 are validated on data from the retrospective analysis by [Collins and Jeffery, 1999] which provides detailed descriptions of the malaria therapy dataset that consists of parasitaemia and fever records. In this dataset, patients with no history of malaria infection were tested in laboratories in Columbia, South Carolina and Milledgeville, Georgia (n=318). Patients were infected with one of three parasite strains (McLendon, Santée-Cooper, or El Limon) either intravenous injection of parasitised blood, or bites from infected mosquitoes or sporozoite injection.

Study	Biological Assumption	Conclusion	Mathematical Model	Data Used
[Roberts et al., 1992]	Antigenic phenotypes switch *in vitro* in the absence of selection pressure, assuming equal growth rates for all variants	The switching rate observed is around 2.4% per generation.	The switching rate was estimated using the closed-form solution of the discrete ODE for the two-state model, $r_{\text{off}} = 1 - (P_n)^{1/n}$	
Horrocks et al. [2004]	Three States of var genes - active, activable, or silenced.	Variable *on* rates were detected for different var variants. Off rates $\geq$ 1%, On rates ranged between 0.025% and 0.25%.	A two-state model was used to monitor transcriptional levels of each gene: $p_{on} = r_{\text{on}} \cdot (1 - r_{\text{on}})^n \cdot n$, where p_{on} is the probability of being on after n cycles. Similarly, the off rate was estimated using the closed-form solution of the discrete ODE for the two-state model, $r_{\text{off}} = 1 - (P_n)^{1/n}$	

Study	**Biological Assumption**	**Conclusion**	**Mathematical Model**	**Data Used**
[Gatton and Cheng, 2004]	Slow & fast switching variants	Parasite replication *in-vivo* is influenced by switching and immune response	Discrete Probabilistic Model	Malariatherapy Dataset (n=90)
[Recker et al., 2004]	No switching	Transient cross reactive immunity can mediate antigenic variation	ODEs for within-host dynamics	
Recker et al, 2011 Recker et al. [2011]	Switching with bias	Non-random, structured switching pattern demonstrated by var transcripts in-vitro	Time-discrete Markov chain with weights $v_{i,c}(t+1) = (1-\omega_i)v_{i,c}(t) + \sum_{j\neq i}^{n}\omega_j\beta ji)v_{j,c}(t)\forall i \in \{1,2,3\ldots n\}$	
Noble and Recker [2012]	Structured switching for each clonal population. The model does not discuss switching rates, but develops the network structure	Same as Buckee and Recker, 2011 Recker et al. [2011]	Time-discrete Markov chain with weights, $v_{i,c}(t+1) = (1-\omega_i)v_{i,c}(t) + \sum_{j\neq i}^{n}\omega_j\beta ji)v_{j,c}(t)\forall i \in \{1,2,3\ldots n\}$	

Study	**Biological Assumption**	**Conclusion**	**Mathematical Model**	**Data Used**
Eckhoff [2012]	Switching and Selection	Shared adaptive immunity and low switching rate extend infection lengths	Time-discrete processes for parasite population, Immune responses as continuous variables. Antigenic switch is modelled as: $N_{n+i,n} = Poisson(K_{antigen}N_n), 1 \leq i \leq n_{antigenicswitch}$	Malariatherapy Dataset
Childs and Buckee [2015]	Switching and Selection	Cross immunity interferes with the development of variant-specific immunity, promoting proliferation when CR response wanes	Time-discrete deterministic model with stochastic parameters, antigenic switch is modelled as $g_i(t+1) \propto \omega_i \beta_{ji} p_j(t)$, where ω is the inherent tendency to switch and the matrix β describes the switching probabilities. This formulation is the same as [Recker et al., 2011]	Malariatherapy Dataset
Pilosof et al. [2019]	Neutral Evolution and Immune Selection	Selection imposed by immunity maintains repertoires with similar properties	Analysis of temporal networks to detect communities by simulating Agent-Based Models	

Study	Biological Assumption	Conclusion	Mathematical Model	Data Used
He and Pascual [2021]	Switching and Selection	Beyond an antigenic threshold, many *var* variants can mutually exist in the population	Agent-based simulations to establish a threshold for diversity, antigenic variation produced through recombination	

Table 1.3: Review of different methods to incorporate antigenic variation in within-host and *in vitro* models

It has also been demonstrated that models that incorporate transcriptional switching of *var* variants have tested the possibility of switching alone as a driver of antigenic diversity and reveal that the mechanism alone is not sufficient to produce chronic infections, as all PfEMP1 variants will eventually appear during the duration of infection Childs and Buckee [2015].

Hence, it is significant for mechanistic models to include not only parasite intrinsic factors but also host-intrinsic variation, specifically arising from heterogeneity in immune responses, which has been repeatedly highlighted with the availability of data from recent studies [Milne et al., 2021; Pickford et al., 2021; Bachmann et al., 2019]. Additionally, the role of antigenic switching rate in shaping the infection duration and investigating the effect of innate immune response in limiting gametocyte success in mosquitoes is still unclear. Most mathematical models that capture chronic infection and variation, have relied heavily on exploiting a limited subset of *var* variants, however, from CHMI studies, even in individuals from endemic area, experimental evidence suggests that most variants are expressed at the beginning of the infection [Bachmann et al., 2016].

1.6 Thesis Objectives

This thesis dissertation is organised in two parts; the first concerns evaluating antigenic variation on a 'short' time scale in a malaria infection. In the second part, we use theoretical models to investigate antigenic variation at a longer time scale which has implications in chronic infections.

- In the first part of this thesis (Chapter 02), we characterise host-pathogen interactions during a Controlled Human Malaria Infection (CHMI). This study was carried out in semi-immune individuals from The Gambia.

  We use data related to both the host (immune responses against *falciparum* antigens) from semi-immune individuals and tried to characterise the dynamics of *var* gene expression and corresponding specific antibody levels against various PfEMP1 domains. The main aims of this project were to estimate the switching rates of *var* genes *in vivo* and comparing them to *in vitro* rates of switching between different groups of *var* genes. By incorporating two deterministic approximations of markov models, we differentiate between different environments for parasite growth. We also contrasted the *var* expression data with infection markers and the corresponding specific immune response dynamics during a single infection. This part of my dissertation work has already been submitted to medarxiv. In this project, I was involved in formal analysis, visualisation and modelling of the data. I also wrote the first draft of the manuscript for this work.

- In the second project (Chapter 03), we adapted a mathematical model of viral antigenic variation to malaria to understand the impact of host immunity on parasite survival in the long term. We study the qualitative behaviour of a mathematical antigenic variation model and establish conditions for peak formation and recurrence analytically. The basic framework used for this model was first used for inferring the dynamics of chronic HIV infections, but with some modified assumptions, it can be adapted to understand malaria infection dynamics as well. We characterise the infection dynamics using a deterministic approach first, beginning with a model with multiple variants present at the start of the infection, we mathematically characterised the

appearance of peaks and formulate necessary conditions. The model includes the variant specific responses and the shared cross-reactive responses separately, and we describe their dynamics both qualitatively and numerically over time. Further, we propose a deterministic ODE model that incorporates switching that we investigate theoretically first, and then study the model numerically using a stochastic implementation using the Gillespie Algorithm to infer the models' short term dynamics. Finally, we study the long-term behaviour of the model using a Random ODE based approach.

CHAPTER 2

CHMI in the Gambia

Diverse *var* gene expression and high turnover facilitate malaria infection.

Inayat Bhardwaj[1,†], Prince B. Nyarko[1,†], Asrar Ba Ashn[1], Camille Cohen[1],
Sukai Ceesay[3], Jane Achan[3], Edgard Dabira[3], Rike Nakajima[5],
Aarti Jain[5], Omid Taghavian[5], Algis Jasinskas[5], Philip L. Felgner[5],
Umberto D'Alessandro[3], Teun Bousema[4], Mark Travassos[2],
Ovidiu Radulescu[1,‡], Antoine Claessens[1,3,4,‡]

[1] LPHI University of Montpellier and CNRS, Montpellier, France,
[2] Malaria Research Program, Center for Vaccine Development and Global Health, University of Maryland School of Medicine, Baltimore, United States of America,
[3]Medical Research Council Unit The Gambia at the London School of Hygiene and Tropical Medicine, Banjul, The Gambia,
[4]Department of Medical Microbiology and Radboud Center for Infectious Diseases, Radboud University Medical Center, Nijmegen, The Netherlands,
[5]Vaccine Research & Development Center, Department of Physiology & Biophysics, School of Medicine, University of California, Irvine, Irvine, California, United States of America.
[†] equal contribution
[‡] corresponding author ovidiu.radulescu@umontpellier.fr, antoine.claessens@umontpellier.fr
June 27, 2024

Abstract

Plasmodium falciparum is believed to escape immunity via antigenic variation, mediated in part by 60 *var* genes. These genes undergo mutually exclusive expression and encode the PfEMP1 surface antigen. The frequency of *var* switching and the immunogenicity of each expressed PfEMP1 remain unclear. To this end, we carried out a Controlled Human Malaria Infection (CHMI) study with 19 adult African volunteers in The Gambia to gain insight into the effect of naturally acquired immunity on the expressed *var* gene repertoire during early phase of an infection. Our findings demonstrated a strong correlation between the diversity of *var* expression, quantified through entropy, and infection outcome. Low-immunity individuals were characterised by high *var* entropy profiles, higher parasitaemia, and lower sero-recognised PfEMP1 domains compared to high-immunity individuals. For the first time we recorded the probability of *var* gene switching *in vitro* and of turnover *in vivo*, enabling us to estimate both intrinsic switching and negative-selection effects. These processes are rapid, resulting in estimated turnover/switching probabilities of 69% - 97% and 7% - 57% per generation, *in vivo* and *in vitro*, respectively. *Var* (PfEMP1) expression triggered time-dependent humoral immune responses in low immunity individuals. Unexpectedly, many PfEMP1 domains did not elicit an antibody response. We conclude that the role of intrinsic *var* switching is to reset and maintain a diverse *var* repertoire. The high *var* switching rates, and possibly weak PfEMP1 immunogenicity, benefit parasite survival during the CHMI.

1 Introduction

While all human-infecting *Plasmodium* species invade, grow and replicate within erythrocytes, *P. falciparum* is distinct in its ability to modify the surface of infected cells.These changes impact erythrocytes' cytoadhesive properties, with late-pigmented trophozoite and schizont stages sequestering within the microvasculature. Sequestration is essential for the avoidance of splenic clearance of late-stage infected red blood cells (iRBC), but can result in microvascular obstruction and the release of pro-inflammatory cytokines, which are key features of malaria pathogenesis [63]. Of the parasite Variant Surface Antigens (VSA), Plasmodium falciparum Erythrocyte Membrane Protein 1 (PfEMP1) is the major ligand binding to human endothelial receptors.

PfEMP1 is encoded by a family of ∼60 *var* genes that undergo mutually exclusive expression; meaning, a single type of *var* gene is expressed at each cycle (with peak transcription at 16 hours post invasion). Each *P. falciparum* isolate typically contains a unique set of 60 *var* sequences, making the worldwide pool of *var* gene sequences virtually infinite [7]. Despite this mind-boggling polymorphism, *var* genes are classified into four main sub-families, named Group A, B, C and E, based on their upstream sequence (Ups) and some conserved motifs [47]. Almost all PfEMP1s have a head structure composed of an N-terminal sequence (NTS), followed by a total of four to nine Duffy binding-like (DBL) and cysteine-rich interdomain region (CIDR) domains, and a semi-conserved intra-cellular acidic terminal sequence (ATS) domain. Crucially, this nomenclature has been repeatedly associated with malaria pathogenesis [65]. In younger children and in cerebral malaria cases, parasites tend to express group A *var* genes; more specifically, PfEMP1s containing a CIDR1α domain that mediates binding the brain endothelial receptor EPCR. Conversely, Group B and group C PfEMP1 are expressed in uncomplicated malaria cases and bind to endothelial cell receptor CD36. The best-characterised PfEMP1 variant expression and infection prognosis is pregnancy-associated malaria, where *var2csa* (group E) binds chondroitin sulfate A (CSA) in the placenta, leading to the sequestration of infected red blood cells in placental blood vessels [37, 62]. Other polymorphic VSA include *rif* (∼180 copies), with a role in dampening anti-malarial immunity [52], and *stevor* (∼30 copies), which are key for iRBC stiffness [39]. Owing to their extracellular exposure, cytoadherent molecules on the surface of infected erythrocytes are also the primary antigenic targets of the immune system, eliciting variant-specific antibody responses. Although anti-RIFIN [22] and anti-STEVOR [40] antibodies have been shown to be functional for promoting immune effector mechanisms, PfEMP1 is thought to be the main target of both total and functional anti-VSA antibodies [12]. Antibodies against group A PfEMP1s are quickly acquired in life and show moderate level of strain-transcending cross-reactivity 21, likely providing protection against the most severe forms of malaria. On the other hand, immunity against Group B and C PfEMP1 takes years, if ever, to develop. Theoretical modeling and experimental data predicts immune acquisition against PfEMP1 variants likely leads to sequential and/or homogeneous *var* expression - a phenomenon postulated to maintain infection chronicity by restricting the number of PfEMP1 variants due to partially cross-reactive and short-lived epitope-specific antibodies [49, 67, 23]. Consequently, in malaria-endemic regions, older children and adults with partially acquired immunity are frequently asymptomatic, i.e. individuals often carry parasite loads without exhibiting symptoms of malaria [35, 19, 13]. *P. falciparum* parasites have thus evolved unique mechanisms of regulating the expression of adhesive surface protein variants to evade the host's adaptive immunity [17, 18]. The proportions of parasites expressing different *var* genes in a population can change through two mechanisms; intrinsic switching and turnover as a result of selection. Intrinsic switching is the probabilistic change of the expressed gene from one intraerythrocytic cycle to the next [63, 54]. *In vivo*, in addition to intrinsic switching, parasites expressing specific PfEMP1 can be recognized and eliminated by the host immune system. Both mechanisms contribute to the turnover rate, describing how frequently the repertoire of expressed *var* genes change. Low switching and turnover rates are thought to promote prolonged infections by preventing the depletion of the entire gene repertoire [14]. However, as discussed in [14], even the lowest *in vitro* rates estimated from [27] are not capable of explaining very long infections such as chronic malaria. Moreover, it is conceivable that rapid, as opposed to slow switching, provides an advantage for parasites, enabling them to evade recognition by the host immune system during the early stages of an infection. Here, we revisit these concepts and perform an investigation of switching under *in vitro* and turnover under *in vivo* conditions using a Controlled Human Malaria Infections (CHMI) study.

CHMI studies in which human volunteers are infected with *P. falciparum* sporozoites or intra-erythrocytic stages, using the NF54/3D7 clone have highlighted the inherent differences in expression of various *var* genes, with group B being predominantly expressed at the early stages of infection, group A to a lesser extent and group C almost entirely absent [4, 3, 38, 26]. Here, we examined *var* gene transcription at multiple timepoints *in vivo* and *in vitro* in a CHMI study carried out with semi-immune individuals in The Gambia, using the NF54/3D7 parasite clone. We measured the intrinsic *var* gene switching rate from *in vitro* culture, while from *in vivo* timepoints we estimated the turnover rate, defined as the result of switching and immune selection. We observed that the breadth of serological responses against 3D7 *var*/PfEMP1 domains affected the pattern of *var* expression at different time points in the CHMI. Exposed individuals with better ability to control infection in endemic regions had a broader breadth of response against 3D7 PfEMP1 domains, and had a distinct *var* expression pattern compared to individuals that were unsuccessful at controlling the infection. Conversely, in non-controller individuals, *var* expression amplified the breadth of response against

3D7 var/PfEMP1 domains, while controllers exhibit a comparatively stable response.

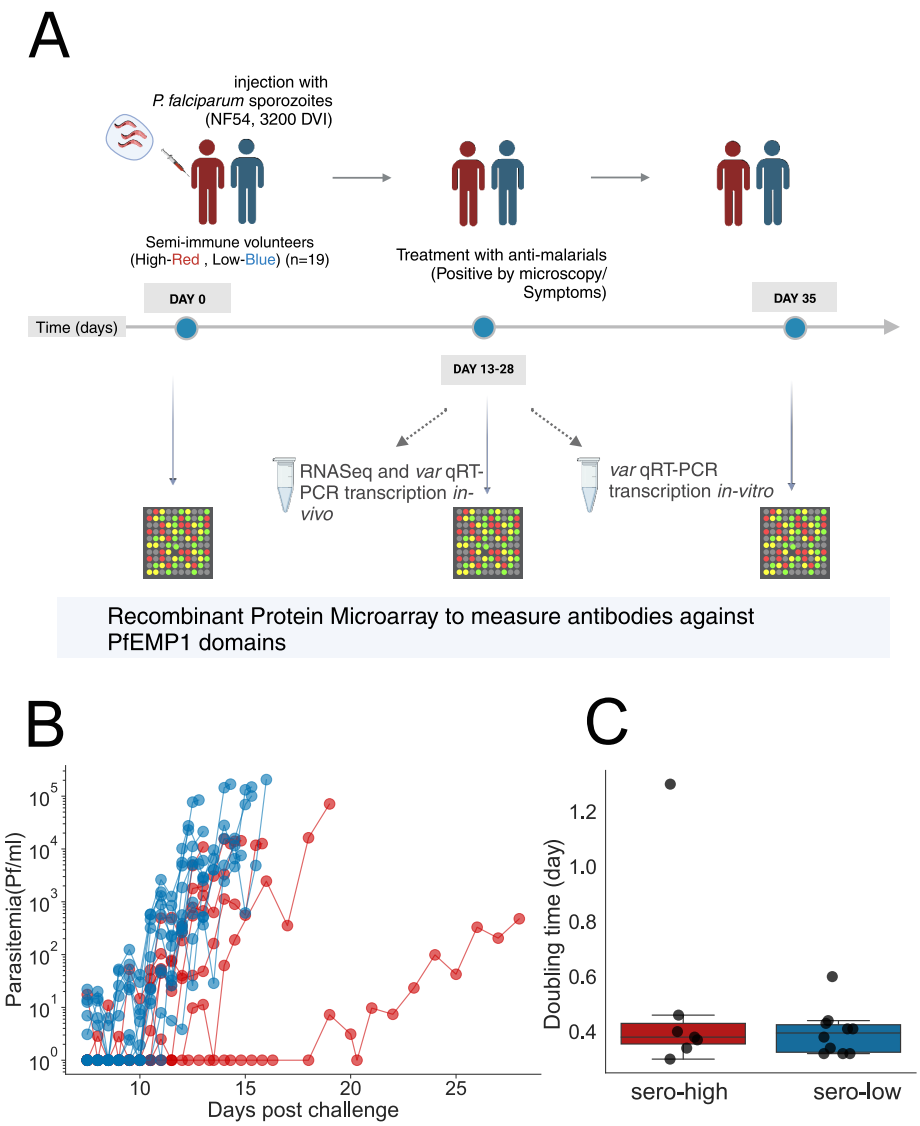

Figure 1: Characteristics of the CHMI for monitoring *var* expression and immune response: A) 19 semi-immune adult males were selected based on their pre-existing antibody levels against six *P. falciparum* antigens and classified as either *sero-high* (red) or *sero-low* (blue) [1]. All volunteers were infected with 3200 sporozoites (NF54/3D7 strain) on the same day and monitored for symptoms of malaria and parasitaemia, *var* gene expression and immune response against PfEMP1 protein domains. Venous blood samples were collected for *var* gene expression at one or two timepoints during the infection; on day 14 post inoculation and day of treatment/termination of study for "long" infections, or only on day of treatment in case an individual was treated before day 14 (short). The immune responses to PfEMP1 and other *P. falciparum* antigens were measured before, during (once or twice, depending on whether the individual was treated before or after day 14) and 2 to 3 weeks after the CHMI. Created with BioRender.com. B) Parasitaemia by qPCR vs days post inoculation, stratified as *sero-high* (red) or *sero-low* (blue). C) Parasite doubling time (time to double the parasitaemia) across the groups of volunteers; classified here as *sero-high* (red) and *sero-low* (blue). DVI - direct venous inoculation.

Volunteer	Immune Response before CHMI	Latency (days)	Entropy	Generation Time (days)	Peak parasitaemia (Pf\ml)
CH001	sero-high	16.00	1.95	1.30	476
CH002	sero-high	10.45	3.00	0.38	1961
CH003	sero-high	9.38	2.64	0.30	5187
CH004	sero-high	11.37	1.60	0.46	10910
CH008	sero-high	9.57	2.89	0.37	12645
CH009	sero-high	9.48	3.58	0.34	14300
CH010	sero-high	7.30	2.64	0.48	15400
CH011	sero-low	9.38	3.30	0.32	21360
CH012	sero-low	10.20	4.00	0.32	22880
CH013	sero-low	6.39	3.85	0.41	27430
CH014	sero-low	6.57	3.50	0.41	27980
CH015	sero-low	6.81	3.40	0.43	71264
CH016	sero-low	6.40	3.85	0.44	84475
CH017	sero-low	9.21	4.06	0.34	100595
CH018	sero-low	5.61	3.22	0.60	148950
CH019	sero-low	8.94	3.69	0.38	168700
CH020	sero-low	8.69	4.01	0.32	205850

Table 1: Parasitaemia characteristics for CHMI volunteers: Different parameters stratified by volunteer immune status before the start of the infection (*sero-low* or *sero-high*). The relationships between these parameters are highlighted in Figure 1. The latency period is defined as number of days until there is detectable parasitaemia. The generation time is the average time taken to double the parasite density. One sero-high individual (CH006) remained negative for the infection throughout the study, while another one (CH007) never reached a parasitaemia sufficient for transcriptome analysis.

2 Results

2.1 Pre-existing immunity determines infection outcome

As previously described, 19 semi-immune adult males living in The Gambia were selected for their antibody levels against six *P. falciparum* antigens and classified as *sero-high* or *sero-low* [1]. All volunteers were inoculated with sporozoites (NF54/3D7 strain) by direct venous inoculation (DVI) and treated with anti-malarials once parasitaemia was detectable by microscopy or at the onset of symptoms. The infection outcome differed significantly in the two groups. *Sero-low* individuals had more symptoms (mean = 4.10, sd = 2.07) than *sero-high* individuals (mean = 5, std = 0.48) with symptoms occurring in both categories approximately 4-5 days after being positive for parasitaemia by PCR [1]. The peak parasitaemia before treatment in individuals classified as *sero-low* was significantly higher than the *sero-high* individuals (Mann Whitney U-Test; p = 0.01). In addition to the parasitaemia peak and clinical symptoms, we also compared the parasite growth rates across volunteers and the pre-patent period (Figure 1, Table 1), defined here as latency. Only two individuals had a long latency period (CH004 = 11 days, CH001 = 16 days), with one of them having an exponential rise in parasite growth rate post latency (CH004). The peak parasitaemia was lowest in the individual with highest latency period and lowest parasite growth rate (CH001). As in [3], we further used the differences in growth rate to classify the individuals as non-controllers (n=17) and controllers (n=2). The "Controllers" were defined as individuals with the longest latency and smallest parasite multiplication rate. Both individuals classified as controllers (CH001 and CH004) were *sero-high* (Figure 1 and Table 1).

2.2 VSAs are the main differentially expressed genes between sero-high and sero-low individuals:

To understand how identical parasites adapt to different hosts, we performed a low input, whole transcriptome analysis of parasites recovered from ten volunteers on the day of treatment. Gene expression and subsequent differential expression analyses are highly influenced by the age and developmental stage of parasites [59]. Thus, we first estimated parasite ages from sequencing reads by calculating the maximum likelihood estimate against data from an *in vitro* time-course experiment [33]. Parasites were $\sim$ 7.6 hours post invasion (hpi) (95% CI; 6.67 – 9.35) (Figure S1 A & Supplementary file S1), with no significant disparity between the ages of *sero-low* and *sero-high* parasites (p=0.28; Student t-test) (Figure S1 B).

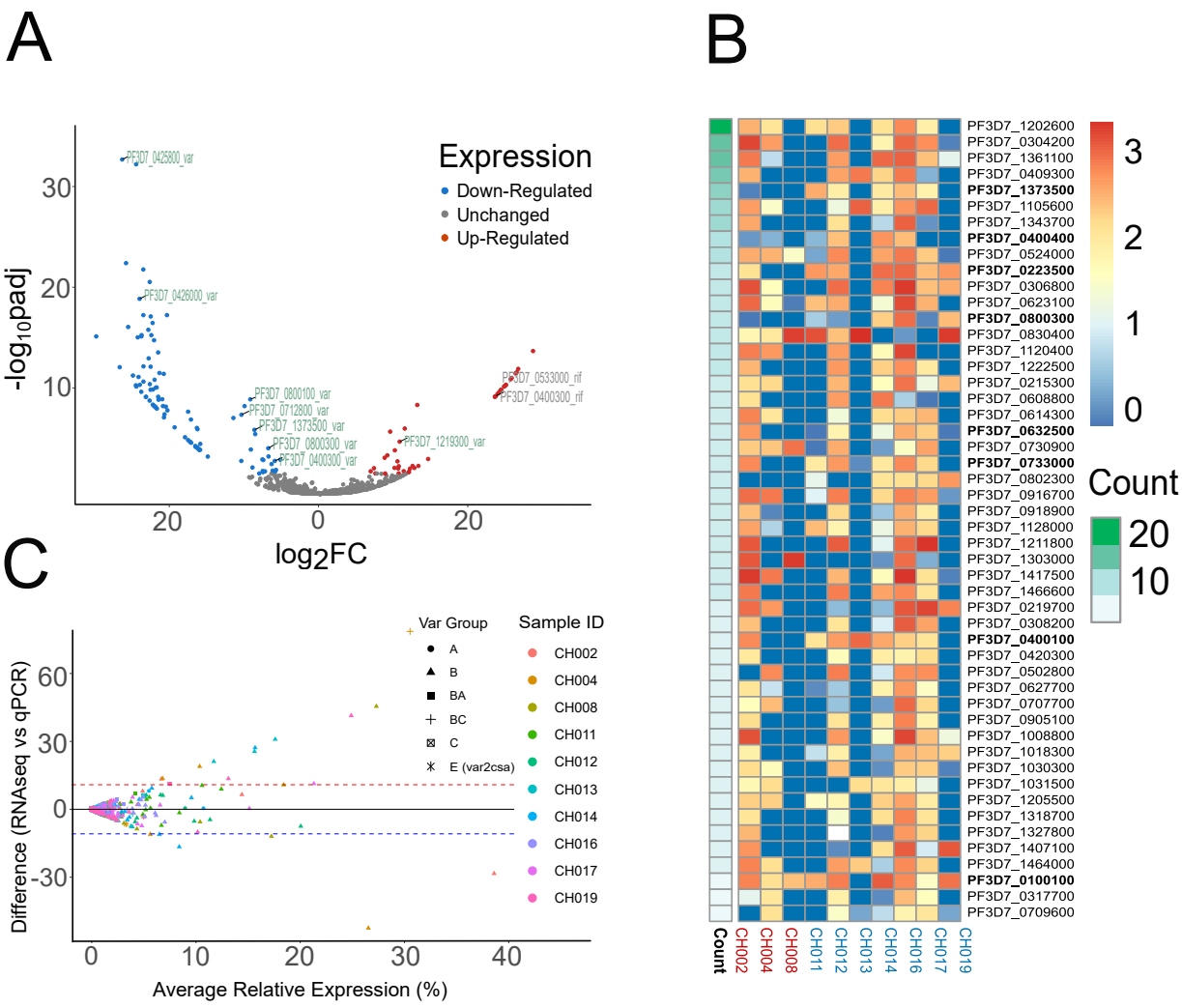

Figure 2: Whole transcriptome expression analysis: A) Differential expression analysis between sero-high and sero-low volunteers. Blue and red represent down and up-regulated genes, respectively. VSAs (*var* and *rif*) are labeled with gene IDs. B) Heat map of the log2 FPKM of the top 50 differentially expressed genes in a pairwise comparison. *Var* genes are in bold. Scale bar represent log2 fold change values. C) Bland-Altman plot of *var* expression by RT-qPCR and RNA sequencing.

Applying a log2 fold change of > 2 (more than 4 fold difference) and Benjamini-Hochberg adjusted p value < 0.01 as cuttoff, 144 *P. falciparum* genes were differentially expressed, of which 103 were down-regulated and 41 up-regulated in *sero-high* compared to *sero-low*. Among these, genes coding for proteins with cell-cell

adhesion predicted function were the most prominent, including 8 *var* genes (Figure 2 A, Supplementary file S2). Due to the nature of clonally variant gene transcription, a pooled analysis might not effectively capture VSAs expressed in a limited number of isolates. Consequently, we undertook pairwise comparisons of all isolates to detect genes displaying differential expression among individuals (Supplementary file S3). Genes were then ranked based on their frequency of appearance in these pairwise comparisons. Remarkably, the top 50 most differentially expressed genes exhibited a notable enrichment of *var* (8 out of the 61 *var* genes were present in the top 50) (Figure 2B). These observations indicated that the most variably expressed genes among individual volunteers were members of the *var* family. Other Variant Surface Antigens (VSAs) including *stevor* (∼30 members) and *rifin* (∼180 members), were poorly detected (Figure S2), likely due to their transcription peaking later in the intra-erythrocytic life cycle [31, 43, 68, 45]. The exception was the *rifin* PF3D7_0401600, which was detected in almost all samples (Supplementary Figure S2B, Supplementary file S4), and was also the major expressed *rifin* in a CHMI study with naive volunteers [38]. In contrast, *var* genes were robustly detected in all samples. To validate the accuracy of our *var* gene observations, we measured *var* expression in each volunteer by RT-qPCR and compared outcomes of both methods. A Bland-Altman plot comprising 610 observations (61 *var* genes in 10 volunteers) showed high c oncordance, with only 15 observations falling outside the 95% confidence interval (Figure 2C). Based on these observations, we focused our attention on *var* gene expression within hosts of varying immunity and the corresponding humoral immune responses.

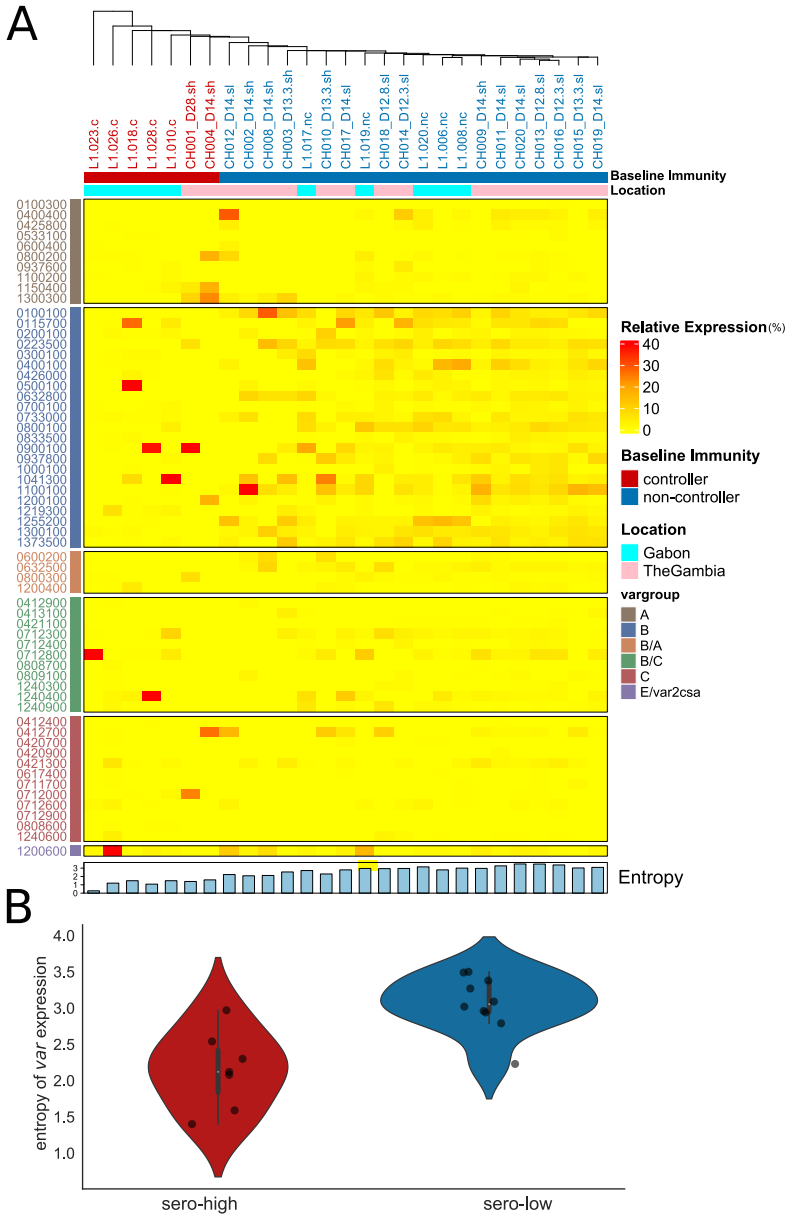

Figure 3: *Var* expression landscape across two CHMIs. A) A heatmap of *var* gene relative expression proportion at the first time point when expression data was available for an individual ; includes data from the current CHMI and from Gabon (at the day of peak infection). The relative expression of each gene is scaled with the total amount of *var* expression, quantified by RT-qPCR and ranges from low to high (0-40%) . The bottom of the heatmap is annotated by the entropy of expression, representing the amount and diversity of *var* genes in each sample. Top annotation is based on immunity and geographical region of origin. All volunteers across different timepoints were hierarchically clustered using an average-linkage method. Distinct clusters formed based on immunity, but not necessarily location. Non-controllers (blue) developed symptoms and patent parasitaemia faster than controllers (red) and expressed a high diversity of *var* genes during the CHMI, independent of the geographical region of origin of the volunteers. B) Entropy of *var* expression: violin plots for the Shannon diversity index of *var* expression across the two categories of volunteers (*sero-high*; red & *sero-low*; blue) whenever the expression data was first available in each volunteer . In the Gambian cohort, the expression entropy was lowest for the two controllers: CH001 and CH004.

2.3 *Var* gene expression pattern is shaped by host-immunity:

To assess the impact of selection due to pre-existing immunity on *var* expression repertoire, *var* gene expression was analysed in all individuals by RT-qPCR. This was either done at day 14 post-inoculation and/or on the day of treatment. Comparison of total *var* quantity from RT-qPCR data showed higher *var* transcript levels in *sero-low* individuals (Mann-Whitney U-test, p-value <0.001). Hierarchically clustering of pooled volunteers from the current study and a previous one in Gabon [3], based on their *var* expression patterns alone showed distinct separation of controllers (CH001 & CH004 from The Gambian CHMI and L1.023, L1.26, L1.010, L.018, L1.028 from the CHMI in Gabon [3]) from *non-controllers* (Figure 3A). To estimate *var* gene heterogeneity, we compared the diversity of *var* repertoires across *sero-high* and *sero-low* groups by computing the Shannon entropy, a measure encompassing both diversity and relative abundance. Significantly higher entropies were observed for *sero-low* individuals (Mann-Whitney U-Statistic, p-value = 0.0002); indicating a larger breadth of *var* expression, in contrast to *sero-high* isolates that exhibited a more restricted repertoire of transcribed *var* genes (Figure 3B). This difference in diversity was also negatively associated with other markers of infection progression including latency (Spearmann Rank Correlation, r = -0.55, p = 0.02) and parasite doubling time (Spearmann Rank Correlation, r= -0.53, p =0.02).
In summary, the distinct (restricted) *var* gene expression pattern in *controllers* could be a proxy for a slow growing *P. falciparum* infection, possibly resulting from selection against specific PfEMP1s.

2.4 *In vitro var* gene switching sustains a steady state with elevated entropy

We aimed to estimate the intrinsic *var* gene switching rate *in vitro*, in the absence of immune selection. Out of the original pool of volunteers (n=19), ten blood isolates drawn from seven volunteers were cultured *in vitro* for 50 to 100 daysseveral cycles to investigate the impact of a lack of host-immunity on *var* expression patterns. Five isolates (CH001-D28, CH002-D14 CH002-D15.8 CH004-D14 & CH004-D20.3) belonged to the *sero-high*, while five isolates (CH012-D14, CH012-D16.3, CH014-D12.3, CH016-D12.3 & CH020-D14)[1] were from the *sero-low* category. For each isolate in culture, we analysed *var* transcription profiles by RT-qPCR at 3 to 8 time points for up to 100 days (Figure S3). Isolates derived from sero-low individuals all converged to near-identical *var* gene expression pattern within 20 days in culture, with all Pearson correlation values above 0.80 (Figure S4). In contrast, sero-high isolates did not demonstrate any uniform expression pattern even after 50 days of culture, with Pearson values ranging from 0.20 to 0.95.

To rigorously assess the hypothesis that the host immunity level may have a lasting impact on *var* gene expression *in vitro*, we integrated data analysis with mathematical modeling.

First, the multi-dimensional traces from the ten timeseries were projected onto a 3D space using PCA. We divided the time points in three categories: early (0-6 days), intermediate (20 $\leq$ 50 days), and late (50-100 days). The projected point clouds from different categories show that the *var* gene global dynamics is quantitatively different for samples from *sero-low* and *sero-high* volunteers (Figure 4). For samples derived from *sero-low* volunteers, *var* gene transcription profiles are more spread at early time points than late time points (Figure 4A), shown quantitatively by using the convex hull of the PCA projected points (Figure 4C). This suggests that after a fast transient phase, the *var* gene transcription profile reaches a steady state; an observation which is similar for all isolates. This can also be seen in Figure 4E where the transcription profiles of all late timepoint samples are compared without projection. *Sero-high* volunteer samples showed a different trend: the variability of the transcription programs starts from smaller values, but not all samples reached a steady state (the final variability is not close to zero) (Figure 4B,D,F). The similarity of the late time *var* gene expression profiles in different samples was also tested to be higher for *Sero-low* compared to *Sero-high* volunteer samples by using an AUC criterion (Figure S5). Nevertheless, when utilizing entropy as a metric to assess the diversity of *var* gene expression within a particular profile, we observed that all samples exhibited a consistent trend of monotonic entropy increase with the highest entropy being reached in the steady state (Figure 4I). Moreover, the primary distinction between *sero-low* and *sero-high* samples appears to be the initial transcription profile, which exhibits higher entropy in the former as opposed to the latter.

[1] the first and second part of the sample symbol indicates the volunteer and the the day after infection when the isolate was drawn, respectively

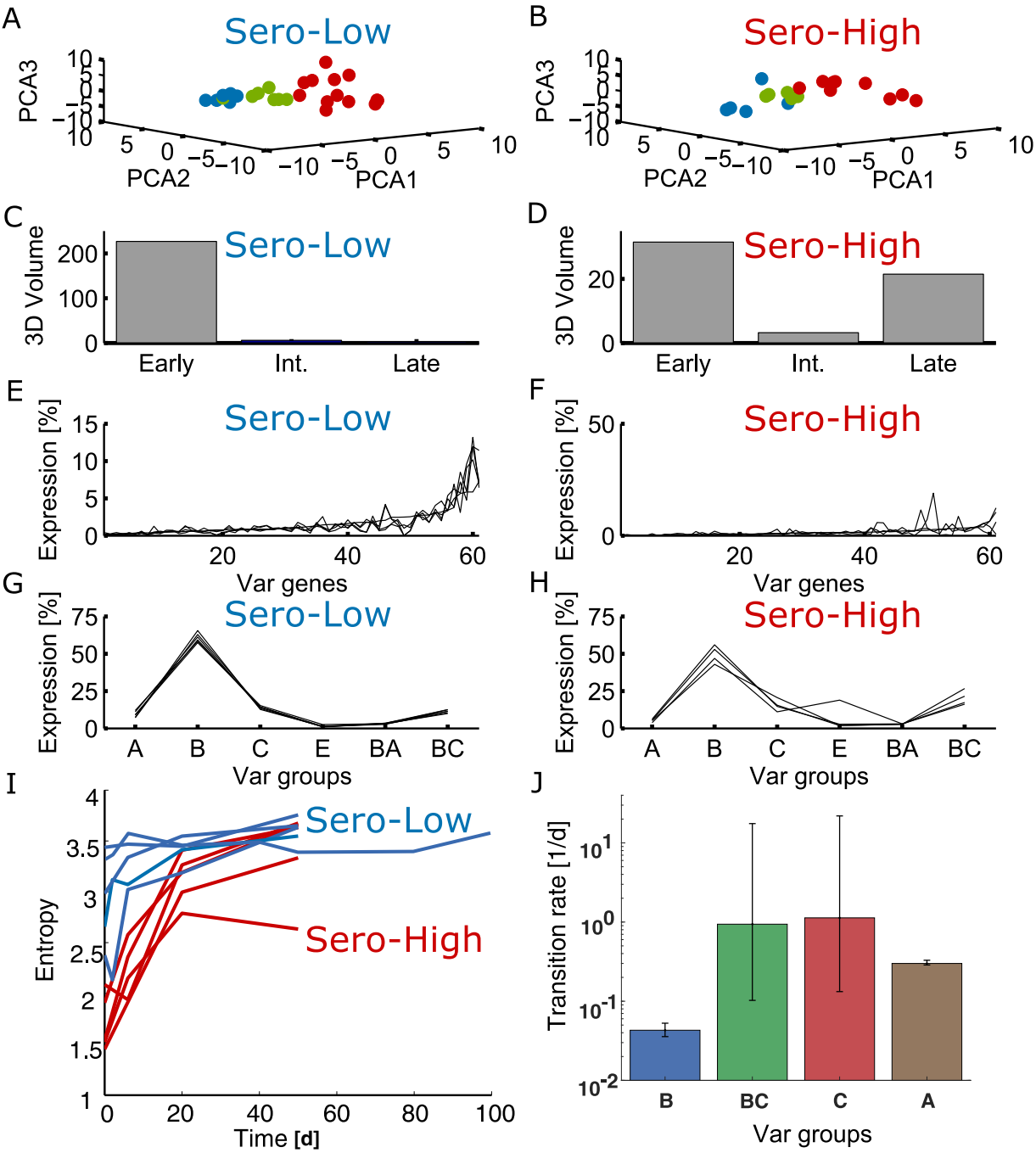

Figure 4: *In vitro* dynamics of *var* gene transcription from 10 isolates by RT-qPCR . A,B) distribution of early (0 to 6 days, red), intermediate (20<50 days, green) and late (50 to 100 days, blue) time samples projected on the 3 first PCA components (36.45 % of the total variance) . C,D) volume of the convex hull of the samples projected on the same 3D space was used as a proxy for the variability of the *var* transcription programs. E,F) probabilities of expression of different *var* genes for all late time samples. G,H) probabilities of expression of different groups of *var* genes for all late time samples. I) *in vitro* evolution of *var* gene expression entropy. J) estimated *in vitro* switching rates. The error bars are uncertainty intervals obtained using the multiple random start points method with an overflow factor $f = 1.2$ (see Methods).

Secondly, we performed a more accurate analysis of the *var* gene transcription dynamics using a mathematical model. In the absence of host immunity, the *in vitro* dynamics is not influenced by selection, but results only from intrinsic switching of the *var* gene system. Under this hypothesis, the *var* gene dynamics can be modelled as a continuous time, four-state Markov chain (see Methods and Materials). The four-states Markov chain model fits well to the data of all the samples (Figure S7). As observed in the first analysis of the data, the theoretical steady state of the inferred Markov chain has high entropy, where many *var* genes are significantly expressed. *Sero-high* samples require more time to reach steady state due to distinct initial data compared to the steady state, while *sero-low* samples have initial states with higher entropy closer to the steady state. The fitted values of the transition rates are represented in the Figure S6. The C and BC switching rates are similar to turnover transition rates *in vivo*, while those for A and B are much smaller than the respective *in vivo* rates (Figure 4J). Altogether, our data indicate that immune selection within sero-high individuals may still impact the *var* gene transcription profile *in vitro* after 25 generations.

2.5 Very high *In vivo var* gene renewal rates *in vivo*

To evaluate *var* transcript profile changes *in vivo*, we compared the expression levels in individuals with two available timepoints, ranging from day 14 to day 20. We then computed the theoretical limits of probability to stop expressing a certain gene, given its expression at the first time point (the turnover probability of that gene). As expected, the turnover probability increased with time between day 14 post-infection and the day of peak infection (Figure 5 A). For the individual with the highest time gap between two time points (CH004), all genes expressed on day 14 were undetectable after three life cycles (6 days).

We further computed the instantaneous transition rates per unit time (days^{-1}) during the CHMI, defined as turnover probability per unit time. On comparing the *var* transition rates per day across different *var* groups, groups A, C and E (*var2csa*) had the highest transition rates. (Figure 5 B). The median transition rates were higher than 1 per day in all three groups, which correspond to transition probabilities higher than 86% per cycle. These high *in vivo* transition rates may arise from a combination of the inherent switching rate and the potential selection pressure acting against parasites that express particular PfEMP1 variants.

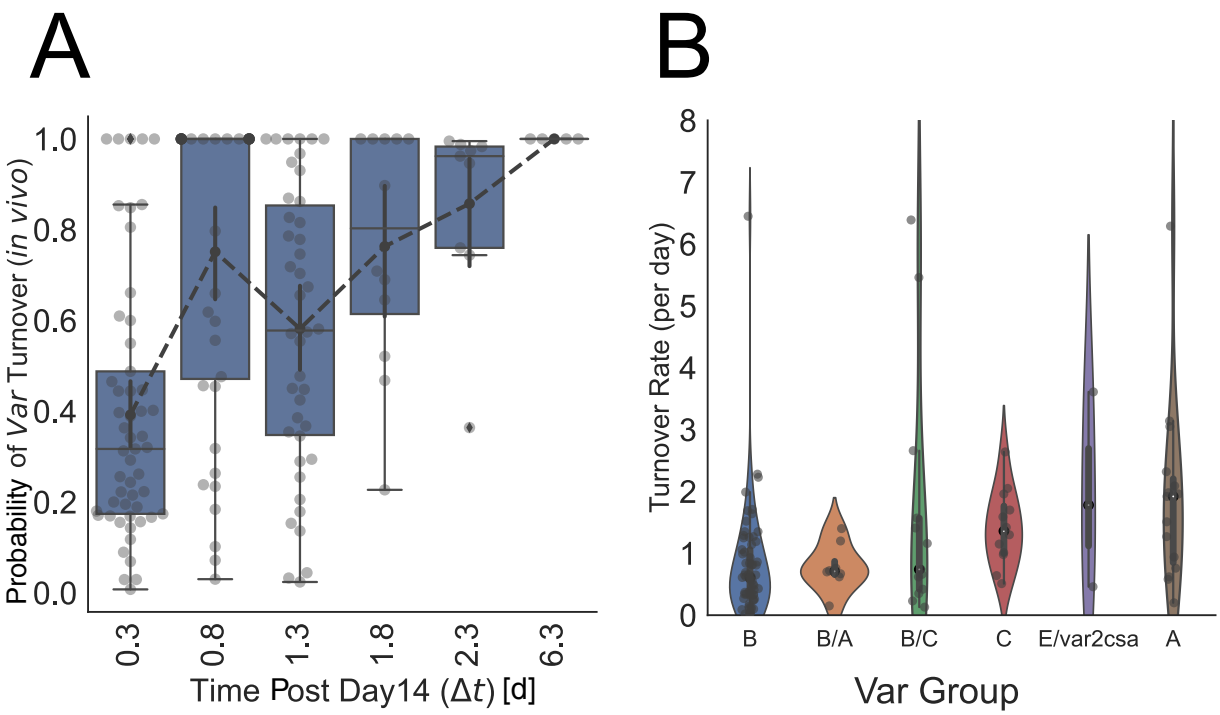

Figure 5: Quantifying change in *var* expression during an infection: A) Finite time turnover probability comparison across different durations indicated that genes expressed at day 14 were no longer detectable by the end of the infection in most volunteers. Each dot is the probability of turnover for a *var* gene in one individual. The lower bounds for turnover probability for each *var* gene in each volunteer are pooled based on the interval between day 14 and treatment time point. This turnover probability is ordered between day 14 and day 20 post-infection. The median of the turnover probability is highest on day 20 (black dashed line). B) The instantaneous turnover rates were calculated for each gene at each time point. The turnover rates for various genes are shown per group pooled by volunteers and time points, ordered by the medians of lower bounds on the turnover rate , in increasing order from left to right. Based on our data, group A *var* genes had the higher turnover rates ~ 1.78 per day as compared to 0.59 per day for group B *var* genes.

2.6 Immune responses against VSAs differ significantly between sero-high and sero-low individuals:

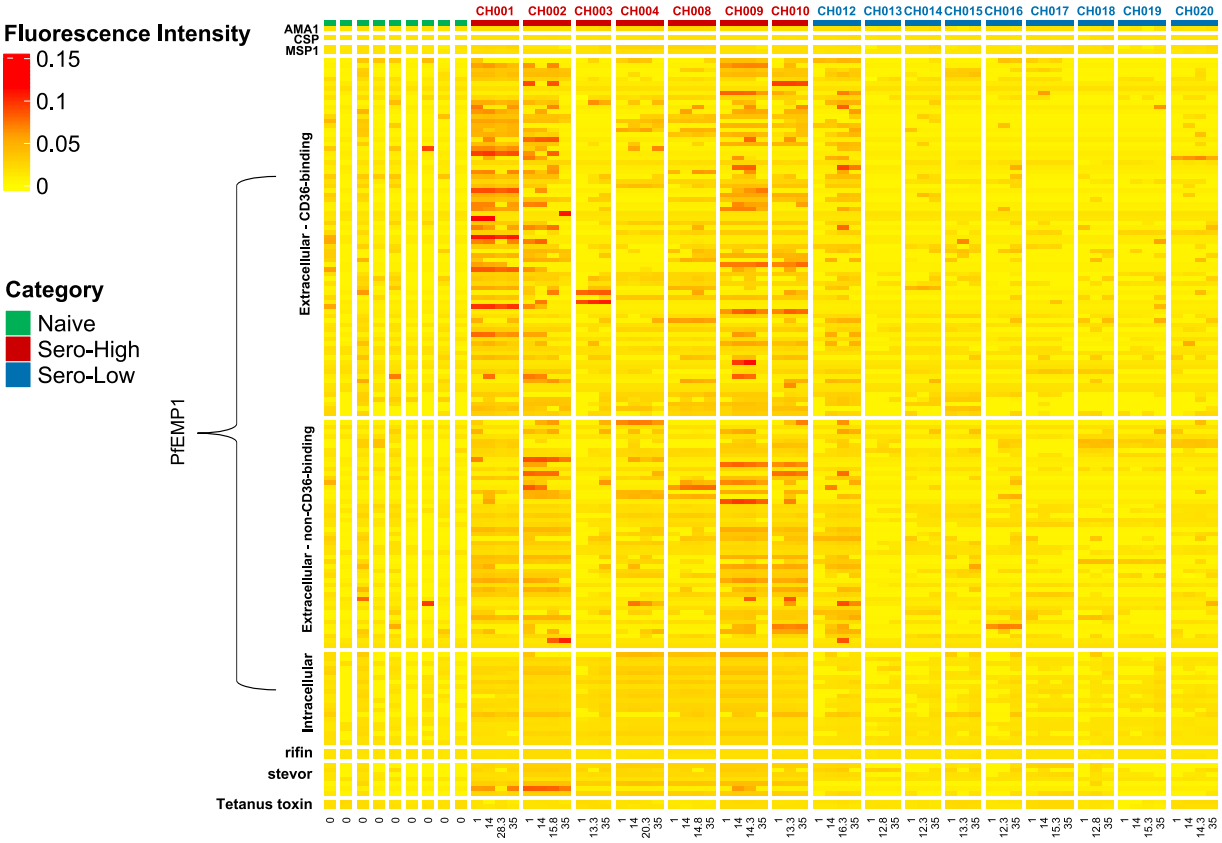

Figure 6: Serorecognition of domains from 3D7 antigens and tetanus across all volunteers. Each column is a time point for a particular volunteer during the infection (top annotation). The *sero-high* and *sero-low* individuals have been annotated in red and blue, respectively. The malaria naive individuals are grouped on the left (labelled and annotated in green). Each row corresponds to a 3D7 domain, grouped based on the host receptors they bind to [**?**] . The fluorescence intensity is scaled for each domain in increasing order (from yellow to red).

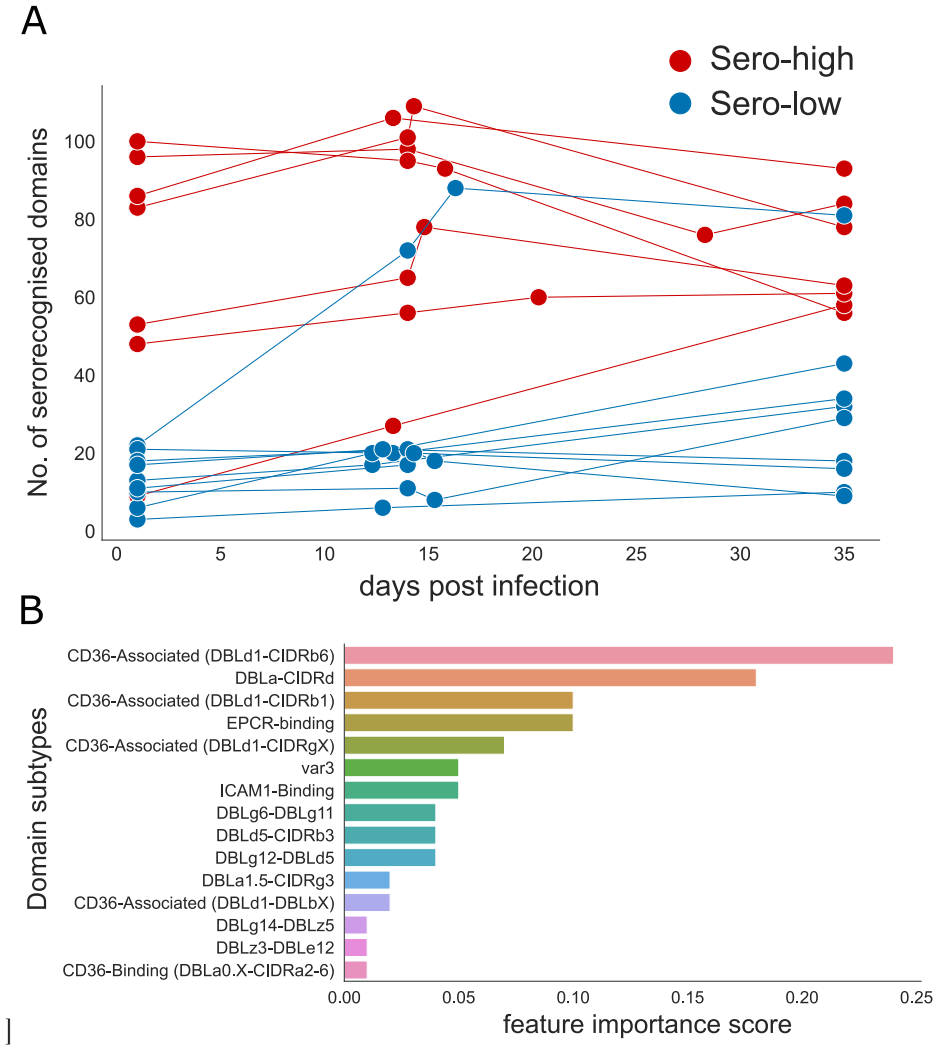

Figure 7: Significant increase of serorecognised 3D7 PfEMP1 domains post-CHMI in *sero-low* individuals. A) Sero-positivity throughout time in CHMI participants (top panel): The scatterplot showing the number of extracellular 3D7 PfEMP1 domains that were sero-recognized at different timepoints during the CHMI across the two groups, *sero-high* (red) and *sero-low* (blue). For each volunteer, the treatment timepoint is considered the peak of infection. B) Relative feature importance score to predict infection outcome: Bar-plot of the relative contribution of each domain sub-type to classify individuals into 'sero-high' and 'sero-low' categories throughout the CHMI calculated using a random-forest classifier.

We evaluated the antibody levels against different antigenic domains corresponding to PfEMP1s and other antigens by exploiting recombinant protein microarray data. Serological responses to a total of 213 *falciparum* PfEMP1 domains (159 from 3D7, 54 from three other strains) and 18 other recombinant antigenic proteins (MSP1, CSP, AMA1, RIFIN and STEVOR) were analysed for each volunteer at several timepoints: before the injection (day 0), during the infection (range: day 13-28) and about 2-3 weeks after treatment (day 35) (Figure 6). At day 0, antibodies against non-PfEMP1 surface antigens were associated with the latency period (AMA1: r= 0.80, $p < 0.01$ & MSP1: r = 0.48, $p < 0.01$ and the peak parasitaemia (AMA1: r= -0.80 , $p < 0.01$, MSP1: r= -0.59,$p < 0.01$) using Spearmann Rank Correlation. These results confirmed previous data from the same CHMI study [1]. We also found that the boost in antibody responses to non-3D7 PfEMP1 domains was correlated with boost in domains associated with 3D7 PfEMP1 domains, (Spearman Correlation >0.9, p-value <0.01), suggesting cross-reactivity across different *falciparum* strains. Anti-CSP antibodies were associated with Latency (r = 0.52, p = 0.03) but not Peak-parasitaemia before treatment

(r = -0.27,p =0.3). Moreover, based on the breadth of response at the beginning of the CHMI, *sero-high* individuals had sero-recognition of a significantly higher number of 3D7 PfEMP1 domains in comparison to *sero-low* individuals before (Mann-Whitney U-Test, $p < 0.01$) and after the infection (Mann-Whitney U-Test, $p < 0.01$) (Figure 7 A). When examining the change in the number of recognized domains before and after the CHMI study, no significant induced response was observed in the *sero-high* group (Mann-Whitney U-Test, $p < 0.01$) (Figure 7A). This is in sharp contrast with the breadth of antibody levels in sero-low individuals, that more than doubled after the infection (mean number of recognized domains pre-infection $\sim$11, $\pm$6; post-infection $\sim$28, $\pm$12, Mann-Whitney U-Test= 17.0, $p < 0.01$). Additionally, we employed a random forest model to predict the subgroup to which the volunteers were linked using microarray data related to PfEMP1 domain responses. Using this model, the subgroups were re-confirmed with a predictive accuracy of 98% (Figure 7B). Feature scores of the model revealed that the most important domains for predicting infection outcome were either DBL-CIDR di-domains, ATS domains or CIDRα-binding domains, with CIDRα-binding domains being the sub-domains that are linked to severe symptoms of *falciparum* infection. The sero-recognition breadth within each individual was negatively correlated with infection markers *in vivo*, i.e. latency (Spearmann Correlation: 0.67,$p < 0.01$) and the peak parasitaemia (Spearmann Correlation: -0.68,$p < 0.01$) (Figure S8). In sero-low individuals, no correlation was found between increase in number of sero-recognized domains and infection characteristics including PMR, latency and peak parasitaemia , indicating that the gain in new antibodies was not sufficient in controlling the infection.

2.7 *Var* expression is moderately associated with pre-existing specific immune response:

To investigate the interplay between pre-existing specific immune responses and PfEMP1 expression, we examined our primary hypothesis that the presence of antibodies targeting specific PfEMP1 domains would impose a selective pressure against infected red blood cells (iRBCs) expressing the corresponding *var* gene during the asexual blood stage. Overall, we observed a moderate association between the breadth of PfEMP1 domain recognition prior to challenge and the Shannon entropy of *var* gene expression during CHMI (day 12-20) (Spearman Rank Correlation = -0.52, $p < 0.05$). This suggests that the diversity of *var* gene expression may be constrained by the breadth of immune responses directed against PfEMP1 domains.

To make inter-PfEMP1 responses throughout the CHMI comparable, we used a discretized method to evaluate both the fluoroscence intensity values for antibody levels per domain and the expression levels of the *var* transcripts (described in Methods and Materials) based on quantiles per domain (for immune response data) and per gene (expression data). On comparing the intensity of recognition at the start of infection to *var* gene expression, we observed a moderate association during the CHMI (Figure 8). This relationship was strongest for *var* groups 'B\C','A' and 'B', indicating that some PfEMP1 expression could have been inhibited by existing specific immune response. However the antibody intensity against PfEMP1s corresponding to the intermediate group 'B/A' and 'var2csa' was not significantly associated with reduction in expression during the CHMI.

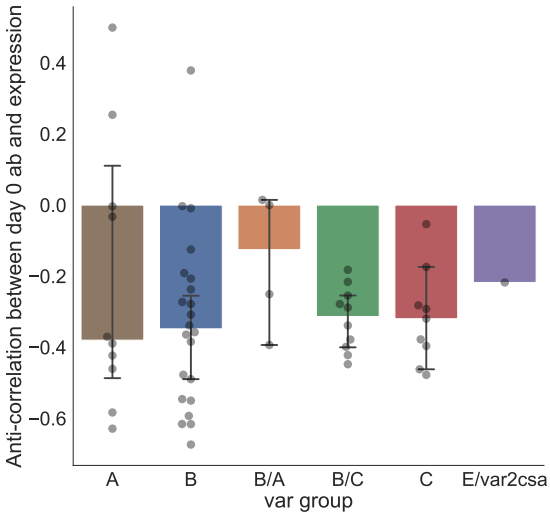

Figure 8: Anti-correlation between pre-existing PfEMP1 antibodies on day 0 and *var* expression during the CHMI: The correlation between existing antibody levels at day 0 and the *var* expression during the infection was calculated across all volunteers for each PfEMP1. Each bar represents the median of the anti-correlation for a group and each point corresponds to a PfEMP1. A PfEMP1 was considered sero-recognised in an individual if at least one of its domains showed antibody signal on the array. For quantifying *var* expression, we used the average expression for each *var* gene if data from two time points was available for a volunteer.

2.8 The increase in antibody levels is not necessarily dependent on the intensity of PfEMP1 expression during the CHMI.

In order to examine the hypothesis that the overall intensity of PfEMP1, specifically the quantity of PfEMP1 expressed at a particular time point within an individual, initiates antibody production, we contrasted the discrete intensity levels at which various *var* genes were expressed during CHMI with the quantity of antibodies acquired against the corresponding PfEMP1. On evaluating the correlation between these two variables, we observed no evident of association in antibody development towards genes expressed at high intensity when compared group-wise for all *var* groups (Figure 9). These results indicate that the gain in antibody levels is not necessarily dependent on the intensity with which a particular gene was expressed during the infection. The possibility of a protein array artefact is low, as, overall, percent of all 3D7 PfEMP1 domains subsequently used for analyses were serorecognised at least once by a plasma sample, validating these recombinant domains as antigens. In summary, our data open up the hypothesis that some PFEMP1s do not necessarily elicit an antibody response.

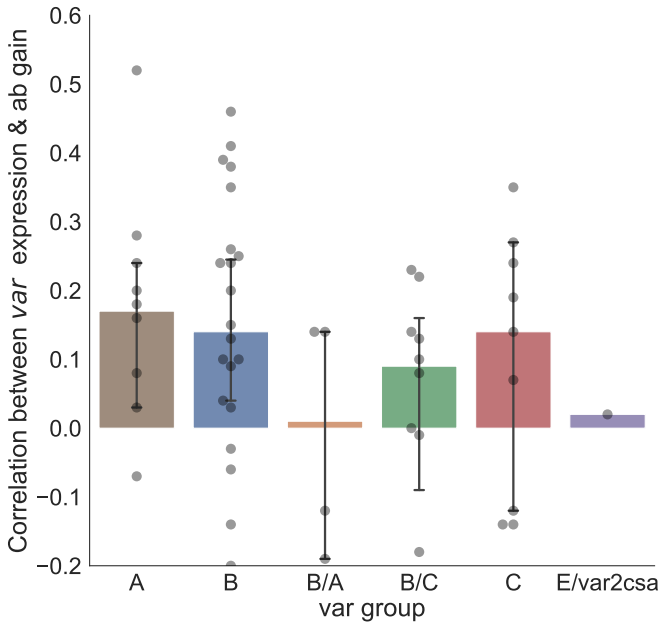

Figure 9: Correlation between expression intensity of PfEMP1s and antibody acquisition at day 35: For each PfEMP1 for which antibody data as well as corresponding *var* gene expression data was available, we calculated the change in antibody levels between the day of the treatment and day 35 of the CHMI and contrasted it against the *var* expression levels across all volunteers. In case two time points were available, the average was used to calculate the expression. The plot shows the correlation for each *var* across all individuals.

3 Discussion

Controlled Human Malaria Infection (CHMI) studies are useful not only for evaluating drug efficacy and vaccine development but also for understanding pathogenesis of *Plasmodium* within the human host and its interactions with the immune system in real time [55]. Leveraging clinical and experimental data from CHMI studies, our aim was to document the heterogeneity in host responses and compare infection characteristics that transcend different geographical regions.

Individuals selected for their previous malarial exposure showed diverse infection outcome and *var* expression heterogeneity, consistent with previous findings in Gabon [3]. In our study, the whole transcriptome sequencing approach underscores *var* genes as the primary cause of transcriptome heterogeneity among isolates. Despite the geographical distance between Gabon and The Gambia, there is a consistent *var* gene expression pattern linked to pre-existing immunity against malaria. The observed similarity suggested an immune response that selectively targeted certain PfEMP1 variants in individuals classified as "controllers". These individuals, characterized by low entropy profiles featuring limited expressed genes, exhibited longer latency periods, lower parasitaemia levels before treatment, and demonstrated recognition of a wide array of PfEMP1 domains prior to the infection challenge. On the other hand, individuals classified as "non-controllers", who had high entropy profiles and a wide range of expressed genes, showed elevated parasitaemia levels, shorter infection delays, and limited recognition of PfEMP1 domains. This is reminiscent of the rodent malaria model, in which *P. chabaudi* parasites express a very limited number of *pir* genes in chronic infections [10]. Antigenic variation, encompassing intrinsic switching of the PfEMP1 proteins that a parasite displays at the red blood cell surface, is regarded as a prominent survival strategy employed by *P. falciparum* during its blood cycle. This process has been extensively studied *in vitro* [27, 48, 70]. Nevertheless,

antigenic variation is also contingent on the host-pathogen interaction, triggered both by intrinsic switching and by elimination of variants through the immune system's negative selection process. Negative-selection eliminates variants and is therefore detrimental to the parasite survival, whereas intrinsic switching replaces one variant with another and maintains the expression diversity of the antigens. Here, from 9 volunteers, two blood isolate timepoints were available, providing a rare opportunity to quantify the turnover rates of *var* genes *in vivo*. Turnover probabilities rapidly increased over time. For instance, in the volunteer that was able to control the infection until the end of the CHMI without turning symptomatic, we found that the initial repertoire of *var* genes had completely changed after three cycles (between day 14 and 20). Given the short interval between timepoints, this shows that the *var* turnover during an infection is much higher than reported previously [42, 20]. Our mathematical estimates based on a Markov chain model lead to turnover probability estimates with group averages between 69% and 97% per generation (corresponding to instantaneous rates from 0.59 to 1.78 per day, see Figure 5B), likely as a result of a combination of intrinsic switching and immune selection. Additionally, group A *var* had the highest rates of transition *in vivo*, a phenomena previously observed *in vitro* [43].

To get an accurate estimate of switching events and rates in the absence of immunity, we modelled the *var* transcripts coming from the CHMI volunteers *in vitro* for several cycles in culture. In our study setting, although smaller than *in vivo* values, intrinsic switching rates were found higher than reported elsewhere [51, 27]. *In vitro* transition (switching) probabilities for *var* genes B and A (7% and 44% per generation, respectively) are over two-fold lower than *in vivo* turnover, whereas the *in vitro* values for var C and BC (57% and 49% per generation, respectively) are close to *in vivo* values. These large, per group values, do not exclude that some rarely transcribed *var* genes have low transition rates, even within fast groups. Furthermore, *var* expression profiles evolved *in vitro* towards a steady-state distribution marked by a significant increase in entropy and many expressed *var* genes. The steady state distribution in both sub-groups comprised as major constituents *var* groups B and C, that is compatible with previous findings 43. In the sero-low groups, the parasite populations reached the corresponding steady state relatively quickly, within fewer than 10 cycles. Remarkably, for sero-high individuals, the parasite cultures took longer to converge to the steady state, with some samples retaining memory of the initial state even after 50 days in culture. We therefore hypothesize that epigenetic imprinting on parasite populations from hosts with robust immune responses led to a *var* gene repertoire significantly divergent from the *in vitro* steady state. However, given that the switching rates were found to be similar, the disparities in time to reach a steady state can be primarily attributed to differences in the expression profiles between the two groups at the peak of infection.

We propose that in all sero-low individuals expressing multiple *var* genes, the *in vivo var* distribution closely mirrors the *in vitro* steady state. This is consistent with the hypothesis that *var* gene expression is reset during mosquito and/or hepatic stage passage [4]. We also hypothesize that a similar state is initially present but is rapidly lost through negative selection in sero-high individuals. This state is reached by parasite intrinsic *var* gene switching as part of a "bet-hedging" strategy in a hostile environment. In all individuals, the observed distribution at later *in vivo* time points evolve to a less diverse repertoire through negative selection. Several studies highlight that the initial probabilities of expression of different variants at the onset of blood stage infection are consistent across multiple CHMI studies with limited stochasticity between individuals [4, 26]. : Similarly, broad group B *var* expression was observed in a CHMI study with the 7G8 clone, although in this instance, a group C *var* was the most dominantly expressed in all volunteers [69][45, 69]. The *in-vivo* reduction in diversity of repertoires is much stronger and more rapid in sero-high individuals that are thus more effective in delaying the infection.

The most common approach to study naturally acquired immunity involves incubating antibodies from semi-immune individuals against parasite recombinant proteins derived from the 3D7 strain [12, 46]. However, to test antibody sero-recognition against the PfEMP1 family, these assays must rely on some level of cross-reactivity, due to the extremely high *var* gene sequence polymorphism. Here, we circumvented this limitation with a 3D7-based protein array and plasma samples from 3D7-infected individuals, allowing us to determine the precise antibody-acquisition against each PfEMP1 variant. The sero-low/sero-high grouping made from Luminex assay [1] was validated with MSP1, CSP and AMA1 on our protein array. As expected, these *sero-high* individuals also sero-recognised a significantly larger proportion of PfEMP1 domains. These pre-existing antibodies decreased the likelihood of reaching the treatment threshold for the infection. The diversity in recognition, coupled with cross-reactivity against VSAs can be considered crucial to prevent symptomatic infections [11, 30, 24] for controlling malaria infections. Our results re-confirm that

anti-PfEMP1 immunity is a marker for infection outcome and severity of malaria infection [66, 8], and that certain PfEMP1 subsets have been linked to shield against severe symptoms of the disease [58, 60, 2, 41]. We also found that the pre-existing specific PfEMP1 antibody levels were at least moderately negatively associated with the expression of *var* genes during the infection, and this stems from acquired immunity to previous malarial infections. The negative correlation was most pronounced for group B and A PfEMP1, which constitute the *var* gene repertoire in early stages of infection.

Although blood-stage infections were artificially shortened by anti-malarial drugs, the breadth of antibody levels against PfEMP1 domains drastically increased by day 35 in sero-low individuals. Among the notable increases in antibodies was against the PfEMP1 domain ATS, located inside the red blood cell. This finding has been consistently demonstrated [61, 46], establishing ATS, the only conserved PfEMP1 domain, as a marker of exposure rather than protection. We did not identify a direct correlation between the *var* genes detected during the infection and the antibody-acquisition by day 35. Merozoites emerge from the liver around day 6, thus the *var* gene expression over the first 3 cycles is unknown, but they could have led to acquisition of novel antibodies observed post-infection. The observation that many highly expressed *var* genes at peak parasitaemia did not trigger an antibody response is intriguing. As each recombinant domain on the array has been serorecognised at least once by one plasma sample, a technical issue with the domain confirmation on the array is unlikely. Hence w We hypothesize that certain PfEMP1 domains are poorly immunogenic. While it is evident that PfEMP1s generally induce a robust immune response, in fact most antibodies targeting surface antigens are against PfEMP1 [12]. However, whether surface expression of a PfEMP1 automatically generates a new antibody had not been previously explored. We argue that *P. falciparum* has evolved not only an extremely polymorphic gene family but also protein domains that are relatively weakly immunogenic. This evolutionary pressure does not apply to the intracellular ATS domain, explaining its higher immunogenicity.

In summary, our findings corroborate the following scenario: The driving force behind maintaining a high-entropy repertoire of PfEMP1 variants is the intrinsic *var* gene switching. The establishment of a high-entropy repertoire occurs through resetting during mosquito and liver passage. This bet-hedging strategy proves to be effective when the parasites are confronted with a less diverse immune response. The high entropy repertoire is maintained by intrinsic switching in *sero-low* individuals, but does not survive negative-selection in *sero-high* individuals. However, some PfEMP1 domains are only poorly immunogenic and can persist. As such, poor immunogenicity combined with bet-hedging insures the parasite survival during CHMI. Intrinsic *var* gene switching is responsible for the reset and maintenance of a diverse *var* repertoire. Its high rates represent a challenge for the immune system during CHMI, because of the limited immunogenicity and duration of the infection. In the case of prolonged infections, such rapid rates of exhaustion of the repertoire could be a disadvantage for the parasite, which then has to depend on alternative mechanisms to generate variability such as recombination [64, 16, 15]. Interestingly, parasites submitted to high negative selection in *sero-high* individuals tend to express more stable variants and recover much slower, the high entropy steady state. This again could work in favor of the host/immune system and contribute to establishing a dynamic asymptomatic equilibrium during extended infections.

4 Methods and Materials

4.1 Epidemiological study design and sample collection

The epidemiological data used in this study was obtained from a previously published, non-randomized clinical trial in the Gambia (low transmission intensity) carried out by the Medical Research Council Unit The Gambia (MRCG) [1]. Briefly, participants aged between 18-35 years were recruited for this study and were screened for various hematological and biochemical abnormalities. Previous malaria exposure in these participants before DVI (Direct Venous Inoculation) was approximated using the LUMINEX platform by comparing responses against 6 malaria antigens (AMA-1, MSP1.19, GLURP.R2, GEXP18, Etramp5, Rh2) known to be markers of malaria exposure. Based on these responses, the volunteers were classified into two groups, *sero-high* and *sero-low* [1]. All volunteers received PfSPZ Challenge (3.2×103 PfSPZ in 0.5 mL, NF54/3D7 strain from Sanaria) by direct venous inoculation. Venous blood samples were collected the day before the inoculation (Day 0), once or twice between day 11 to 28, and at at day 35. All volunteers were treated with artemether-lumefantrine once thick blood smears were positive with *P. falciparum*.

4.2 Parasite enrichment and sorting

Infected venous erythrocytes frozen in glycerolyte were thawed and immediately treated with Streptolysin O (SLO) from Streptococcus pyogens (Sigma) as previously described [28, 9], with few modifications. Briefly, lyophilized SLO was reconstituted at 25U/µL stock concentrations, activated at room temperature for 15 minutes with 1M dithiothreitol (DTT) and used at a final activity of 1U/µL. Cells were lysed at room temperature for 6 minutes and reaction quenched with 5% PBS-BSA. Cell pellets were resolved on 60% Percoll gradient to remove cell debris, by centrifugation at 2500 x g for 3 minutes. Pellets were washed twice with PBS and stained with 500µL of 1:2000 dilutions of Vybrant DyeCycle Green Stain (Thermo Fisher) for 30 minutes at 37oC. Where possible, 100 infected erythrocytes were sorted in triplicates with a BD FACSAria flow cytometer (BD Biosciences) into wells containing lysis buffer of 2µL 0.8% Triton-X100, 1µL of 10mM dNTP mix (Thermo Fisher), 0.1µL of 20U/µL RNase Inhibitor (SUPERase•In™; Thermo Fisher), 0.1µL of 100µM non-anchored oligo dT (IDT) [50], 0.4µL of 50% polyethylene glycol (PEG8000) (Sigma) and 0.4µL nuclease-free water. Plates were snap-frozen on dry ice and stored at -80oC until use.

4.3 Whole transcriptome amplification with SMARTseq2

Complementary DNA (cDNA) were synthesized from sorted cells with a modified version of the SMARTseq2 protocol which has been optimized for *Plasmodium* [50], with few modifications. Briefly, a molecular crowding step [5] was included to improve library yield by adding 5% polyethylene glycol (PEG8000) (Sigma) to the lysis buffer [25]. Additionally, the SmartScribe (Clontech) reverse transcriptase was substituted with the better performing Maxima H (Thermo Fisher) at the cDNA synthesis step [5, 25, 72]. Frozen plates were thawed and incubated at 72oC for 5 minutes. cDNA synthesis master mix with final concentrations of 1X Maxima H RT buffer, 10µM TSO (Qiagen), 5U SUPERase•In RNase Inhibitor, 25U Maxima H enzyme, and nuclease-free water in 6µL volumes were added to each well. The cDNA was synthesized at 42oC for 90 minutes, followed by 10 cycles of 2 minutes at 50oC and 2 minutes at 42oC, and deactivation at 85oC for 5 minutes. cDNA was then amplified at 26 cycles with the KAPA HiFi HotStart ReadyMix PCR Kit (KAPA Biosystems), using the following conditions: denaturation at 98oC for 3 minutes, cycling steps of denaturing at 98oC for 20 seconds, annealing at 67oC for 15 seconds, extension at 72oC for 6 minutes, and final extension at 72oC for 5 minutes. PCR products were cleaned with 1X AMPure XP beads (Beckman Coulter), and eluted with 20µL of nuclease-free water. cDNA quantity and quality were assessed with Qubit dsDNA HS Assay (Invitrogen) and Agilent High Sensitivity DNA Assay (Agilent), on a Qubit 4 fluorometer and Agilent 2100 Bioanalyzer, respectively.

4.4 Whole transcriptome sequencing and data analysis

Amplified whole transcriptomes were sequenced by BGI genomics (Hong Kong). Paired-end fastQ files were aligned with HISAT2 (default alignment parameters) [29] and bam files made with SAMtools [34]. The SummarizeOverlaps feature of the GenomicAlignments package [32] was used to count reads against the *P. falciparum* 3D7 reference genome (version 3.0) and DESeq2 [36] used for differential expression analysis in R.

4.5 Parasite culturing

Cryopreserved parasites were thawed with NaCl solution [56], and parasites cultured in RPMI-1640 (sigma) supplemented with 25mM HEPES, 2mM L-glutamine, 0.5% Albumax II (sigma) and 50µg/L gentamicin (sigma). Parasites were cultured in 10mL volumes at 2% haematocrit in a blood gas environment of 90% N2, 5% CO2 and 5% oxygen. Parasites were harvested for RNA extraction at respective timepoints after synchronization with 5% D-sorbitol.

4.6 RNA extraction from samples stored in RNAprotect and cultured isolates

Total RNA was extracted by the phenol-chloroform extraction method with TRIzol reagent. For *in vivo* samples stored in RNAprotect Cell Reagent (Qiagen), five volumes of TRIzol reagent (Ambion) was added for homogenisation. For *in vitro* samples, 1mL of TRIzol was added to 200µL erythrocyte pellets and

homogenised. One-fifth TRIzol volumes of chloroform (Sigma-Aldrich) were added, and phase-separated by centrifuged at 16,000xg for 15 minutes at 4oC. RNA was precipitated from the aqueous phase with ice-cold isopropanol and 15µg of glycogen (GlycoBlue™ Coprecipitant; Invitrogen) for 2 hours or overnight at 4oC. After centrifugation at 16,000xg for 30 minutes (at 4oC), the precipitated RNA pellets were washed with 75% ethanol, air-dried at room temperature and solubilized in 87.5µL of DEPC-treated water (Invitrogen). Residual genomic DNA was subsequently removed by in-solution digestion with 7U of RNase-free DNase I (Qiagen). The RNA was then cleaned up by a second phenol-chloroform extraction step, and finally solubilized in 15µL DEPC-treated water. Absence of genomic DNA was determined by 35 cycles of RT-qPCR, using the skeleton binding protein 1 (*SBP1*) as target gene. If Ct values were less than 32, DNase digestion and re-extraction was repeated. The RNA was either used immediately or stored at -80oC.

4.7 Estimation of primer efficiency

Primers used for 3D7 *var* gene expression analysis were selected from previous studies [53, 3]. All primers were synthesized by Eurofins Genomics at 0.01 µmole with HPSF purification. *P. falciparum* 3D7 genomic DNA was serially diluted over 5-log concentrations and applied in a qPCR assay to determine primer amplification efficiency, using the SensiFAST™ SYBR No-Rox kit (Bioline) and primers at 300nM concentration. PCR was run with a LightCycler® 480 System (Roche). A two-step PCR was applied, with initial denaturation at 95oC for 3 minutes, followed by 40 cycles of annealing and extension at 62oC ramping at 4.8o C/s. A melting curve step was included to ascertain the specificity of the primers. Only primers with efficiencies between 1.8 and 2.2 were used for further analyses.

4.8 Real time (RT)-qPCR

cDNA was synthesized with the PrimeScript™ RT reagent Kit (Takara) using a combination of random hexamers (100µM) and oligo dT (50µM) primers in 20µL reaction volumes. cDNA was used in qPCR for the quantification of *var* genes in each sample. RT-qPCR assays were run with the SensiFAST™ SYBR No-Rox kit (Bioline) and primers at 300nM concentration on a LightCycler® 480 System (Roche). A two-step PCR was used, with initial denaturation at 95oC for 3 minutes followed by 40 cycles of annealing and extension at 62oC with 4.8oC/s ramp. Each assay included a 2.5µg genomic DNA positive control and no template (water) negative control. A melting curve step was included to ascertain the specificity of the primers. Four Plasmodium genes; *SBP1* (PF3D7_0501300), fructose-bisphosphate aldolase (PF3D7_1444800), arginyl-tRNA synthetase (PF3D7_1218600) and seryl tRNA synthetase (PF3D7_0717700) were included as housekeeping genes (references). Normalisation and calibration were done as previously described [3]. In brief, *SBP1* was used as the normalizer while 2.5ng genomic DNA was used for calibration. Relative quantification was calculated using $2^{-\Delta\Delta CT}$ taking into consideration the individual primer amplification efficiencies [44].

4.9 Estimating infection characteristics:

For comparing infection progression in-terms of growth rate, we calculated the PMR using a piece-wise log-linear model with latency as an additional parameter, given by:

$$y(t) = \begin{cases} 0 & , t \leq d \\ y_d \exp[m(t-d)] & , t > d \end{cases}$$

where d is the latency period, i.e. the time during which parasitaemia is undetectable, and m is the intrinsic growth rate of the parasite in each individual, y is the measured parasitaemia level, and y_d is a small undetectable parasitaemia value. In the model we approximate to zero the undetectable parasitaemia during latency and consider that after latency the parasitaemia grows exponentially.

4.10 Estimating *var* gene expression changes:

var gene expression probabilities were estimated as frequencies, i.e. ratios of the number of specific reads to the total number of reads. All probabilities less than a cut-off of 2% of the total *var* expression were considered

as vanishing. Because each parasite expresses only one *var* gene at a time, the expression probability of a gene also represents the proportion of parasites expressing that gene.

To quantify the heterogeneity of the population of parasites in terms of quantity and type of *var* genes, we used the above expression probabilities to compute a Shannon diversity index as follows:

$$S = -\sum_{P_i \neq 0} P_i \log(P_i),$$

where P_i represents the probability that the *var* gene i is expressed.

To model the change in *var* gene expression across time we considered a two state, continuous time [2] Markov chain described by the diagram:

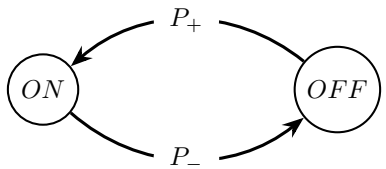

The two possible states for each variant are "ON" and "OFF" and P_+ and P_- are the probabilities of transition from one state to the other. The state "ON" means that the variant is expressed in a given parasite. The 'OFF' state corresponds to both events in which the parasite has switched away to expressing another gene, as well as the parasite expressing the same gene was recognized and eliminated by the host immune system.

The probabilities of a gene being expressed at various times $t + \Delta t$ and at t are related by the following expression:

$$P^{ON}_{t+\Delta t} = P^{ON}_t(1 - P_-(\Delta t)) + P^{OFF}_t P_+(\Delta t) \tag{1}$$

where $P_-(\Delta t)$, $P_+(\Delta t)$ are the finite time transition probabilities from OFF to ON and from ON to OFF, respectively. Using Eq.1, we can find bounds for the finite time transition probabilities $P_-(\Delta t)$ and $P_+(\Delta t)$. The probability bounds for P_- can be given as:

$$\max(0, \frac{P^{ON}_t - P^{ON}_{t+\Delta t}}{P^{ON}_t}) \leq P_-(\Delta t) \leq \min(\frac{1 - P^{ON}_{t+\Delta t}}{P^{ON}_t}, 1). \tag{2}$$

Similarly, the finite time transition probability from OFF to ON state satisfies:

$$\max(0, \frac{P^{ON}_{t+\Delta t} - P^{ON}_t}{1 - P^{ON}_t}) \leq P_+(\Delta t) \leq \min(\frac{P^{ON}_{t+\Delta t}}{1 - P^{ON}_t}, 1). \tag{3}$$

The finite time transition probabilities thus calculated depend on the time interval Δt. To quantify the transition probabilities independently of the time interval, we estimate the instantaneous transition rate (per unit time) p_- from ON to OFF, for each gene. Neglecting switching to events, instantaneous transition rate is related to the finite-time transition probability, as described by the formula:

$$P_-(\Delta t) = 1 - \exp(-p_- \Delta t). \tag{4}$$

The finite time transition probability along a time Δt equal to the generation time T_g is equivalent to the rates derived previously in [27], using the discrete difference equations. Indeed, let us suppose that the gene only changes from ON to OFF. Then, the changes of the proportion of parasites expressing a variant P_t over successive generations, starting with a monoclonal population $P_0 = 1$ to represent the experimental conditions from [27], are described as:

$$P_{t+1} = P_t - r_{\text{off}} P_t, \tag{5}$$

$$\text{where} \quad r_{\text{off}} = 1 - P_n^{1/n}. \tag{6}$$

[2] Even if one parasite switches the variant only at discrete times, multiples of the generation time, a continuous-time model is appropriate for modeling a population of non-synchronized parasites.

Comparing Eq. (1) with $P_+ = 0$ to Eq. (5) we find the equivalence between $P_-(T_g)$ and the discrete model rate r_{off}:

$$r_{\text{off}} = P_-(T_g) = 1 - \exp(-p_- T_g). \tag{7}$$

To summarize, in this paper we use both instantaneous transition rates (measured in d^{-1}) and finite time transition probabilities (measured in % per generation) to estimate rates of changes of *var* gene expression. The above definitions are general and apply to both *in vivo* turnover and to *in vitro* switching, even if the mechanisms of gene population change are different. The definition of rates used in previous works [27], based on discrete Markov chains models and concerning *in-vitro* switching, is the same as our definition of finite time transition probabilities.

4.11 Modeling *in vitro* data

The analysed data consists of ten time series with up to six time points. The time series is multi-dimensional, as for each time point one has the probability of expression of each of the 61 *var* genes.

First, the high-dimensional traces were projected onto a 3D space using Principal Component Analysis.

This can be modelled as a continuous time, four-state Markov chain. The number of states in the model is obtained by using the following principles: i) each state corresponds to genes from the same group, ii) var gene groups such as E and BA have very low probabilities at late times for all sero-low samples and most sero-high samples (see Figure 4 g,h) and are therefore excluded from the analysis.

The *var* genes dynamics is described by a continuous time, four-state Markov chain model. The master equation for this model reads:

$$\frac{d\mathbf{p}}{dt} = \mathbf{Q}\mathbf{p},\ \mathbf{p}(0) = \mathbf{p}_0, \tag{8}$$

where $\mathbf{p}(t) = (p_1(t), p_2(t), p_3(t), p_4(t))^T$ and $\mathbf{p}_0$ are the time dependent and initial ($t = 0$) probabilities of the four states (in order, *var* gene groups A, B, C, BC), respectively, $\mathbf{Q}$ is the adjoint transition-rate matrix (also named adjoint infinitesimal generator matrix), satisfying $Q_{ii} = -\sum_{j\neq i} Q_{ji}$ (zero sum columnwise).

In this model, each state is a group of *var* genes. The element $Q_{ji}, j \neq i$ represents the instantaneous transition rate from a state i to the state j. The instantaneous transition rates are estimated by optimisation and correspond to the minimum of the objective function

$$\mathcal{O}(\mathbf{Q}) = \sum_{i=1}^{4}\sum_{j=1}^{n_k}\sum_{k=1}^{10} |(p_i(t_{jk};\mathbf{Q}) - p_i^{obs}(t_{jk})|^2, \tag{9}$$

where $p_i(t_{ij};\mathbf{Q})$ are solutions of (8) with initial conditions $\mathbf{p}_0 = \mathbf{p}^{obs}(0)$ and $p_i^{obs}(t_{jk})$ are measured expression probabilities; the index $1 \leq k \leq 10$ designates the sample and $n_k \leq 6$ is the number of time points for the sample k.

The instantaneous rates to switch away from each state are given by

$$\begin{aligned} q_1 &= -Q_{11} = Q_{21} + Q_{31} + Q_{41}, \\ q_2 &= -Q_{22} = Q_{12} + Q_{32} + Q_{42}, \\ q_3 &= -Q_{33} = Q_{13} + Q_{23} + Q_{43}, \\ q_4 &= -Q_{44} = Q_{14} + Q_{24} + Q_{34}. \end{aligned} \tag{10}$$

The finite time, per generation, probabilities to switch away can be computed from the diagonal elements of the matrix $\exp(T_g\mathbf{Q})$, where T_g is the generation time, namely

$$\begin{aligned} Q_1 &= 1 - [\exp(T_g\mathbf{Q})]_{11}, \\ Q_2 &= 1 - [\exp(T_g\mathbf{Q})]_{22}, \\ Q_3 &= 1 - [\exp(T_g\mathbf{Q})]_{33}, \\ Q_4 &= 1 - [\exp(T_g\mathbf{Q})]_{44}, \end{aligned} \tag{11}$$

where $\exp(*)$ represents the matrix exponential.

The inter-individual similarity of the large time *var* gene transcription profiles was tested using an AUC criterion. For an arbitrarily chosen late time sample the *var* genes were sorted in decreasing order of their expression values. Then a normalized rank was assigned to each *var* gene representing the rank in the particular sample divided by the total number of *var* genes. For all genes that have ranks smaller than a given one and for all samples, we computed the fraction of common genes that is the proportion of highly expressed *var* genes that are common to all late time samples. The AUC index was defined as the area comprised between the diagonal (fraction of common genes = normalized rank) and the fraction of common genes vs. normalised rank curve, low AUC meaning large similarity.

4.12 Protein microarray

We developed a custom microarray featuring extensive coverage of the PfEMP1 domains in the reference genome 3D7 as previously described [60] as well as 79 protein fragments from PfEMP1s from the IT4, HB3, and DD2 reference strains, as well as PfEMP1s sequenced from field isolates. PfEMP1 fragments were typically expressed as consecutive constitutive domains [47], as we have previously done with the reference genome 3D7 [60]. Intracellular acidic terminal segments (ATS) of PfEMP1s were expressed as stand-alone fragments. The microarray also included additional antigen malaria proteins, including the 3D7 variants of apical membrane antigen 1, circumsporozoite protein, and merozoite surface protein-1. Three concentrations of tetanus toxin were also included as positive controls. Construction of microarrays has been previously described elsewhere [**?** 57, 6]. The microarray was probed with plasma from study participants as previously described and then scanned [71]. Fluorescence intensity was defined as the raw signal intensity corrected by global median scaling for no-DNA negative controls.

4.13 Protein microarray data analysis

All statistical analyses were carried out in python version 3.9. MFI-bkg values smaller than or equal to zero, were replaced with the average value of blank responses (in this case with a value of 2 so that the $log2FC$ value can be computed) and log-transformed. Sero-recognition threshold for all domains was determined by the median + 2 S.D. response levels in naive North-American individuals (n=10). Each domain on the array corresponds to a domain represented on the PfEMP1 protein encoded by the *var* genes. The random forest regressors and classifiers to predict relationships between immune response and infection outcome were implemented using scikit-learn 1.1.2. For data validation, we used responses against Tetanus antigens as control across naive and semi-immune individuals. The classification of the volunteers for immune response was retained as per the method described in the Epidemiological study design, based on another study, and later re-confirmed by several of our analyses. A PfEMP1 was considered recognised in an individual even if only one domain corresponding to the protein was recognised (in the event of multiple domains present per protein). The prediction of volunteer sub-groups was carried out based on immune responses using a random-forest classifier with Bootstrapping and Grid-Search to obtain optimal parameters for prediction of volunteers and a feature importance score was calculated to distinguish domain types useful in prediction the outcome of infection. We also calculated the change in breadth of response; as a cumulative total of domains recognised at different time-points in an individual, as well as the fold change in responses to each antigenic domain, between the first and the last time-point during the study.

4.14 *Var* expression and anti-PfEMP1 antibodies

A discretization method was used to compare inter-PfEMP1 responses throughout the CHMI. In this method, we converted the quantitative Fluorescence Intensity values per PfEMP1 to discrete values across all individuals, using quantile based classification. To discretize the domains, we used the following scheme: For each domain, we had a distribution of data points from samples defined as: $x_1, x_2, x_3, \ldots, x_n$, where n is the number of individual samples per PfEMP1. We discretized the dataset into $k+1$ bins using quantiles, where the quantiles are represented by $q_1, q_2, \ldots, q_k$. First, the quantile values $q_1, q_2, \ldots, q_k$ were calculated based on the chosen number of categories. These quantiles divide the data into k+1 intervals. Then each data point x_i was assigned to a specific interval based on its value. For instance, if x_i falls in the interval

$(q_{j-1}, q_j]$, it is assigned to the j-th bin. Mathematically, this function can be represented as:

$$\text{qcut}(x, q) = \begin{cases} k & \text{if } x > q_k, \\ k-1 & \text{if } q_{k-1} < x \leq q_k, \\ \vdots & \\ 1 & \text{if } q_1 < x \leq q_2, \\ 0 & \text{if } x \leq q_1, \end{cases}$$

where x is a data point from the dataset, $q = (q_1, q_2, \ldots, q_k)$, k is the number of quantiles.

We then grouped domains based on the PfEMP1 that they correspond to, and to each PfEMP1 group we associate the maximum domain response. Finally, only the PfEMP1s for which there was data available for both qPCR expression as well immune response were selected for the analysis.

Authors competing interests

The authors declare to have no competing interests.

Acknowledgments

We thank Isaie Reuling for helping setting up the CHMI. This work was funded by grants from the joint MRC/LSHTM fellowship, the French National Research Agency (18-CE15- 0009-01), Méditérannée Infection (InfectioPole Sud), ATIP-Avenir, Fonds Médical de la Recherche (FRM).

Supplementary figures

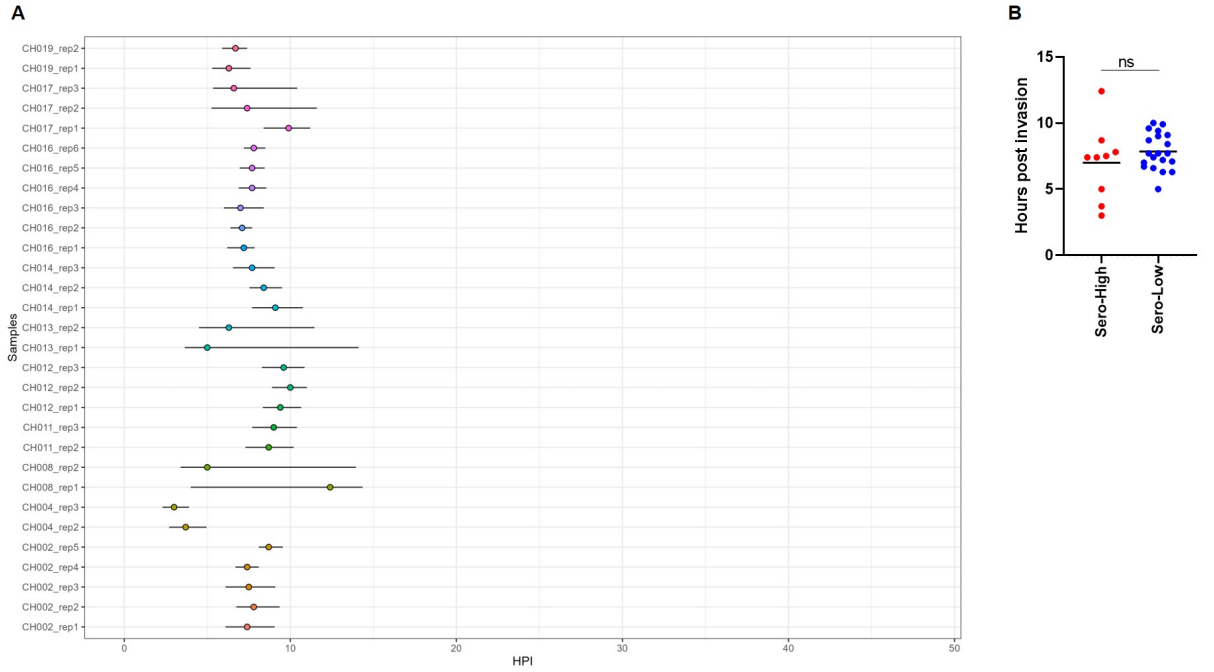

Figure S1: Developmental age of parasites by maximum likelihood estimated based on the captured transcriptomes *in vivo*. (A) All isolates were estimated to be ring-stages. (B) No significant difference between *sero-low* and *sero-high* derived isolates.

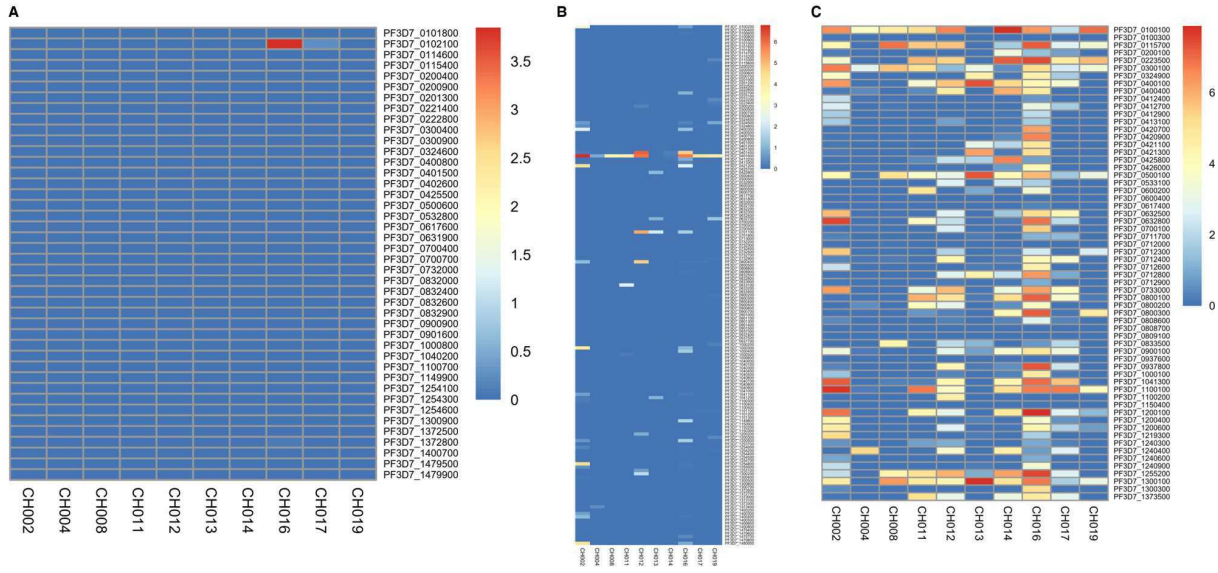

Figure S2: *In vivo* expression levels of variant surface antigens (VSA) from bulk RNA-seq.:Heatmap shows Log2FPKM values in each isolate. (A) *stevor* genes., (B) *rif* genes. (C) *var* genes.

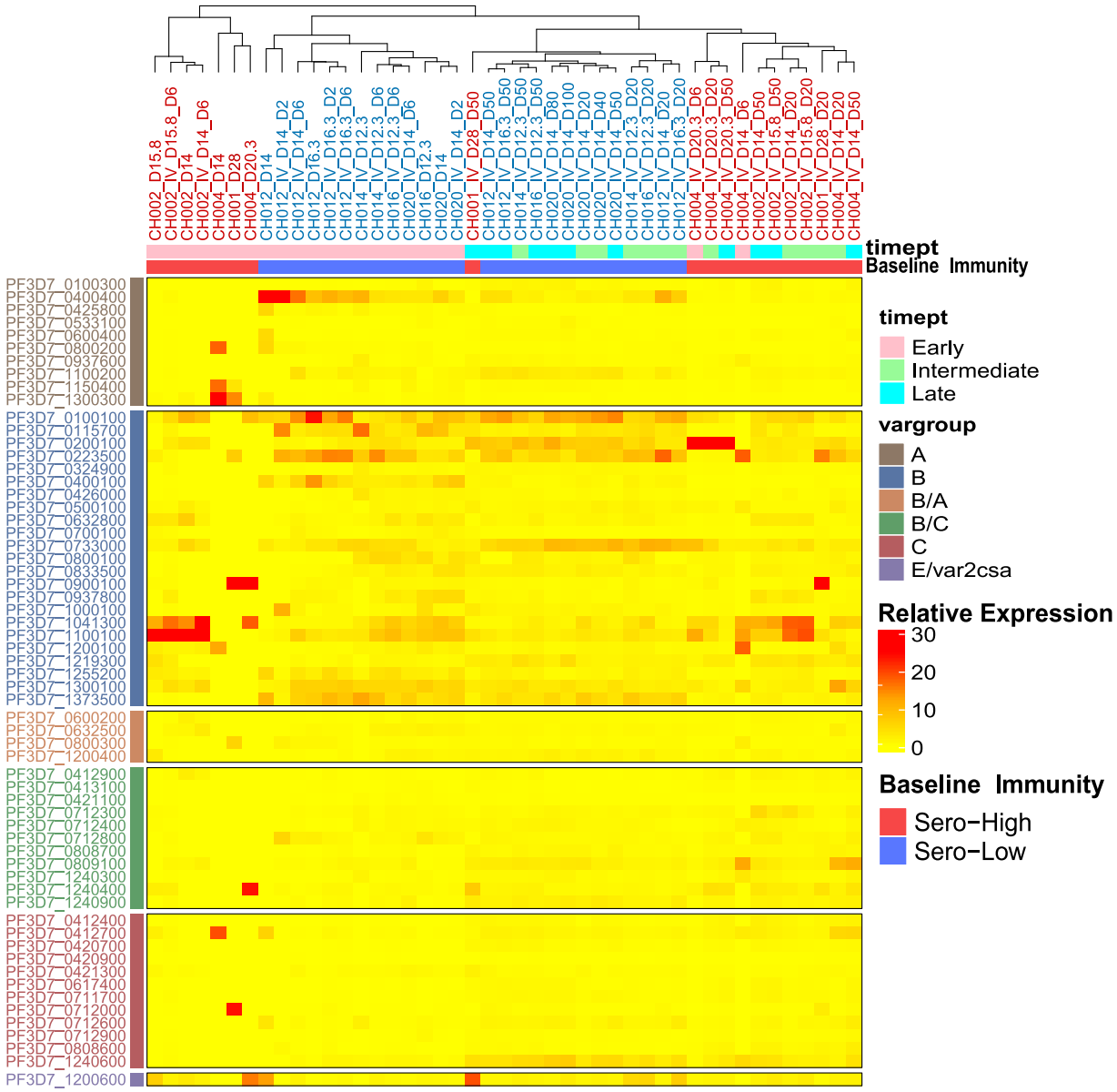

Figure S3: *In vitro var* expression landscape across time for ten isolates derived from *sero-low* and *sero-high* individuals. The heatmap is hierarchically clustered for relative expression of *var* genes at timepoints 6, 20 and 50 days *in vitro* after the *in vivo* infection timepoint. For CH020 (*sero-low* individual) there was an additional timepoint at 100 days post *in vivo*. Relative expression of each gene is shown from *low* to *high*, between 0% (yellow) to 30% (red). *Var* genes were grouped based on upstream sequence as A, B, C,E or intermediate groups B/A and B/C. Individuals were clustered based on expression and stratified by infection outcome.

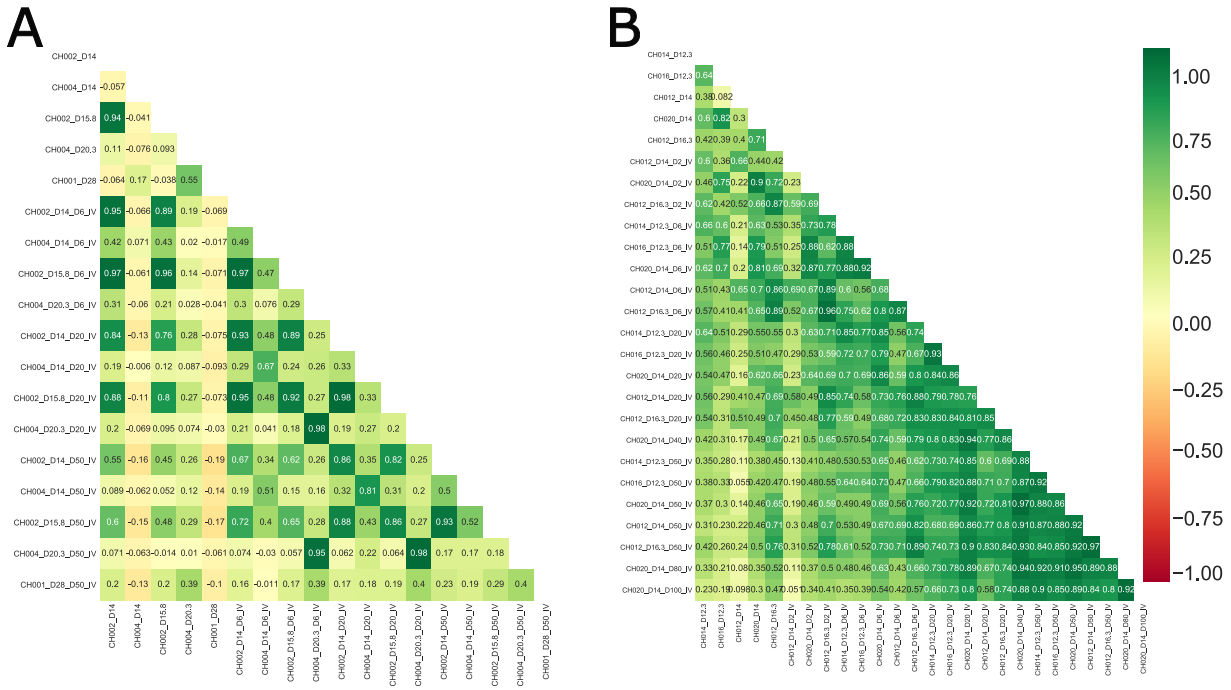

Figure S4: Pearson correlation between the *var* expression times series of A) *sero-high* individuals during *in vitro* culture and B) sero-low individuals. The color gradient is ordered from red (least) to green (highest).

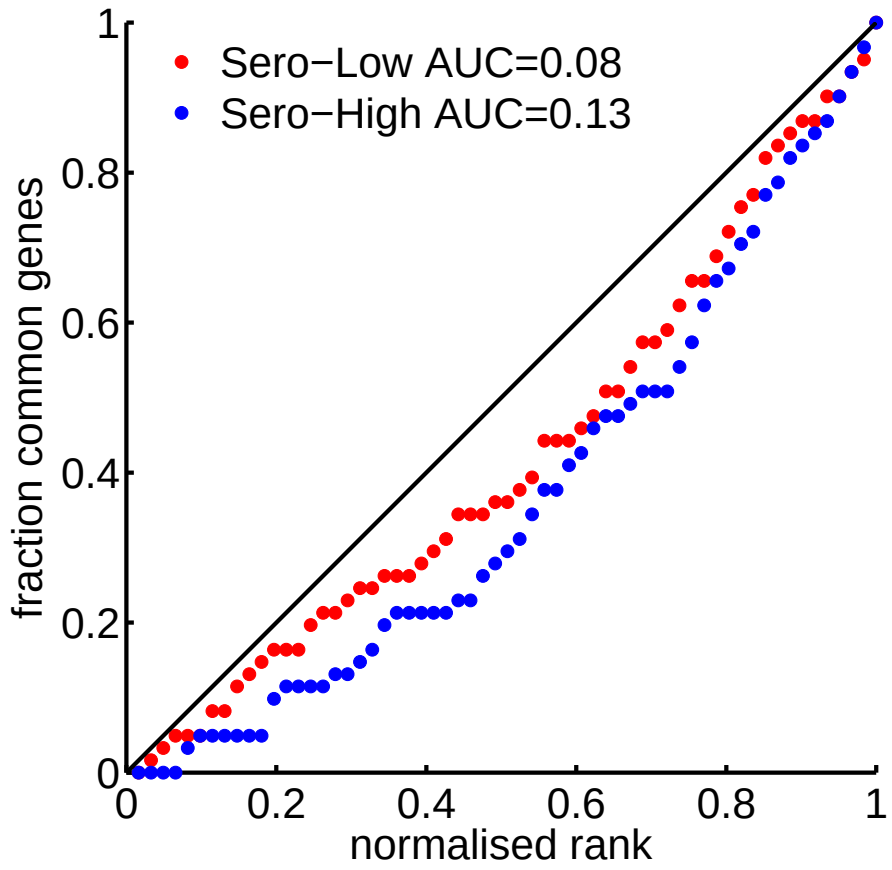

Figure S5: AUC method for testing the similarity of *var* genes distribution in all late time samples *in vitro*. The normalised rank represent the rank divided by total number of *var* genes after sorting them with respect to expression value in decreasing order. The fraction of common genes is the proportion of *var* genes that have ranks smaller than a given one in all late time samples. The diagonal represents the perfect similarity. The AUC index is defined as the area comprised between the diagonal and the curve, lower AUC meaning larger similarity.

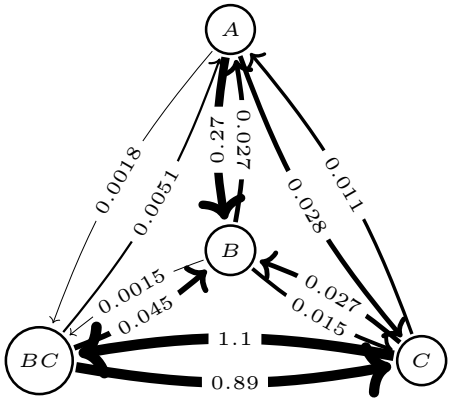

Figure S6: Transition graph and instantaneous switching rates of the four states *var* genes model resulting from fitting the model to the *in vitro* data. The gene groups E and BA where not included in this model because they reach rapidly very low steady state probabilities (see Figure 4 g,h).

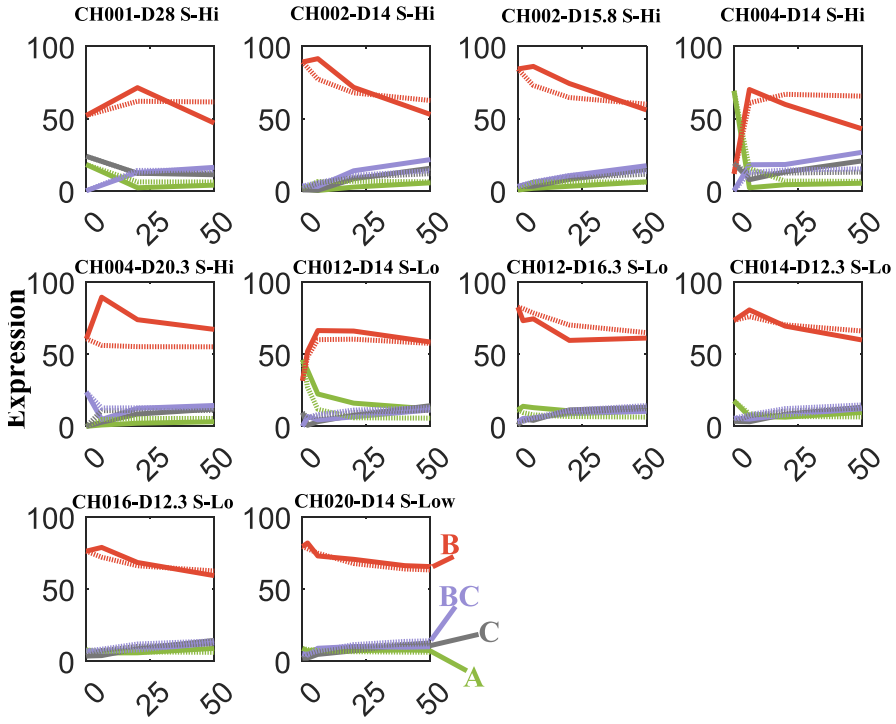

Figure S7: Fitting the four-state model to the *in vitro* expression data. Dotted lines are the model predictions.

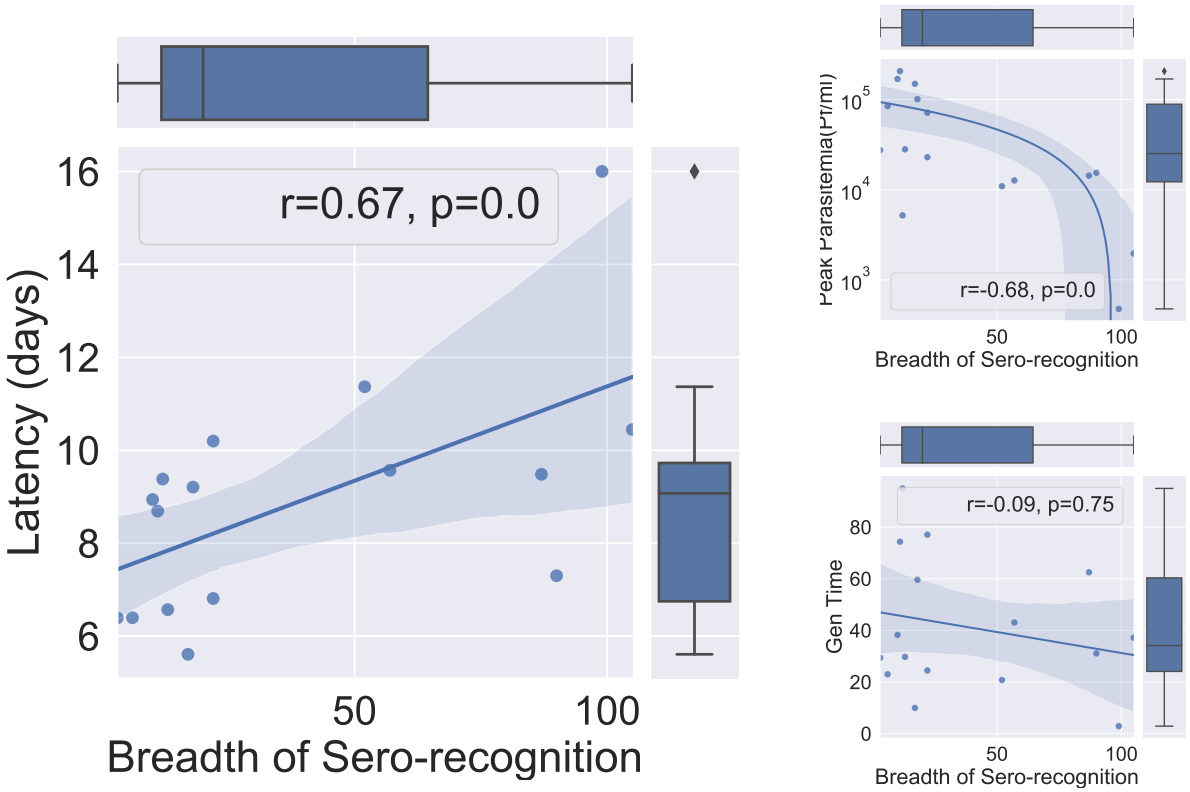

Figure S8: Pre-infection breadth of immune response and parasite growth dynamics. A) Spearmann Rank correlation between the number of 3D7 PfEMP1 domains recognized by the host at the beginning of the infection and the latency period (days until patent parasitaemia). B) Sero-recognition at day 0 and peak of parasitaemia: The log-peak of parasitaemia (Pf/ml) correlation with respect to the number of sero-recognized domains at the start of infection in an individual. C) Spearmann Correlation plot for parasite multiplication rate vs breadth of sero-recognition in each individual.

References

[1] Jane Achan, Isaie J Reuling, Xi Zen Yap, Edgard Dabira, Abdullahi Ahmad, Momodou Cox, Davis Nwakanma, Kevin Tetteh, Lindsey Wu, Guido JH Bastiaens, et al. Serologic markers of previous malaria exposure and functional antibodies inhibiting parasite growth are associated with parasite kinetics following a plasmodium falciparum controlled human infection. *Clinical Infectious Diseases*, 70(12):2544–2552, 2020.

[2] Marion Avril, Abhai K Tripathi, Andrew J Brazier, Cheryl Andisi, Joel H Janes, Vijaya L Soma, David J Sullivan Jr, Peter C Bull, Monique F Stins, and Joseph D Smith. A restricted subset of var genes mediates adherence of plasmodium falciparum-infected erythrocytes to brain endothelial cells. *Proceedings of the National Academy of Sciences*, 109(26):E1782–E1790, 2012.

[3] Anna Bachmann, Ellen Bruske, Ralf Krumkamp, Louise Turner, J Stephan Wichers, Michaela Petter, Jana Held, Michael F Duffy, B Kim Lee Sim, Stephen L Hoffman, et al. Controlled human malaria infection with plasmodium falciparum demonstrates impact of naturally acquired immunity on virulence gene expression. *PLoS pathogens*, 15(7):e1007906, 2019.

[4] Anna Bachmann, Michaela Petter, Ralf Krumkamp, Meral Esen, Jana Held, Judith AM Scholz, Tao Li, B Kim Lee Sim, Stephen L Hoffman, Peter G Kremsner, et al. Mosquito passage dramatically changes var gene expression in controlled human plasmodium falciparum infections. *PLoS pathogens*, 12(4):e1005538, 2016.

[5] Johannes W Bagnoli, Christoph Ziegenhain, Aleksandar Janjic, Lucas E Wange, Beate Vieth, Swati Parekh, Johanna Geuder, Ines Hellmann, and Wolfgang Enard. Sensitive and powerful single-cell rna sequencing using mcscrb-seq. *Nature communications*, 9(1):2937, 2018.

[6] Jason A Bailey, Andrea A Berry, Mark A Travassos, Amed Ouattara, Sarah Boudova, Emmanuel Y Dotsey, Andrew Pike, Christopher G Jacob, Matthew Adams, John C Tan, et al. Microarray analyses reveal strain-specific antibody responses to plasmodium falciparum apical membrane antigen 1 variants following natural infection and vaccination. *Scientific reports*, 10(1):3952, 2020.

[7] Alyssa E Barry, Aleksandra Leliwa-Sytek, Livingston Tavul, Heather Imrie, Florence Migot-Nabias, Stuart M Brown, Gilean A V McVean, and Karen P Day. Population genomics of the immune evasion (var) genes of plasmodium falciparum. *PLoS pathogens*, 3(3):e34, 2007.

[8] Alyssa E Barry, Angela Trieu, Freya JI Fowkes, Jozelyn Pablo, Mina Kalantari-Dehaghi, Algis Jasinskas, Xiaolin Tan, Matthew A Kayala, Livingstone Tavul, Peter M Siba, et al. The stability and complexity of antibody responses to the major surface antigen of plasmodium falciparum are associated with age in a malaria endemic area. *Molecular & Cellular Proteomics*, 10(11), 2011.

[9] Audrey C Brown, Christopher C Moore, and Jennifer L Guler. Cholesterol-dependent enrichment of understudied erythrocytic stages of human plasmodium parasites. *Scientific reports*, 10(1):4591, 2020.

[10] Thibaut Brugat, Adam James Reid, Jing-wen Lin, Deirdre Cunningham, Irene Tumwine, Garikai Kushinga, Sarah McLaughlin, Philip Spence, Ulrike Boehme, Mandy Sanders, et al. Antibody-independent mechanisms regulate the establishment of chronic plasmodium infection. *Nature microbiology*, 2(4):1–9, 2017.

[11] Jo-Anne Chan, Michelle J Boyle, Kerryn A Moore, Linda Reiling, Zaw Lin, Wina Hasang, Marion Avril, Laurens Manning, Ivo Mueller, Moses Laman, et al. Antibody targets on the surface of plasmodium falciparum–infected erythrocytes that are associated with immunity to severe malaria in young children. *The Journal of infectious diseases*, 219(5):819–828, 2019.

[12] Jo-Anne Chan, Katherine B Howell, Linda Reiling, Ricardo Ataide, Claire L Mackintosh, Freya JI Fowkes, Michaela Petter, Joanne M Chesson, Christine Langer, George M Warimwe, et al. Targets of antibodies against plasmodium falciparum–infected erythrocytes in malaria immunity. *The Journal of clinical investigation*, 122(9):3227–3238, 2012.

[13] Ingrid Chen, Siân E Clarke, Roly Gosling, Busiku Hamainza, Gerry Killeen, Alan Magill, Wendy O'Meara, Ric N Price, and Eleanor M Riley. "asymptomatic" malaria: a chronic and debilitating infection that should be treated. *PLoS medicine*, 13(1):e1001942, 2016.

[14] Lauren M Childs and Caroline O Buckee. Dissecting the determinants of malaria chronicity: why within-host models struggle to reproduce infection dynamics. *Journal of The Royal Society Interface*, 12(104):20141379, 2015.

[15] Antoine Claessens, William L Hamilton, Mihir Kekre, Thomas D Otto, Adnan Faizullabhoy, Julian C Rayner, and Dominic Kwiatkowski. Generation of antigenic diversity in plasmodium falciparum by structured rearrangement of var genes during mitosis. *PLoS genetics*, 10(12):e1004812, 2014.

[16] Kirk W Deitsch, Amy del Pinal, and Thomas E Wellems. Intra-cluster recombination and var transcription switches in the antigenic variation of plasmodium falciparum. *Molecular and biochemical parasitology*, 101(1-2):107–116, 1999.

[17] Kirk W Deitsch and Ron Dzikowski. Variant gene expression and antigenic variation by malaria parasites. *Annual review of microbiology*, 71:625–641, 2017.

[18] Manoj T Duraisingh and David Horn. Epigenetic regulation of virulence gene expression in parasitic protozoa. *Cell host & microbe*, 19(5):629–640, 2016.

[19] Beatriz Galatas, Quique Bassat, and Alfredo Mayor. Malaria parasites in the asymptomatic: looking for the hay in the haystack. *Trends in parasitology*, 32(4):296–308, 2016.

[20] Michelle L Gatton, Jennifer M Peters, Elizabeth V Fowler, and Qin Cheng. Switching rates of plasmodium falciparum var genes: faster than we thought? *Trends in Parasitology*, 19(5):202–208, 2003.

[21] Ashfaq Ghumra, Jean-Philippe Semblat, Ricardo Ataide, Carolyne Kifude, Yvonne Adams, Antoine Claessens, Damian N Anong, Peter C Bull, Clare Fennell, Monica Arman, et al. Induction of strain-transcending antibodies against group a pfemp1 surface antigens from virulent malaria parasites. *PLoS pathogens*, 8(4):e1002665, 2012.

[22] Suchi Goel, Mia Palmkvist, Kirsten Moll, Nicolas Joannin, Patricia Lara, Reetesh R Akhouri, Nasim Moradi, Karin Öjemalm, Mattias Westman, Davide Angeletti, et al. Rifins are adhesins implicated in severe plasmodium falciparum malaria. *Nature medicine*, 21(4):314–317, 2015.

[23] Michael F Good and Stephanie K Yanow. Hiding in plain sight: an epitope-based strategy for a subunit malaria vaccine. *Trends in Parasitology*, 2023.

[24] Sunetra Gupta, Robert W Snow, Christl A Donnelly, Kevin Marsh, and Chris Newbold. Immunity to non-cerebral severe malaria is acquired after one or two infections. *Nature medicine*, 5(3):340–343, 1999.

[25] Michael Hagemann-Jensen, Christoph Ziegenhain, Ping Chen, Daniel Ramsköld, Gert-Jan Hendriks, Anton JM Larsson, Omid R Faridani, and Rickard Sandberg. Single-cell rna counting at allele and isoform resolution using smart-seq3. *Nature Biotechnology*, 38(6):708–714, 2020.

[26] Regina Hoo, Ellen Bruske, Sandra Dimonte, Lei Zhu, Benjamin Mordmüller, B Kim Lee Sim, Peter G Kremsner, Stephen L Hoffman, Zbynek Bozdech, Matthias Frank, et al. Transcriptome profiling reveals functional variation in plasmodium falciparum parasites from controlled human malaria infection studies. *EBioMedicine*, 48:442–452, 2019.

[27] Paul Horrocks, Robert Pinches, Zóe Christodoulou, Sue A Kyes, and Chris I Newbold. Variable var transition rates underlie antigenic variation in malaria. *Proceedings of the National Academy of Sciences*, 101(30):11129–11134, 2004.

[28] Katherine E Jackson, Tobias Spielmann, Eric Hanssen, Akinola Adisa, Frances Separovic, Matthew WA Dixon, Katharine R Trenholme, Paula L Hawthorne, Don L Gardiner, Tim Gilberger, et al. Selective permeabilization of the host cell membrane of plasmodium falciparum-infected red blood cells with streptolysin o and equinatoxin ii. *Biochemical Journal*, 403(1):167–175, 2007.

[29] Daehwan Kim, Ben Langmead, and Steven L Salzberg. Hisat: a fast spliced aligner with low memory requirements. *Nature methods*, 12(4):357–360, 2015.

[30] Hannah W Kimingi, Ann W Kinyua, Nicole A Achieng, Kennedy M Wambui, Shaban Mwangi, Roselyne Nguti, Cheryl A Kivisi, Anja TR Jensen, Philip Bejon, Melisa C Kapulu, et al. Breadth of antibodies to plasmodium falciparum variant surface antigens is associated with immunity in a controlled human malaria infection study. *Frontiers in Immunology*, 13, 2022.

[31] Sue Kyes, Robert Pinches, Chris Newbold, et al. A simple rna analysis method shows var and rif multigene family expression patterns in plasmodium falciparum. *Molecular and biochemical parasitology*, 105(2):311–315, 2000.

[32] Michael Lawrence, Wolfgang Huber, Hervé Pagès, Patrick Aboyoun, Marc Carlson, Robert Gentleman, Martin T Morgan, and Vincent J Carey. Software for computing and annotating genomic ranges. *PLoS computational biology*, 9(8):e1003118, 2013.

[33] Jacob E Lemieux, Natalia Gomez-Escobar, Avi Feller, Celine Carret, Alfred Amambua-Ngwa, Robert Pinches, Felix Day, Sue A Kyes, David J Conway, Chris C Holmes, et al. Statistical estimation of cell-cycle progression and lineage commitment in plasmodium falciparum reveals a homogeneous pattern of transcription in ex vivo culture. *Proceedings of the National Academy of Sciences*, 106(18):7559–7564, 2009.

[34] Heng Li, Bob Handsaker, Alec Wysoker, Tim Fennell, Jue Ruan, Nils Homer, Gabor Marth, Goncalo Abecasis, Richard Durbin, and 1000 Genome Project Data Processing Subgroup. The sequence alignment/map format and samtools. *bioinformatics*, 25(16):2078–2079, 2009.

[35] Kim A Lindblade, Laura Steinhardt, Aaron Samuels, S Patrick Kachur, and Laurence Slutsker. The silent threat: asymptomatic parasitemia and malaria transmission. *Expert review of anti-infective therapy*, 11(6):623–639, 2013.

[36] Michael I Love, Wolfgang Huber, and Simon Anders. Moderated estimation of fold change and dispersion for rna-seq data with deseq2. *Genome biology*, 15(12):1–21, 2014.

[37] Rui Ma, Tengfei Lian, Rick Huang, Jonathan P Renn, Jennifer D Petersen, Joshua Zimmerberg, Patrick E Duffy, and Niraj H Tolia. Structural basis for placental malaria mediated by plasmodium falciparum var2csa. *Nature microbiology*, 6(3):380–391, 2021.

[38] Kathryn Milne, Alasdair Ivens, Adam J Reid, Magda E Lotkowska, Aine O'Toole, Geetha Sankaranarayanan, Diana Munoz Sandoval, Wiebke Nahrendorf, Clement Regnault, Nick J Edwards, et al. Mapping immune variation and var gene switching in naive hosts infected with plasmodium falciparum. *Elife*, 10:e62800, 2021.

[39] Bernina Naissant, Florian Dupuy, Yoann Duffier, Audrey Lorthiois, Julien Duez, Judith Scholz, Pierre Buffet, Anais Merckx, Anna Bachmann, and Catherine Lavazec. Plasmodium falciparum stevor phosphorylation regulates host erythrocyte deformability enabling malaria parasite transmission. *Blood, The Journal of the American Society of Hematology*, 127(24):e42–e53, 2016.

[40] Makhtar Niang, Amy Kristine Bei, Kripa Gopal Madnani, Shaaretha Pelly, Selasi Dankwa, Usheer Kanjee, Karthigayan Gunalan, Anburaj Amaladoss, Kim Pin Yeo, Ndeye Sakha Bob, et al. Stevor is a plasmodium falciparum erythrocyte binding protein that mediates merozoite invasion and rosetting. *Cell host & microbe*, 16(1):81–93, 2014.

[41] Sofia Nunes-Silva, Sébastien Dechavanne, Azizath Moussiliou, Natalia Pstrąg, Jean-Philippe Semblat, Stéphane Gangnard, Nicaise Tuikue-Ndam, Philippe Deloron, Arnaud Chêne, and Benoît Gamain. Beninese children with cerebral malaria do not develop humoral immunity against the it4-var19-dc8 pfemp1 variant linked to epcr and brain endothelial binding. *Malaria journal*, 14(1):1–15, 2015.

[42] Jennifer Peters, Elizabeth Fowler, Michelle Gatton, Nanhua Chen, Allan Saul, and Qin Cheng. High diversity and rapid changeover of expressed var genes during the acute phase of plasmodium falciparum infections in human volunteers. *Proceedings of the National Academy of Sciences*, 99(16):10689–10694, 2002.

[43] Michaela Petter, Malin Haeggström, Ayman Khattab, Victor Fernandez, Mo-Quen Klinkert, and Mats Wahlgren. Variant proteins of the plasmodium falciparum rifin family show distinct subcellular localization and developmental expression patterns. *Molecular and biochemical parasitology*, 156(1):51–61, 2007.

[44] Michael W Pfaffl. A new mathematical model for relative quantification in real-time rt–pcr. *Nucleic acids research*, 29(9):e45–e45, 2001.

[45] Anastasia K Pickford, Lucas Michel-Todó, Florian Dupuy, Alfredo Mayor, Pedro L Alonso, Catherine Lavazec, and Alfred Cortés. Expression patterns of plasmodium falciparum clonally variant genes at the onset of a blood infection in malaria-naive humans. *Mbio*, 12(4):10–1128, 2021.

[46] Sai Sundar Rajan Raghavan, Louise Turner, Rasmus W Jensen, Nicolai Tidemand Johansen, Daniel Skjold Jensen, Pontus Gourdon, Jinqiu Zhang, Yong Wang, Thor Grundtvig Theander, Kaituo Wang, et al. Endothelial protein c receptor binding induces conformational changes to severe malaria-associated group a pfemp1. *Structure*, 31(10):1174–1183, 2023.

[47] Thomas S Rask, Daniel A Hansen, Thor G Theander, Anders Gorm Pedersen, and Thomas Lavstsen. Plasmodium falciparum erythrocyte membrane protein 1 diversity in seven genomes–divide and conquer. *PLoS computational biology*, 6(9):e1000933, 2010.

[48] Mario Recker, Caroline O Buckee, Andrew Serazin, Sue Kyes, Robert Pinches, Zóe Christodoulou, Amy L Springer, Sunetra Gupta, and Chris I Newbold. Antigenic variation in plasmodium falciparum malaria involves a highly structured switching pattern. *PLoS Pathogens*, 7(3):e1001306, 2011.

[49] Mario Recker, Sean Nee, Peter C Bull, Sam Kinyanjui, Kevin Marsh, Chris Newbold, and Sunetra Gupta. Transient cross-reactive immune responses can orchestrate antigenic variation in malaria. *Nature*, 429(6991):555–558, 2004.

[50] Adam J Reid, Arthur M Talman, Hayley M Bennett, Ana R Gomes, Mandy J Sanders, Christopher JR Illingworth, Oliver Billker, Matthew Berriman, and Mara KN Lawniczak. Single-cell rna-seq reveals hidden transcriptional variation in malaria parasites. *elife*, 7:e33105, 2018.

[51] David J Roberts, Anthony R Berendt, Robert Pinches, Gerard Nash, Kevin Marsh, Christopher I Newbold, et al. Rapid switching to multiple antigenic and adhesive phenotypes in malaria. *Nature*, 357(6380):689–692, 1992.

[52] Fumiji Saito, Kouyuki Hirayasu, Takeshi Satoh, Christian W Wang, John Lusingu, Takao Arimori, Kyoko Shida, Nirianne Marie Q Palacpac, Sawako Itagaki, Shiroh Iwanaga, et al. Immune evasion of plasmodium falciparum by rifin via inhibitory receptors. *Nature*, 552(7683):101–105, 2017.

[53] Ali Salanti, Trine Staalsoe, Thomas Lavstsen, Anja TR Jensen, MP Kordai Sowa, David E Arnot, Lars Hviid, and Thor G Theander. Selective upregulation of a single distinctly structured var gene in chondroitin sulphate a-adhering plasmodium falciparum involved in pregnancy-associated malaria. *Molecular microbiology*, 49(1):179–191, 2003.

[54] A Scherf, R Hernandez-Rivas, P Buffet, E Bottius, C Benatar, B Pouvelle, J Gysin, and M Lanzer. Antigenic variation in malaria: in situ switching, relaxed and mutually exclusive transcription of var genes during intra-erythrocytic development in plasmodium falciparum. *The EMBO journal*, 17(18):5418–5426, 1998.

[55] Danielle I Stanisic, James S McCarthy, and Michael F Good. Controlled human malaria infection: applications, advances, and challenges. *Infection and immunity*, 86(1):e00479–17, 2018.

[56] LB Stewart, O Diaz-Ingelmo, A Claessens, J Abugri, RD Pearson, S Goncalves, E Drury, DP Kwiatkowski, GA Awandare, and DJ Conway. Intrinsic multiplication rate variation and plasticity of human blood stage malaria parasites. commun biol 3: 624, 2020.

[57] Emily M Stucke, Antoine Dara, Ankit Dwivedi, Theresa Hodges, Drissa Coulibaly, Abdoulaye K Kone, Karim Troaore, Boureima Guindo, Bourama Tangara, Amadou Niangaly, et al. Identification of expressed vars in whole blood clinical samples with a custom capture array versus rna enrichment methods. In *AMERICAN JOURNAL OF TROPICAL MEDICINE AND HYGIENE*, volume 101, pages 498–498. AMER SOC TROP MED & HYGIENE 8000 WESTPARK DR, STE 130, MCLEAN, VA 22101 USA, 2019.

[58] Sofonias K Tessema, Rie Nakajima, Algis Jasinskas, Stephanie L Monk, Lea Lekieffre, Enmoore Lin, Benson Kiniboro, Carla Proietti, Peter Siba, Philip L Felgner, et al. Protective immunity against severe malaria in children is associated with a limited repertoire of antibodies to conserved pfemp1 variants. *Cell host & microbe*, 26(5):579–590, 2019.

[59] Richard Thomson-Luque, Lasse Votborg-Novél, Wanangwa Ndovie, Carolina M Andrade, Moussa Niangaly, Charalampos Attipa, Nathalia F Lima, Drissa Coulibaly, Didier Doumtabe, Bouréima Guindo, et al. Plasmodium falciparum transcription in different clinical presentations of malaria associates with circulation time of infected erythrocytes. *Nature Communications*, 12(1):4711, 2021.

[60] Mark A Travassos, Amadou Niangaly, Jason A Bailey, Amed Ouattara, Drissa Coulibaly, Kirsten E Lyke, Matthew B Laurens, Jozelyn Pablo, Algis Jasinskas, Rie Nakajima, et al. Children with cerebral malaria or severe malarial anaemia lack immunity to distinct variant surface antigen subsets. *Scientific reports*, 8(1):6281, 2018.

[61] Noah T Ventimiglia, Emily M Stucke, Drissa Coulibaly, Andrea A Berry, Kirsten E Lyke, Matthew B Laurens, Jason A Bailey, Matthew Adams, Amadou Niangaly, Abdoulaye K Kone, et al. Malian adults maintain serologic responses to virulent pfemp1s amid seasonal patterns of fluctuation. *Scientific Reports*, 11(1):14401, 2021.

[62] Nicola K Viebig, Emily Levin, Sebastien Dechavanne, Stephen J Rogerson, Jürg Gysin, Joseph D Smith, Artur Scherf, and Benoit Gamain. Disruption of var2csa gene impairs placental malaria associated adhesion phenotype. *PloS one*, 2(9):e910, 2007.

[63] Mats Wahlgren, Suchi Goel, and Reetesh R Akhouri. Variant surface antigens of plasmodium falciparum and their roles in severe malaria. *Nature Reviews Microbiology*, 15(8):479–491, 2017.

[64] Christopher P Ward, George T Clottey, Mark Dorris, Dar-Der Ji, and David E Arnot. Analysis of plasmodium falciparum pfemp-1/var genes suggests that recombination rearranges constrained sequences. *Molecular and biochemical parasitology*, 102(1):167–177, 1999.

[65] George M Warimwe, Gregory Fegan, Jennifer N Musyoki, Charles RJC Newton, Michael Opiyo, George Githinji, Cheryl Andisi, Francis Menza, Barnes Kitsao, Kevin Marsh, et al. Prognostic indicators of life-threatening malaria are associated with distinct parasite variant antigen profiles. *Science translational medicine*, 4(129):129ra45–129ra45, 2012.

[66] George M Warimwe, Thomas M Keane, Gregory Fegan, Jennifer N Musyoki, Charles RJC Newton, Arnab Pain, Matthew Berriman, Kevin Marsh, and Peter C Bull. Plasmodium falciparum var gene expression is modified by host immunity. *Proceedings of the National Academy of Sciences*, 106(51):21801–21806, 2009.

[67] George M Warimwe, Mario Recker, Esther W Kiragu, Caroline O Buckee, Juliana Wambua, Jennifer N Musyoki, Kevin Marsh, and Peter C Bull. Plasmodium falciparum var gene expression homogeneity as a marker of the host-parasite relationship under different levels of naturally acquired immunity to malaria. *PLoS One*, 8(7):e70467, 2013.

[68] JS Wichers, JAM Scholz, J Strauss, S Witt, A Lill, LI Ehnold, N Neupert, B Liffner, R Lühken, M Petter, et al. Dissecting the gene expression, localization, membrane topology, and function of the plasmodium falciparum stevor protein family. mbio 10: e01500-19. *CAS PubMed PubMed Central Article*, 2019.

[69] Jan Stephan Wichers-Misterek, Ralf Krumkamp, Jana Held, Heidrun von Thien, Irene Wittmann, Yannick Daniel Höppner, Julia M Ruge, Kara Moser, Antoine Dara, Jan Strauss, et al. The exception that proves the rule: Virulence gene expression at the onset of plasmodium falciparum blood stage infections. *PLoS Pathogens*, 19(6):e1011468, 2023.

[70] Xu Zhang, Francesca Florini, Joseph E Visone, Irina Lionardi, Mackensie R Gross, Valay Patel, and Kirk W Deitsch. A coordinated transcriptional switching network mediates antigenic variation of human malaria parasites. *Elife*, 11:e83840, 2022.

[71] Albert E Zhou, Aarti Jain, Rie Nakajima, Biraj Shrestha, Emily M Stucke, Sudhaunshu Joshi, Kathy A Strauss, Per N Hedde, Andrea A Berry, Philip L Felgner, et al. Protein microarrays as a tool to analyze antibody responses to variant surface antigens expressed on the surface of plasmodium falciparum–infected erythrocytes. In *Malaria Immunology: Targeting the Surface of Infected Erythrocytes*, pages 343–358. Springer, 2022.

[72] Daniel Zucha, Peter Androvic, Mikael Kubista, and Lukas Valihrach. Performance comparison of reverse transcriptases for single-cell studies. *Clinical Chemistry*, 66(1):217–228, 2020.

CHAPTER 3

Mathematical Models of Antigenic Variation

As discussed earlier in Section 1.5, mathematical models in malaria encompass different fields in biology and epidemiology, including but not limited to ecology, evolution, and genetics of both the host and the parasite. To address these diverse questions, multiple types of mathematical models have been developed. Models incorporating population genetics investigate the parasite's evolution and transmission in a complicated environment characterized by variable host immunity, host death, medication availability, and mosquito availability [Mandal et al., 2011]. Additionally modelling approaches have been explored to understand malaria biology, including individual-based models[Smith et al., 2018] and habitat-modelling of transmission [Kulkarni et al., 2010; Gu and Novak, 2005].

The exact switching mechanisms exhibited by *P. falciparum* parasites expressing different antigenic variants are not completely described. Additionally, the effect of selection pressure on the transcriptional switching is also not fully quantified. Earlier models of *P. falciparum* within-host dynamics incorporating switching mechanisms allow the transcription of a number of variants in the parasite population at the earlier stages. Cross-reactive immune responses, suggested as a mechanism necessary for chronic infections and included explicitly in [Gatton et al., 2003; Childs and Buckee, 2015; Eckhoff, 2012] does not permit chronic infections [Camponovo et al., 2021].

However, contrary to the assumptions of existing models, parasites may express a large range of variants during the initial blood stage, as has been shown in data from CHMI studies [Bachmann et al., 2016, 2019; Milne et al., 2021]. Other recent models, such as those by [Challenger et al., 2017] have tried to simplify this caveat by not focusing on variant specific sub-populations, modelling only the overall parasitemia. Models by [McKenzie and Bossert, 2005; Gurarie et al., 2012; Recker et al., 2004] also offer simpler alternatives without delving into variant-switching mechanisms. Even though these models exhibit persistence of parasite populations under simplified conditions, host-pathogen interactions in long term *falciparum* infections are biologically poorly understood to validate the accuracy of most theoretical models.

To understand the role of immune responses in shaping malaria infections, evaluation of immunological markers at baseline and their correlation with the time to infection makes it feasible to pinpoint that acquired immunity is critical for protecting against malaria, but it is challenging to ascertain whether measured responses actually mediate protection or are merely markers of prior exposure, given that most immune responses to malaria increase with age and cumulative exposure to malaria antigens anyway[Sarr et al., 2007; Tongren et al., 2006]. Therefore, mathematical approaches that incorporate host-pathogen interactions have proven useful to understand infection dynamics to distinguish between different mechanisms that sustain infections.
In the early models of mathematical modelling of immunity to malaria, proposed by [Aron and May, 1982], maintenance of acquired immunity in response to repeated exposure was defined as the rate of reversion, γ, which is defined as the average duration for which immunity lasts, assuming that immunity can only last up to a few years (incorporated as τ if repeated exposure does not occur), in a completely susceptible population experiencing a rate of h infections per year. Mathematically, the rate of reversion was defined a monotonically decreasing function given by: $\gamma(h) = \frac{he^{-h\tau}}{1-e^{-h\tau}}$
The rate of loss of immunity thus defined, as proposed by Aron, decayed faster in the absence of exposure. Incorporating exposure dependent immunity functions thus paved for understanding immuno-epidemiology of malaria infection in regions of varying transmission. However, to design strategies to combat malaria, we need to better understand host-pathogen dynamics and this involves understanding

mechanisms that shape the parasite population in chronic infections. Since within-host data pertaining to 'naive' or 'non-naive' individuals is critically limited, malaria research has benefited from mathematical modelling. In this chapter, we emphasize one such class of mathematical models that captures events within an individual host: "within host" models that take into account the parasite's interaction with the host's immune system [Dietz et al., 2006; Childs and Buckee, 2015; Recker et al., 2004; Camponovo et al., 2021].

We include switching mechanisms to an ODE based model because continuous models have the advantage of being studied analytically. Theoretical models and *in vitro* data [Horrocks et al., 2004; Recker et al., 2011; Noble and Recker, 2012; Noble et al., 2013] indicate that differences in the rate at which the parasite switches the expressed *var*genes or differences in the growth rates of parasites expressing different *var* genes [Molineaux et al., 2001] are the primary processes by which the parasite avoids diminishing its *var* repertoire early in the infection. However, unlike other species that exploit antigenic variation to elude the immune system, *P. falciparum* has a smaller *var* gene repertoire per haploid genome. Because the number of asexual parasites at the height of a primary acute infection is extremely high (in the order of many billions), even low switching rates would result in the immune system seeing all variations early in an infection. To address this caveat, malaria models have investigated the role of a transient cross-reactive response against variants at the blood stage [Recker et al., 2004; Klein et al., 2014] and we incorporate the same approach in our model.

The model that is analysed mathematically in the following sections, originally proposed by [Nowak and May, 2000] and currently adapted to malaria accounts for antigenic variation in the parasite population. Additionally, the model also describes the production of immune responses directed against (i) antigens unique to particular parasite variations (variant specific) and (ii) antigens shared by all parasite variants (cross-reactive). Model analysis allows us to assess the relative impact of variant-specific and cross-reactive immune responses in parasite control in long-lasting infections.

In the case of chronic malaria infections in endemic regions, specific and cross-reactive responses differ by targeting unique or shared epitopes on the infected cell's surface, and this phenomenon coupled with antigenic variation exhibited by the

parasite add to the complexity of modelling the within- host dynamics. Although the mathematical model was initially used to understand viral infection exhibiting antigenic variation, it can be easily adapted to study malaria and its development, as described in the following sections.

3.1 Nowak's Model of Antigenic Variation

In the 1990's Nowak proposed a mathematical theory for the progression of HIV infection as an evolutionary process. The basic idea of this theory was that the virus evolution during individual infections enables the virus to escape the immune system response. This process was called antigenic variation. A basic model of antigenic variation was built using the following assumptions:

(**i**) the virus is recognized by the immune response.

(**ii**) the virus can mutate during the course of infection producing variants.

(**iii**) the presence of each variant induces a specific immune response that recognizes and eliminates the specific variant .

(**iv**) viruses induce also a cross-reactive immune response that recognize and eliminate a large variety of viruses with shared epitopes.

This model is generic enough to be applied to any pathogen undergoing antigenic variation. In our case we apply it to malaria parasites and correct parameter assumptions based on literature. In our case, we adapt the cross-reactive response as a shared adaptive response which captures the effects of cross-reactivity between specific variants implicitly like in the model[Molineaux et al., 2001].

The basic model is described by a a set of ordinary differential equations (ODEs) Nowak and May [2000]. The ODE variables are the antigenic variants used to define the system of a parasite population interacting with the immune system during a single

infection, as well as the intensities of the specific and cross-reactive immune responses:

$$\dot{v}_i = v_i(r - px_i - qz) \tag{3.1}$$

$$\dot{x}_i = av_i \tag{3.2}$$

$$\dot{z} = k\sum_i v_i - bz, \tag{3.3}$$

for all $i \in [1, N]$.

The following interpretation elements are provided for the understanding of the system of ODEs:

- The first set of equations (3.1), represent the rate of change of the variable v_i over time, where v_i is the number of parasites of the variant i in the population. r is the growth rate, considered even for each variant; the parasites are under selective pressure due to elimination by the specific and cross-reactive immune responses, x_i and z, which are moderated by the rate constants p and q, respectively.

- The second set of equations (3.2) represent the dynamics of the specific response against each unique variant, which is directly proportional to the amount of parasites expressing the variant v_i. Like in the original Nowak's model, we assume that the specific response to a unique variant has infinite memory, which means that these equations contain no degradation terms.

- The third equation (3.3) represents the dynamics of the cross-reactive response z, influenced by the collective presence of all v_i, and also experiencing a natural decay. The term $k\sum_i v_i$ represents the cumulative effect of all variants v_i, while bz represents the natural decay of z. In other models, the cross-reactive immune response, z, has been modelled by including only the number of minor epitopes shared amongst variants. For simplicity, we assume that the cross-reactive response acts on all variants equally.

- N is the number of *var* genes.

In this system, we assume that both x_i and z are absent at $t = 0$, i.e. there is no immune response at the beginning of infection and both specific and cross-reactive immune responses are triggered by the parasite growth in the host.

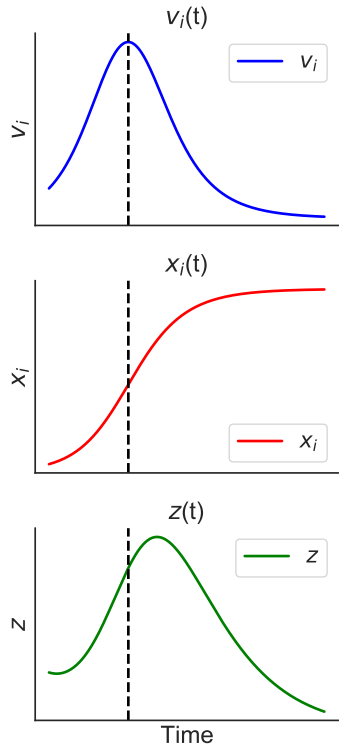

Figure 3.1: General Solution for the time series of the parasite (v_i) and host specific $(x_i$ and cross-reactive (z) immune responses, for a given antigent variant i

3.1.1 Matched asymptotic solutions of the model with non-overlapping parasitemia peaks

The model is a system of $2N + 1$ ODEs, among which N are non-linear. The system is not integrable and it is not possible to obtain analytic solutions. However, under certain approximations, it is possible to compute solutions analytically. By experimenting with the model, we notice that solutions present peaks when the parasite population increases while expressing a single gene i (Figure 3.1); successive peaks can express different genes and co-expression of two or more different genes by the same population is possible (peaks can overlap). In order to obtain analytic solutions, we consider first that peaks are well separated and that the overlap can be

neglected.

Although this condition is appropriate for antigenic variation in HIV [Lipsitch and O'Hagan, 2007] and also *Trypanosoma brucei* infections [Horn, 2014], the simplified model does not handle all the intricacies of the *Plasmodium falciparum* infection that involves parasites expressing many different variants. We will release this constraint in the models that will be studied numerically in the next sections.

We will use matched asymptotic expansions [Holmes, 2012; Lagerstrom, 2013] to describe solutions with non-overlapping peaks. The principle of this method is to consider that the solution has several parts, called inner or boundary layers, where parasitemia and the intensities of immune responses change quickly and other parts, called outer layers, where these variables change slowly. Continuity conditions (Prandl's matching principle) allow the matching of boundary layer and outer solutions. When boundary layers are in between outer solutions the fast variation of the boundary layer fast variables results in a jump of the solution from one outer layer to another.

In order to justify this approach we start by rescaling the variables and parameters of the model. Let us define the new variables and parameters $\tilde{x}_i = x_i/a$, $\tilde{z} = z/k$, $\tilde{v}_i = v_i/r$, $\bar{t} = rt$, $\tilde{p} = pa/r$, $\tilde{q} = qK/r$, $\epsilon = b/r$. Using these variables and parameters the system of ODEs reads:

$$\begin{aligned}
\frac{d\tilde{v}_i}{d\bar{t}} &= \tilde{v}_i(1 - \tilde{p}\tilde{x}_i - \tilde{q}\tilde{z}),\\
\frac{d\tilde{x}_i}{d\bar{t}} &= \tilde{v}_i,\\
\frac{d\tilde{z}}{d\bar{t}} &= \sum_{i=1}^{N} \tilde{v}_i - \epsilon\tilde{z},\\
&\quad \text{for all } i \in [1, N].
\end{aligned} \tag{3.4}$$

We consider that the parameter ϵ is small, which means that the memory of the cross-reactive immune response is large compared to the parasite generation time.

Under this assumption we look for the inner layer solution as an expansion in

powers of ϵ:

$$\begin{pmatrix} \tilde{v} \\ \tilde{\mathbf{x}} \\ \tilde{z} \end{pmatrix}_{in} = \begin{pmatrix} \tilde{v}_0 \\ \tilde{\mathbf{x}}_0 \\ \tilde{z}_0 \end{pmatrix}_{in} + \epsilon \begin{pmatrix} \tilde{v}_1 \\ \tilde{\mathbf{x}}_1 \\ \tilde{z}_1 \end{pmatrix}_{in} + \dots \tag{3.5}$$

Inserting (3.5) in (3.4) we find that the lowest (zero-th) order in ϵ term in the solution has to satisfy the inner layer equation:

$$\begin{aligned} \frac{d\tilde{v}_i}{d\bar{t}} &= \tilde{v}_i(1 - \tilde{p}\tilde{x}_i - \tilde{q}\tilde{z}), \\ \frac{d\tilde{x}_i}{d\bar{t}} &= \tilde{v}_i, \\ \frac{d\tilde{z}}{d\bar{t}} &= \sum_{i=1}^{N} \tilde{v}_i, \\ & \text{for all } i \in [1, N]. \end{aligned} \tag{3.6}$$

Under the assumption that each inner layer involves a single antigen ($\tilde{v}_j = 0$ for all $j \neq i$), this reads

$$\begin{aligned} \frac{d\tilde{v}_i}{d\bar{t}} &= \tilde{v}_i(1 - \tilde{p}\tilde{x}_i - \tilde{q}\tilde{z}), \\ \frac{d\tilde{x}_i}{d\bar{t}} &= \tilde{v}_i, \\ \frac{d\tilde{z}}{d\bar{t}} &= \tilde{v}_i, \end{aligned} \tag{3.7}$$

Changing the time variable to $\tau = \epsilon\bar{t}$ (slow time) in (3.4) we obtain

$$\begin{aligned} \epsilon\frac{d\tilde{v}_i}{d\tau} &= \tilde{v}_i(1 - \tilde{p}\tilde{x}_i - \tilde{q}\tilde{z}), \\ \epsilon\frac{d\tilde{x}_i}{d\tau} &= \tilde{v}_i, \\ \epsilon\frac{d\tilde{z}}{d\tau} &= \sum_{i=1}^{N} \tilde{v}_i - \epsilon\tilde{z}, \\ & \text{for all } i \in [1, N]. \end{aligned} \tag{3.8}$$

The outer solution is a solution of (3.8) expressed as an expansion in powers of ϵ.

$$\begin{pmatrix} \tilde{v} \\ \tilde{\mathbf{x}} \\ \tilde{z} \end{pmatrix}_{out} = \begin{pmatrix} \tilde{v}_0 \\ \tilde{\mathbf{x}}_0 \\ \tilde{z}_0 \end{pmatrix}_{out} + \epsilon \begin{pmatrix} \tilde{v}_1 \\ \tilde{\mathbf{x}}_1 \\ \tilde{z}_1 \end{pmatrix}_{out} + \dots \tag{3.9}$$

Inserting (3.9) in (3.8) we find that the lowest order (zero-th order) term of the outer solution should verify the outer equation:

$$\begin{aligned} \tilde{v}_i &= 0, \\ \frac{d\tilde{x}_i}{d\tau} &= 0, \\ \frac{d\tilde{z}}{d\tau} &= -\tilde{z}, \\ &\text{for all } i \in [1, N]. \end{aligned} \tag{3.10}$$

Solution of the inner layer equation

Let us first show (3.7) has two first integrals, i.e. it is an integrable system.

Indeed, substraction of the last two equations of (3.7) leads to

$$\frac{d\left(\tilde{x}_i - \tilde{z}\right)}{d\bar{t}} = 0 \implies \tilde{x}_i - \tilde{z} = \text{const.} \tag{3.11}$$

In other words, $\tilde{x}_i - \tilde{z}$ is a linear first integral, indicating that the projection of orbits on the plane $(\tilde{x}_i, \tilde{z})$ are lines.

Using (3.7) we find that

$$\frac{d\left[\tilde{v}_i + \frac{(1-\tilde{p}x_i - \tilde{q}\tilde{z})^2}{2(\tilde{p}+\tilde{q})}\right]}{d\bar{t}} = 0 \implies \tilde{v}_i + \frac{(1-\tilde{p}x_i - \tilde{q}\tilde{z})^2}{2(\tilde{p}+\tilde{q})} = \text{const.} \tag{3.12}$$

In other words, $\tilde{v}_i + \frac{(1-\tilde{p}x_i - \tilde{q}\tilde{z})^2}{2(\tilde{p}+\tilde{q})}$ is a quadratic first integral indicating that the projection of orbits on the plane $(\tilde{x}_i, \tilde{v}_i)$ are parabolas (see Figure 3.2).

We can use the two first integrals to eliminate the variables $\tilde{z}$ and $\tilde{v}_i$ and write a reduced ODE for the variable $\tilde{x}_i$. However, it is instructive to do it stepwise, and eliminate first $\tilde{z}$.

Using (3.11) we find that

$$\tilde{z} = \tilde{x}_i + \tilde{z}^- - \tilde{x}_i^-, \tag{3.13}$$

where $\tilde{x}_i^- = \lim_{\bar{t}\to-\infty} \tilde{x}_i$, $\tilde{z}^- = \lim_{\bar{t}\to-\infty} \tilde{z}$.

Substituting in the first two equations of (3.7) we obtain

$$\begin{aligned} \frac{d\tilde{v}_i}{d\bar{t}} &= \tilde{v}_i(r' - (\tilde{p}+\tilde{q})\tilde{x}_i), \\ \frac{d\tilde{x}_i}{d\bar{t}} &= \tilde{v}_i, \end{aligned} \tag{3.14}$$

where $r' = 1 + \tilde{q}(\tilde{x}_i^- - \tilde{z}^-)$.

Analysis of the Reduced 2-D System

The reduced model described by (3.14) is well known. It is the same as the reduced SIR model obtained from the compartmental epidemiological model SIR [Kermack and McKendrick, 1927] after elimination of the S variable using the conservation law $S + I + R = \text{const.}$. Like the SIR model, our 2D reduced model (3.14) has a phase portrait with parabolic orbits (Figure 3.2). Indeed, from (3.12) and utilizing $\lim_{\bar{t}\to\infty} \tilde{v}_i = 0$ we find that all orbits of the dynamical system are parabolas defined by the equation

$$\tilde{v}_i + \frac{(r' - (\tilde{p}+\tilde{q})x_i)^2}{2(\tilde{p}+\tilde{q})} = \frac{(r' - (\tilde{p}+\tilde{q})x_i^-)^2}{2(\tilde{p}+\tilde{q})}. \tag{3.15}$$

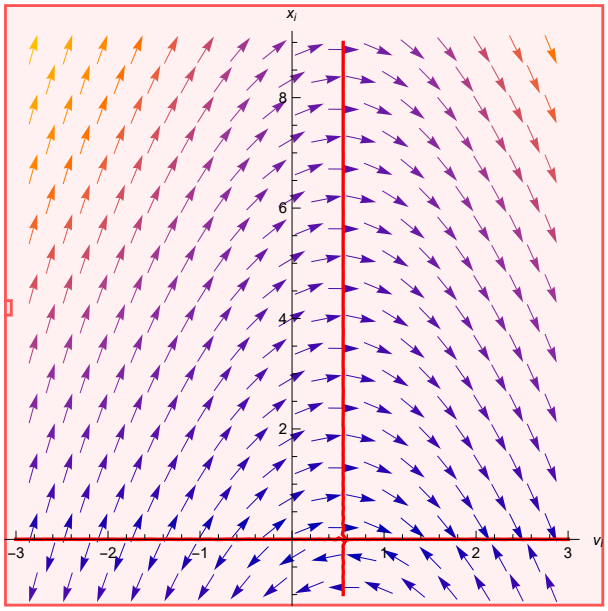

Figure 3.2: The trajectories of both $\tilde{v}_i$ and $\tilde{x}_i$ are highlighted by the vector field and the x and y nullclines (red) are given by the solutions $\frac{d\tilde{x}_i}{d\bar{t}} = 0$ & $\frac{d\tilde{v}_i}{d\bar{t}} = 0$ respectively.

The reduced form of the system can be visualized using a phase-portrait of the variant in which $\tilde{v}_i$ and the corresponding immune response $\tilde{x}_i$ are represented over time. The steady states of the reduced system are degenerate, corresponding to vanishing parasitemia $\tilde{v}_i = 0$. The steady states

$$\tilde{v}_i = 0, \tilde{x}_i > r'/(\tilde{p}+\tilde{q}),$$

situated at the right of the vertical $\tilde{v}_i-$ nullcline are stable, whereas the steady states

$$\tilde{v}_i = 0, \tilde{x}_i < r'/(\tilde{p}+\tilde{q}),$$

situated at the left of the vertical $\tilde{v}_i-$ nullcline are unstable. Typically, an orbit goes from $\tilde{x}_i^- < r'/(\tilde{p}+\tilde{q})$ to $2r'/(\tilde{p}+\tilde{q}) - \tilde{x}_i^- > r'/(\tilde{p}+\tilde{q})$ corresponding to corresponding to to $\bar{t} = -\infty$ and $\bar{t} = \infty$, respectively. There is a parasitemia peak at $\tilde{x}_i = r'/(\tilde{p}+\tilde{q})$ where $\tilde{v}_i = \frac{(r'-(\tilde{p}+\tilde{q})x_i^-)^2}{2(\tilde{p}+\tilde{q})}$ (see (3.15)).

Computing the inner layer solution

Using the first integral (3.12) we can now reduce the system to only one ODE:

$$\frac{d\tilde{x}_i}{d\bar{t}} = \frac{(r'-(\tilde{p}+\tilde{q})x_i^-)^2}{2(\tilde{p}+\tilde{q})} - \frac{(r'-(\tilde{p}+\tilde{q})x_i)^2}{2(\tilde{p}+\tilde{q})}. \tag{3.16}$$

(3.16) is integrable by separation of variables.

Considering that the time origin is the parasitemia peak of the variant i, from (3.16)

it follows

$$\int_{r'/(\tilde{p}+\tilde{q})}^{\tilde{x}_i} \frac{dx}{\frac{(r'-(\tilde{p}+\tilde{q})x_i^-)^2}{2(\tilde{p}+\tilde{q})} - \frac{(r'-(\tilde{p}+\tilde{q})x)^2}{2(\tilde{p}+\tilde{q})}} = \bar{t}. \tag{3.17}$$

In order to compute (3.17) we define $y = \frac{(\tilde{p}+\tilde{q})x - r'}{r'-(\tilde{p}+\tilde{q})x_i^-}$ that satisfies

$$-1 < y < 1, \text{ for all } x \in (x_i^-, 2r' - x_i^-).$$

From (3.17) it follows that

$$\int_0^{y(\tilde{x}_i^-)} \frac{dy}{1-y^2} = \log \frac{1+y(\tilde{x}_i^-)}{1-y(\tilde{x}_i^-)} = (r' - (\tilde{p}+\tilde{q})x_i^-)\bar{t},$$

and finally

$$\tilde{x}_i(\bar{t}) = \frac{r' + (r' - (\tilde{p}+\tilde{q})\tilde{x}_i^-)}{\tilde{p}+\tilde{q}} = \frac{r'}{\tilde{p}+\tilde{q}} + \left[\frac{r'}{\tilde{p}+\tilde{q}} - x_i^-\right] \frac{1 - \exp\left[(r' - (\tilde{p}+\tilde{q})x_i^-)\bar{t}\right]}{1 + \exp\left[(r' - (\tilde{p}+\tilde{q})x_i^-)\bar{t}\right]} \tag{3.18}$$

Using (3.15) we find

$$\tilde{v}_i(\bar{t}) = \frac{(r' - (\tilde{p}+\tilde{q})x_i^-)^2}{2(\tilde{p}+\tilde{q})} - \frac{(r' - (\tilde{p}+\tilde{q})\tilde{x}_i(\bar{t}))^2}{2(\tilde{p}+\tilde{q})}. \tag{3.19}$$

Let us introduce a new function $\mu_i(\bar{t}) = 1 - \tilde{p}\tilde{x}_i(\bar{t}) - \tilde{q}\tilde{z}(\bar{t})$ and consider the following

Condition 1. $\mu_i(-\infty) = 1 - \tilde{p}\tilde{x}_i^- - \tilde{q}\tilde{z}^- > 0$.

The following property summarizes the behavior of the inner layer solution

Proposition 2. *The inner layer problem has solutions $(\tilde{v}_i(\bar{t}), \tilde{x}_i(\bar{t}), \tilde{z}(\bar{t}))$ defined for $-\infty < \bar{t} < \infty$. If the Condition 1 is satisfied, then the solutions of the model behave in the following way:*

i) *the specific immune response against variant i, $\tilde{x}_i$, increases from $\tilde{x}_i(-\infty) = \tilde{x}_i^-$ to $\tilde{x}_i(\infty) = \tilde{x}_i^- + \frac{2}{\tilde{p}+\tilde{q}}(1 - \tilde{q}\tilde{z}^- - \tilde{p}\tilde{x}_i^-)$,*

ii) *the cross reactive immune response increases from $\tilde{z}(-\infty) = \tilde{z}^-$ to $\tilde{z}(\infty) = \tilde{z}^- + \frac{2}{\tilde{p}+\tilde{q}}(1 - \tilde{q}\tilde{z}^- - \tilde{p}\tilde{x}_i^-)$,*

iii) *μ_i decreases from $\mu_i(-\infty) = 1 - \tilde{p}\tilde{x}_i^- - \tilde{q}\tilde{z}^- > 0$ to $\mu_i(\infty) = -\mu_i(-\infty)$,*

iv) *the parasitemia $\tilde{v}_i$ has a peak at $\bar{t} = 0$ $\tilde{v}(0) = \frac{(1-\tilde{q}\tilde{z}^- - \tilde{p}\tilde{x}_i^-)^2}{2(\tilde{p}+\tilde{q})}$, and vanishes when $\bar{t} \to \pm\infty$.*

Proof. i) Condition 1 implies that $\tilde{x}_i = \tilde{x}_i^-, \tilde{z} = \tilde{z}^-, \tilde{v}_i = 0$ is an unstable steady state and the infection peak can develop from any arbitrary neighborhood of this state. Therefore this state is the α-limit of the trajectory (see also (3.1.1)). The ω-limit of the trajectory is the second solution of the equation (3.15) with $\tilde{v}_i = 0$, i.e.

$$\frac{r' - (\tilde{p}+\tilde{q})\tilde{x}_i^+}{2(\tilde{p}+\tilde{q})} = -\frac{r' - (\tilde{p}+\tilde{q})\tilde{x}_i^-}{2(\tilde{p}+\tilde{q})},$$

where $\tilde{x}_i^+ = \lim_{\bar{t}\to\infty} \tilde{x}_i(\bar{t})$. It follows that

$$\tilde{x}_i(\infty) = \tilde{x}_i^- + \frac{2}{\tilde{p}+\tilde{q}}(1 - \tilde{q}\tilde{z}^- - \tilde{p}\tilde{x}_i^-).$$

ii) Using (3.1.1) it follows that

$$\tilde{z}(-\infty) = \tilde{z}^+ = \tilde{x}_i^+ + \tilde{z}^- - \tilde{x}_i^- = \tilde{z}^- + \frac{2}{\tilde{p}+\tilde{q}}(1 - \tilde{q}\tilde{z}^- - \tilde{p}\tilde{x}_i^-).$$

iii) Using the definition

$$\mu_i(\bar{t}) = 1 - \tilde{p}\tilde{x}_i(\bar{t}) - \tilde{q}\tilde{z}(\bar{t}),$$

and the two previous results it follows

$$\mu_i(\infty) = 1 - \tilde{p}\tilde{x}_i^+ - \tilde{q}\tilde{z}^+ = -(1 - \tilde{p}\tilde{x}_i^- - \tilde{q}\tilde{z}^-) = -\mu_i(-\infty).$$

iv) Here we only need to compute the parasitemia at the peak, i.e. when $\frac{d\tilde{v}_i}{d\bar{t}} = 0$, which means

$$\tilde{x}_i(0) = \frac{r'}{\tilde{p}+\tilde{q}}.$$

Using the conservation law (3.15) we find

$$\tilde{v}_i(0) = \frac{(r' - (\tilde{p}+\tilde{q})\tilde{x}_i^-)^2}{2(\tilde{p}+\tilde{q})} - \frac{(r' - (\tilde{p}+\tilde{q})\tilde{x}_i(0))^2}{2(\tilde{p}+\tilde{q})} = \frac{(1 - \tilde{q}\tilde{z}^- - \tilde{p}\tilde{x}_i^-)^2}{2(\tilde{p}+\tilde{q})}.$$

□

Solution of the outer layer equation

The solution of the outer later equation is straightforward from (3.10). It reads

$$\begin{aligned} \tilde{v}_i &= v_i^{out}(0), && (3.20)\\ \tilde{x}_i &= x_i^{out}(0), && (3.21)\\ \tilde{z} &= \tilde{z}^{out}(0)\exp(-\tau), && (3.22) \end{aligned}$$

Matching condition

In the matched asymptotic expansion method, the inner and outer solutions should match. We use here Prandl's condition [Lagerstrom, 2013] that reads

$$\begin{pmatrix} \tilde{v}(\infty) \\ \tilde{\mathbf{x}}(\infty) \\ \tilde{z}(\infty) \end{pmatrix}_{in} = \begin{pmatrix} \tilde{v}(0) \\ \tilde{\mathbf{x}}(0) \\ \tilde{z}(0) \end{pmatrix}_{out} \tag{3.23}$$

At the zero-th order in ϵ this leads to

$$\begin{aligned} v_i^{out}(0) &= 0,\\ x_i^{out}(0) &= \tilde{x}_i^- + \frac{2}{\tilde{p}+\tilde{q}}(1-\tilde{q}\tilde{z}^- - \tilde{p}\tilde{x}_i^-),\\ \tilde{z}^{out}(0) &= \tilde{z}^- + \frac{2}{\tilde{p}+\tilde{q}}(1-\tilde{q}\tilde{z}^- - \tilde{p}\tilde{x}_i^-). \end{aligned} \tag{3.24}$$

3.1.2 Multiple peak solutions

The arguments from the preceding section work also when there are multiple peaks of infection. An assumption of the model is that each peak corresponds to the development of a different variant i. Supposing that there are N variants $i \in \{1,\dots N\}$ we denote by $i_1, i_2, \dots, i_n, \dots$ $\tau_1, \tau_2, \dots, \tau_n, \dots$ the variant and the time of maximum parasitemia for successive peaks. Here $i_n \in \{1,2,\dots,N\}$ but variants can repeat in the series.

In order to analyze solutions we consider that each peak has short duration and represents an inner layer, whereas between successive inner layers there are outer layers. Inner and outer solutions are computed like in the preceding sections.

Let us denote by $\tilde{z}_n^-$, $\tilde{z}_n^+$ the values of the inner layer solution at times $\bar{t} \to -\infty$ and $\bar{t} \to \infty$, respectively. Similarly μ_n^-, $\mu_n^+ = -\mu_n^-$ are values of μ at $\bar{t} \to -\infty$ and $\bar{t} \to \infty$, respectively. Finally, $\tilde{x}_n^i$ is the value of $\tilde{x}_i$ in the n-th inner layer at $\bar{t} \to -\infty$.

Equivalently, we have the one-sided limits

$$\begin{aligned}
\lim_{\tau \to \tau_n^+} \tilde{x}_i(\tau) &= \tilde{x}_{n+1}^i, \lim_{\tau \to \tau_n^-} \tilde{x}_i(\tau) = \tilde{x}_n^i, && (3.25)\\
\lim_{\tau \to \tau_n^+} \tilde{z}(\tau) &= \tilde{z}_n^+, \lim_{\tau \to \tau_n^-} \tilde{z}(\tau) = \tilde{z}_n^-, && (3.26)\\
\lim_{\tau \to \tau_n^+} \mu(\tau) &= -\mu_n, \lim_{\tau \to \tau_n^-} \mu(\tau) = \mu_n. && (3.27)
\end{aligned}$$

Between two subsequent peaks, the outer solution can be expressed as:

$$\begin{aligned}
\tilde{v}_i(\tau) &= 0,\\
\tilde{x}_i(\tau) &= \tilde{x}_n^i\\
\tilde{z}(\tau) &= \tilde{z}_{n-1}^+ \exp(\tau - \tau_{n-1})\\
&\quad \text{for } \tau_{n-1} < \tau \leq \tau_n \qquad (3.28)
\end{aligned}$$

From one peak to another, one has the following recursion

$$\tilde{x}_{n+1}^i = \tilde{x}_n^i + \frac{2}{\tilde{p}+\tilde{q}}(1 - \tilde{q}\tilde{z}_n^- - \tilde{p}x_n^i), \qquad (3.29)$$

$$\tilde{x}_{n+1}^j = \tilde{x}_n^j, \text{ for all } j \neq i, \qquad (3.30)$$

$$\tilde{z}_n^+ = \tilde{z}_n^- + \frac{2}{\tilde{p}+\tilde{q}}(1 - \tilde{q}\tilde{z}_n^- - \tilde{p}x_n^i), \qquad (3.31)$$

provided the antigen i developed at the n-th peak.

In other words, the parasites expressing the antigen i have developed and have been cleared during the peak n by inducing equal increases of the rescaled specific and cross-reactive immune responses.

Equation (3.28) shows that the specific immune response remains constant between peaks, whereas the cross-reactive immune response decreases exponentially from one

peak to another. In particular, one has

$$\tilde{z}_n^- = \tilde{z}_{n-1}^+ \exp(\tau_n - \tau_{n-1}). \tag{3.32}$$

In order to write a recursion for $\tilde{z}_n^-$ let us notice that the cross-reactive immune response before peak satisfies two conditions.

The first condition follows from Condition 1. The peak can occur only if the Condition 1 is fulfilled, which for the $n+1$-th peak reads

$$\mu_{n+1}^i > 0.$$

The following identity is straightforward

$$\mu_{n+1}^i = \frac{\tilde{q}-\tilde{p}}{\tilde{p}+\tilde{q}}\mu_n^i + \tilde{q}(\tilde{z}_n^- - \tilde{z}_{n+1}^-)), \tag{3.33}$$

and leads to the following peak development condition

$$\tilde{z}_{n+1}^- < \tilde{z}_n^- + \frac{\tilde{q}-\tilde{p}}{\tilde{p}+\tilde{q}}(1 - \tilde{p}\tilde{x}_n^i - \tilde{q}z_n^-). \tag{3.34}$$

Immediately after the peak of the variant i the quantity μ_n^i is negative and therefore there is a latency period during which no new peak of the antigen i can occur. During this latency period the cross-reactive immune response has to decrease sufficiently enough to make μ_n^i positive again.

Because of the exponential decrease (3.32), the cross-reactive response also satisfies

$$\tilde{z}_{n+1}^- < \tilde{z}_n^+ = \tilde{z}_n^- + \frac{2}{\tilde{p}+\tilde{q}}(1 - \tilde{q}\tilde{z}_n^- - \tilde{p}x_n^i) \tag{3.35}$$

z_{n+1}^- satisfying (3.34) and (3.35) belongs to an interval

$$z_{n+1}^- \in (0, \min(\tilde{z}_n^- + \frac{2}{\tilde{p}+\tilde{q}}(1 - \tilde{q}\tilde{z}_n^- - \tilde{p}x_n^i), \tilde{z}_n^- + \frac{\tilde{q}-\tilde{p}}{\tilde{p}+\tilde{q}}(1 - \tilde{p}\tilde{x}_n^i - \tilde{q}z_n^-))) \tag{3.36}$$

Although the precise position can be computed using higher order terms in the matched asymptotic expansion, the region that should be investigated correspond to parasitemia close to zero, in which case the deterministic model fails and one has to

consider stochastic effects. For the sake of simplicity, we modify the model to account for some stochasticity and simply assume that the next peak occur for any z^-_{n+1} distributed uniformly in the interval (3.36). More precisely we consider the following modelling assumption

Assumption 3. $z^-_{n+1} \sim U(0, \min(\tilde{z}^-_n + \frac{2}{\tilde{p}+\tilde{q}}(1-\tilde{q}\tilde{z}^-_n - \tilde{p}x^i_n), \tilde{z}^-_n + \frac{\tilde{q}-\tilde{p}}{\tilde{p}+\tilde{q}}(1-\tilde{p}\tilde{x}^i_n - \tilde{q}z^-_n)))$, where U stands for the uniform continuous distribution.

Multiple peaks in the absence of antigenic variation

Let us consider that the parasite can express only one antigen i. In this case the parasite can infect the host at multiple times because the specific response is not sufficient for eliminating the parasite and the cross-reactive response ensures protection for a finite time. This leads to multiple peak solutions. However, the amplitude of the peaks becomes lower and eventually vanishes after a number of peaks. In order to prove this property mathematically we consider the following recursion model:

$$\tilde{x}^i_{n+1} = \tilde{x}^i_n + \frac{2}{\tilde{p}+\tilde{q}}(1-\tilde{q}\tilde{z}^-_n - \tilde{p}x^i_n), \tag{3.37}$$

$$z^-_{n+1} \sim U(0, \tilde{z}^-_n + \frac{\tilde{q}-\tilde{p}}{\tilde{p}+\tilde{q}}(1-\tilde{p}\tilde{x}^i_n - \tilde{q}z^-_n)). \tag{3.38}$$

Indeed, in this case the min in Assumption 3 is always the second term because $\frac{2}{\tilde{p}+\tilde{q}} > \frac{\tilde{q}-\tilde{p}}{\tilde{p}+\tilde{q}}$.

From the Proposition 2 the peak amplitudes in this model are

$$\tilde{v}^{max}_n = \frac{(\mu^i_n)^2}{2(\tilde{p}+\tilde{q})}$$

We can prove the following

Proposition 4. *Suppose that $\tilde{q} > \tilde{p}$ which means that the cross-reactive response is more effective than the specific response. Then, for almost all trajectories we have:*

i) $\lim_{n\to\infty} \tilde{x}^i_n = 1$,

ii) $\lim_{n\to\infty} \tilde{z}^-_n = 0$,

iii) $\lim_{n\to\infty} \tilde{v}_n^{max} = 0$.

For the proof we need a Lemma.

Lemma 1. *For all* $0 < \zeta < 1$ *and series* u_n, v_n *satisfying*

$$u_{n+1} = u_n + (1-\zeta)(1-u_n-v_n), \tag{3.39}$$
$$v_{n+1} \sim U(0, v_n + \zeta(1-u_n-v_n)), \tag{3.40}$$

where U *denotes the uniform continuous distribution* (*independent on* u_n *and* v_n) *we have*

i) $\lim_{n\to\infty} u_n = 1$, *almost surely,*

ii) $\lim_{n\to\infty} v_n = 0$, *almost surely.*

Proof of the Lemma 1. Let us define $w_n = 1 - u_n$. It follows that

$$w_{n+1} = \zeta w_n + (1-\zeta)v_n,$$
$$v_{n+1} \sim U(0, (1-\zeta)v_n + \zeta w_n)).$$

We find that

$$\begin{pmatrix} \mathbb{E}\left[w_{n+1}^2\right] \\ \mathbb{E}\left[v_{n+1}^2\right] \\ \mathbb{E}[w_{n+1}v_{n+1}] \end{pmatrix} = A \begin{pmatrix} \mathbb{E}\left[w_n^2\right] \\ \mathbb{E}\left[v_n^2\right] \\ \mathbb{E}[w_n v_n] \end{pmatrix},$$

where A is the following matrix

$$A = \begin{pmatrix} \zeta^2 & (1-\zeta)^2 & 2\zeta(1-\zeta) \\ \frac{1}{3}\zeta^2 & \frac{1}{3}(1-\zeta)^2 & \frac{2}{3}\zeta(1-\zeta) \\ \frac{1}{2}\zeta^2 & \frac{1}{2}(1-\zeta)^2 & \zeta(1-\zeta) \end{pmatrix}$$

A has two eigenvalues equal to zero and the non-zero eigenvalue is smaller than one, $\lambda_g = \frac{\zeta^2+\zeta+1}{3} < 1$.

It follows that

$$\mathbb{E}\left[w_n^2 + v_n^2 + w_n v_n\right] \leq C\lambda_g^{n-1},$$

and

$$\sum_{n\geq 1} \mathbb{E}\Big[w_n^2 + v_n^2 + w_n v_n\Big] < \infty.$$

As w_n, v_n are positive variables we also have

$$\sum_{n\geq 1} \mathbb{E}\Big[w_n^2 + v_n^2\Big] < \infty,$$

which means that $\lim_{n\to\infty} w_n = \lim_{n\to\infty} v_n = 0$ almost surely.

□

Remark 5. The Lemma holds if the uniform continuous distribution is replaced by any continuous distribution with the same support. The proof in this more general case follows the same lines.

Proof of the Proposition 4. The proof of the proposition is now straightforward. It is enough to identify u_n, v_n, ζ with $\tilde{x}_n^i$, $\tilde{z}_n^-$, $\frac{\tilde{q}-\tilde{p}}{\tilde{q}+\tilde{p}}$, respectively. □

Multiple peaks in the presence of antigenic variation

In order to compute the peaks of parasites expressing different antigens, we consider the following modelling assumptions:

Assumption 6. At each step n the variant i_n is drawn uniformly from the set $\{1,2,\ldots,N\}$ independently on the history.

With this assumption the model reads

$$\begin{aligned}
i_{n+1} &\sim U\{1,2,\ldots,N\}, && (3.41)\\
\tilde{x}_{n+1}^{i_n} &= \tilde{x}_n^{i_n} + \frac{2}{\tilde{p}+\tilde{q}}(1-\tilde{q}\tilde{z}_n^- - \tilde{p}x_n^{i_n}), && (3.42)\\
\tilde{x}_{n+1}^{j} &= \tilde{x}_n^{j}, \text{ for all } j \neq i_n, && (3.43)\\
z_{n+1}^- &\sim U(0, \min(\tilde{z}_n^- + \frac{2}{\tilde{p}+\tilde{q}}(1-\tilde{q}\tilde{z}_n^- - \tilde{p}x_n^{i_n}), \tilde{z}_n^- + \frac{\tilde{q}-\tilde{p}}{\tilde{p}+\tilde{q}}(1-\tilde{p}\tilde{x}_n^{i_n} - \tilde{q}z_n^-)) && (3.44)
\end{aligned}$$

where the discrete and continuous uniform distributions are independent among themselves and with respect to the past $(\tilde{x}_{\leq n}^i, z_{\leq n}^-)$.

Proposition 7. *Suppose that $\tilde{q} > \tilde{p}$ which means that the cross-reactive response is more effective than the specific response. Then, for almost all trajectories of the model described by* (3.41) *we have:*

i) $\lim_{n\to\infty} \tilde{x}_n^i = 1$, *for all* $i \in \{1,2,\ldots,N\}$,

ii) $\lim_{n\to\infty} \tilde{z}_n^- = 0$,

iii) $\lim_{n\to\infty} \tilde{v}_n^{max} = 0$, *where* v_n^{max} *represents the maximal parasitemia at peak* n.

We define the extinction time as the time needed to have peaks below a small fraction of the maximal amplitude (the amplitude of the first peak). In order to compute this time and compare it across different situations (various numbers of antigens) we need the time between successive peaks. This result from the relation

$$\tilde{z}_{n+1}^- = \tilde{z}_n^+ \exp(\tau_{n+1} - \tau_n) = (\tilde{z}_n^- + \frac{2}{\tilde{p}+\tilde{q}}(1 - \tilde{q}\tilde{z}_n^- - \tilde{p}x_n^{i_n}))\exp(-\tau_{n+1} + \tau_n),$$

that leads to

$$\tau_n = \sum_{k=1}^{n-1} \log \frac{\tilde{z}_k^- + \frac{2}{\tilde{p}+\tilde{q}}(1 - \tilde{q}\tilde{z}_k^- - \tilde{p}x_k^{i_k})}{\tilde{z}_{k+1}^-}. \tag{3.45}$$

We have simulated the model described by (3.41) for several values of the parameters N and $\frac{\tilde{q}-\tilde{p}}{\tilde{q}+\tilde{p}}$. The result is illustrated in Figure 3.3. Comparing Figure 3.3 a) and b) we realize that, even if the infection extincts after some number of peaks, the extinction time is much larger in the case of many antigens compared to the case when there is only one antigen.

Antigenic variation definitely extends the duration of infection. This is shown in Figure 3.3c where the persistence time scales linearly with the number of antigens and in Figure 3.3 a & b where the infection length is elongated by the number of variants. Furthermore, the persistence time is also strongly influenced by the parameter $\frac{\tilde{q}-\tilde{p}}{\tilde{q}+\tilde{p}}$ representing the differential relative importance of cross-reactive and specific immune response. The extinction time can be very large for many antigens and for a cross-reactive response more efficient (in terms of building-up, recognizing and eliminating parasites) than the specific response. Given that the time τ is measured in units $1/b$ (lifetime of cross-reactive response) the extinction time also scales proportionally with the lifetime of the cross-reactive response.

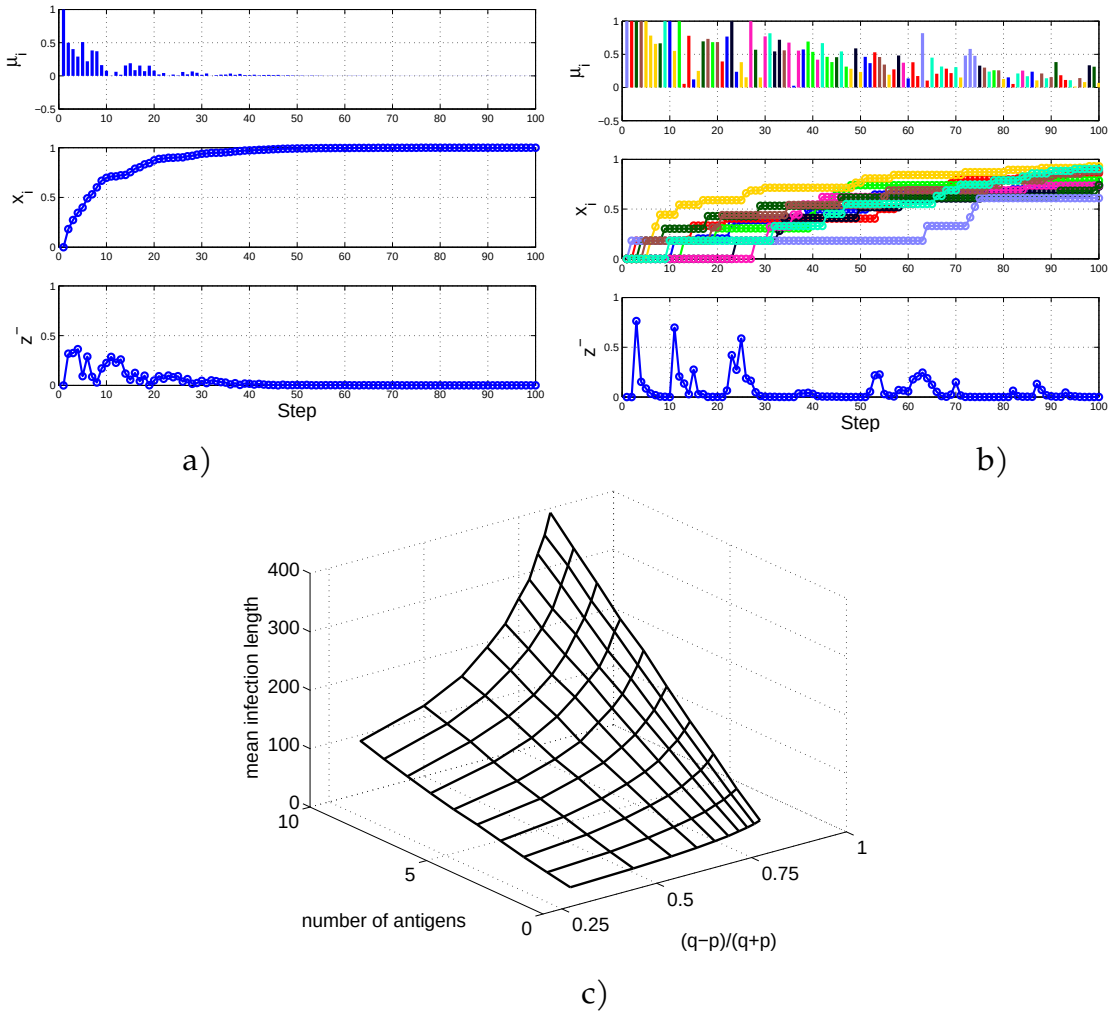

Figure 3.3: Nowak's model. a) one variant b) ten variant c) dependence of the mean infection duration on the model's parameters. The duration of the infection (persistence time) was defined as the time after which the peak parasitemia drops to 1% of the maximum value. Although the infection ultimately disappears, the persistence time can be very long. Here time is represented by the re-scaled variable τ whose units are b^{-1} i.e. lifetime of the cross-reactive immune response.

3.2 Deterministic Antigenic Variation Model with Switching

To represent the effect of variant switching on parasite heterogeneity we build on previous mathematical models [McQueen et al., 2013; Eckhoff, 2012; Recker et al., 2011; Klein et al., 2014; Childs and Buckee, 2015]. We made the assumption that within a single infection, *P. falciparum* parasites can switch the variant surface antigens (PfEMP1) that they exhibit to the immune system [Deitsch and Dzikowski, 2017]. The decision to switch from a variant to another takes place at the end of the cell cycle: a parasite can give rise of offspring expressing a different *var* gene. Although the switching is probabilistic we adopt here a deterministic approach, consisting in writing ODEs for evolution of the numbers of parasites of different types. The deterministic can be justified rigorously using the law of large numbers for Markov processes (see next section). Here we modify Nowak's models introduced in the previous section by adding switching terms. In the modified model the population of parasites expressing different genes $g_i, 1 \leq i \leq N$, follows the differential equations:

$$\frac{dg_i}{dt} = g_i(\alpha(1 - \sum_{j \neq i} P_{ij}) - \beta_i x_i - qz) + \alpha \sum_{j \neq i} P_{ji} g_j, \tag{3.46}$$

where i denotes the antigenic variant g_i, α is the intrinsic growth rate of the parasite, P_{ij} is the transition that parasites switch from expressing gene group i to gene group j, β_i is the rate at which the specific immune response x_i acts on gene group i and is proportional to the density of parasites expressing that group, and qz is the cross-reactive naturally acquired immunity that acts on all parasites expressing different variants of the *var* family. The specific immune response to each PfEMP1 is described by the following differential equation:

$$\frac{dx_i}{dt} = \gamma_i g_i - c x_i, \tag{3.47}$$

where γ_i is the rate at which the immune system acquires immunity to gene group i. The specific responses corresponding to each variant gradually declines over time with the rate c in the absence of consistent exposure [Staalsoe et al., 2001]. The cross-reactive immune response z is accumulated as a result of exposure to all gene groups, and its

rate of accumulation is described by the following differential equation:

$$\frac{dz}{dt} = \mu \sum_{i=1}^{N} g_i - pz \tag{3.48}$$

where μ is the rate at which the immune system acquires cross-reactive immunity, proportional to the total density of parasites expressing any gene group, and p is the rate at which the cross-reactive immunity declines naturally.

In order to study the Eqs. (3.46), (3.47), (3.48), we use a singular perturbations method. We consider that the characteristic times of immunity decay are much larger than the characteristic times of development of the infection.

Let us consider the following rescaled variables $\bar{g}_i = g_i/\alpha$, $\bar{t} = t\alpha$, $\bar{x}_i = x_i/\gamma_i$, $\bar{z} = z/\mu$, $\epsilon_1 = p/\alpha$, $\epsilon_2 = c/p$, $\bar{\beta}_i = \beta_i$, $\bar{q} = q\mu/\alpha$. In these variables the equations describing the model read:

$$\begin{aligned}
\frac{d\bar{g}_i}{d\bar{t}} &= \bar{g}_i((1 - \sum_{j\neq i} P_{ij}) - \bar{\beta}_i\bar{x}_i - \bar{q}\bar{z}) + \sum_{j\neq i} P_{ji}\bar{g}_j, \\
\frac{d\bar{x}_i}{d\bar{t}} &= \bar{g}_i - \epsilon_1\epsilon_2\bar{x}_i, \\
\frac{d\bar{z}}{d\bar{t}} &= \sum_{i=1}^{N} \bar{g}_i - \epsilon_1\bar{z}.
\end{aligned} \tag{3.49}$$

When ϵ_1, ϵ_2 are small parameters, we have a three time scales singular perturbation problem. $\bar{g}_i$ are the fast time scale variables, $\bar{q}$ is a slow variable and $\bar{x}_i$ are slower variables. Geometric singular perturbation theory applies to this situation [Cardin and Teixeira, 2017]. The fast dynamics is obtained by setting $\epsilon_1 = \epsilon_2 = 0$ in (3.49):

$$\frac{d\bar{g}_i}{d\bar{t}} = \bar{g}_i((1 - \sum_{j\neq i} P_{ij}) - \bar{\beta}_i\bar{x}_i - \bar{q}\bar{z}) + \sum_{j\neq i} P_{ji}\bar{g}_j, \tag{3.50}$$

$$\frac{d\bar{x}_i}{d\bar{t}} = \bar{g}_i, \tag{3.51}$$

$$\frac{d\bar{z}}{d\bar{t}} = \sum_{i=1}^{N} \bar{g}_i. \tag{3.52}$$

The fast equations (3.50), (3.51), (3.52) describe the development of the infection. Like in the Section 3.1, the fast equations have a steady state $\bar{g}_i = 0$ which develops

into an infection peak, provided that this state is unstable. As the steady state $\bar{g}_i = 0$ is degenerate in the directions $\bar{x}_i$ and $\bar{z}$, we test the instability condition with respect to the normal directions $\bar{g}_i$ (in terms of geometric singular perturbation theory, this boils down to ensuring that $\bar{g}_i = 0$ approximates a normally hyperbolic attractive invariant manifold of (3.49), see [Fenichel, 1979; Cardin and Teixeira, 2017]).

Let J be the Jacobian matrix of the system (3.50) with respect to the variables $\bar{g}_i$, computed at the steady state $\bar{g}_i = 0$. The instability condition means that all the eigenvalues of J are in the right complex half-plane, or equivalently, that all eigenvalues of $-J$ are in the left complex half-plane, i.e. $-J$ is a stable matrix. In order to find the stability conditions for $-J$, we apply the Routh-Hurwitz theory that we recall here.

Let $p(\lambda) = det(-J - \lambda I)$ be the characteristic polynomial of $-J$. Then, the eigenvalues of the $-J$ are computed by solving $p(\lambda) = 0$, which is equivalent to solving the polynomial equation

$$a_0\lambda^n + a_1\lambda^{n-1} + \ldots a_{n-1}\lambda + a_n = 0,$$

where $a_0 = 1$ (the l.h.s. of the equation is the characteristic polynomial of $-J$ multiplied by 1 or -1, if n is even or odd, respectively).

The Hurwitz matrix a (n, n) matrix obtained in the following way:

- the first row contains the coefficients with odd indices,
- in each column the next element is a coefficient of index lowered by one with respect to the predecessor,
- all coefficients of indices smaller than 0 or larger than n are considered zero.

$$H = \begin{bmatrix} a_1 & a_3 & a_5 & \dots & 0 & 0 & 0 \\ a_0 & a_2 & a_4 & \dots & 0 & 0 & 0 \\ 0 & a_1 & a_3 & \dots & 0 & 0 & 0 \\ 0 & a_0 & a_2 & \dots & 0 & 0 & 0 \\ 0 & 0 & a_1 & \ddots & a_n & 0 & 0 \\ 0 & 0 & a_0 & \ddots & a_{n-1} & 0 & 0 \\ \vdots & \vdots & \vdots & \dots & a_{n-2} & a_n & 0 \\ \vdots & \vdots & \vdots & \dots & a_{n-3} & a_{n-1} & 0 \\ 0 & 0 & 0 & \dots & a_{n-4} & a_{n-2} & a_n \end{bmatrix}$$

The following result, due to Hurwitz, is well established [DeJesus and Kaufman, 1987]:

Proposition 8. *$-J$ is stable (i.e. all its roots have negative real parts) if and only if all the leading principal minors of the Hurwitz matrix are positive and the minors$\Delta_k(p)$ are called the Hurwitz determinants.*

$$\begin{aligned} \Delta_1 &= |a_1| = a_1 > 0, \\ \Delta_2 &= \begin{vmatrix} a_1 & a_3 \\ a_0 & a_2 \end{vmatrix} = a_1 a_2 - a_0 a_3 > 0, \\ \Delta_3 &= \begin{vmatrix} a_1 & a_3 & a_5 \\ a_0 & a_2 & a_4 \\ 0 & a_1 & a_3 \end{vmatrix} = a_3 \Delta_2 - a_1 (a_1 a_4 - a_0 a_5) > 0, \\ &\vdots \end{aligned} \tag{3.53}$$

In the case when $n = 3$ (three variants model) the Jacobian matrix is:

$$J = \begin{bmatrix} 1 - P_{12} - P_{13} - \bar{\beta}_1 \bar{x}_1 - \bar{q}\bar{z} & P_{21} & P_{31} \\ P_{12} & 1 - P_{21} - P_{23} - \bar{\beta}_2 \bar{x}_2 - \bar{q}\bar{z} & P_{32} \\ P_{13} & P_{23} & 1 - P_{31} - P_{32} - \bar{\beta}_3 \bar{x}_3 - \bar{q}\bar{z} \end{bmatrix}$$

The eigenvalues of $-J$ satisfy the polynomial equation

$$\lambda^3 + a_1\lambda^2 + a_2\lambda + a_3 = 0,$$

where

$$a_1 = 3 - P_{13} - P_{21} - P_{23} - P_{31} - P_{32} - P_{12} - \bar{\beta}_1\bar{x}_1 - \bar{\beta}_2\bar{x}_2 - \bar{\beta}_3\bar{x}_3 - 3\bar{q}\bar{z}, \tag{3.54}$$

$$\begin{aligned} a_2 = {} & 3\bar{q}^2\bar{z}^2 - 2P_{13} - 2P_{21} - 2P_{23} - 2P_{31} - 2P_{32} - 2P_{12} + P_{13}P_{21} + P_{12}P_{23} + P_{13}P_{23} + \\ & + P_{12}P_{31} + P_{12}P_{32} + P_{13}P_{32} + P_{21}P_{31} + P_{21}P_{32} + P_{23}P_{31} - 2\bar{b}_1\bar{x}_1 - 2\bar{b}_2\bar{x}_2 - 2\bar{b}_3\bar{x}_3 - \\ & - 6\bar{q}\bar{z} + \bar{b}_2P_{12}\bar{x}_2 + \bar{b}_2P_{13}\bar{x}_2 + \bar{b}_3P_{12}\bar{x}_3 + \bar{b}_3P_{13}\bar{x}_3 + \bar{b}_1P_{21}\bar{x}_1 + \bar{b}_1P_{23}\bar{x}_1 + \\ & + \bar{b}_3P_{21}\bar{x}_3 + \bar{b}_3P_{23}\bar{x}_3 + \bar{b}_1P_{31}\bar{x}_1 + \bar{b}_1P_{32}\bar{x}_1 + \bar{b}_2P_{31}\bar{x}_2 + \bar{b}_2P_{32}\bar{x}_2 + 2P_{12}\bar{q}\bar{z} + \\ & + 2P_{13}\bar{q}\bar{z} + 2P_{21}\bar{q}\bar{z} + 2P_{23}\bar{q}\bar{z} + 2P_{31}\bar{q}\bar{z} + 2P_{32}\bar{q}\bar{z} + \bar{b}_1\bar{b}_2\bar{x}_1\bar{x}_2 + \bar{b}_1\bar{b}_3\bar{x}_1\bar{x}_3 + \\ & + \bar{b}_2\bar{b}_3\bar{x}_2\bar{x}_3 + 2\bar{b}_1\bar{q}\bar{x}_1\bar{z} + 2\bar{b}_2\bar{q}\bar{x}_2\bar{z} + 2\bar{b}_3\bar{q}\bar{x}_3\bar{z} + 3, \end{aligned} \tag{3.55}$$

$$\begin{aligned} a_3 = {} & 3\bar{q}^2\bar{z}^2 - P_{13} - P_{21} - P_{23} - P_{31} - P_{32} - P_{12} - \bar{q}^3\bar{z}^3 + P_{13}P_{21} + P_{12}P_{23} + P_{13}P_{23} + \\ & + P_{12}P_{31} + P_{12}P_{32} + P_{13}P_{32} + P_{21}P_{31} + P_{21}P_{32} + P_{23}P_{31} - \bar{b}_1\bar{x}_1 - \\ & - \bar{b}_2\bar{x}_2 - \bar{b}_3\bar{x}_3 - 3\bar{q}\bar{z} - P_{12}\bar{q}^2\bar{z}^2 - P_{13}\bar{q}^2\bar{z}^2 - P_{21}\bar{q}^2\bar{z}^2 - P_{23}\bar{q}^2\bar{z}^2 - P_{31}\bar{q}^2\bar{z}^2 - P_{32}\bar{q}^2\bar{z}^2 + \\ & + \bar{b}_2P_{12}\bar{x}_2 + \bar{b}_2P_{13}\bar{x}_2 + \bar{b}_3P_{12}\bar{x}_3 + \bar{b}_3P_{13}\bar{x}_3 + \bar{b}_1P_{21}\bar{x}_1 + \bar{b}_1P_{23}\bar{x}_1 + \bar{b}_3P_{21}\bar{x}_3 + \bar{b}_3P_{23}\bar{x}_3 + \\ & + \bar{b}_1P_{31}\bar{x}_1 + \bar{b}_1P_{32}\bar{x}_1 + \bar{b}_2P_{31}\bar{x}_2 + \bar{b}_2P_{32}\bar{x}_2 + 2P_{12}\bar{q}\bar{z} + \\ & + 2P_{13}\bar{q}\bar{z} + 2P_{21}\bar{q}\bar{z} + 2P_{23}\bar{q}\bar{z} + 2P_{31}\bar{q}\bar{z} + \\ & + 2P_{32}\bar{q}\bar{z} - \bar{b}_3P_{13}P_{21}\bar{x}_3 - \bar{b}_3P_{12}P_{23}\bar{x}_3 - \bar{b}_3P_{13}P_{23}\bar{x}_3 - \\ & - \bar{b}_2P_{12}P_{31}\bar{x}_2 - \bar{b}_2P_{12}P_{32}\bar{x}_2 - \bar{b}_2P_{13}P_{32}\bar{x}_2 - \\ & - \bar{b}_1P_{21}P_{31}\bar{x}_1 - \bar{b}_1P_{21}P_{32}\bar{x}_1 - \bar{b}_1P_{23}P_{31}\bar{x}_1 + \bar{b}_1\bar{b}_2\bar{x}_1\bar{x}_2 + \bar{b}_1\bar{b}_3\bar{x}_1\bar{x}_3 + \bar{b}_2\bar{b}_3\bar{x}_2\bar{x}_3 - \\ & - P_{13}P_{21}\bar{q}\bar{z} - P_{12}P_{23}\bar{q}\bar{z} - P_{13}P_{23}\bar{q}\bar{z} - P_{12}P_{31}\bar{q}\bar{z} - P_{12}P_{32}\bar{q}\bar{z} - \\ & - P_{13}P_{32}\bar{q}\bar{z} - P_{21}P_{31}\bar{q}\bar{z} - P_{21}P_{32}\bar{q}\bar{z} - \\ & - P_{23}P_{31}\bar{q}\bar{z} + 2\bar{b}_1\bar{q}\bar{x}_1\bar{z} + 2\bar{b}_2\bar{q}\bar{x}_2\bar{z} + 2\bar{b}_3\bar{q}\bar{x}_3\bar{z} - \bar{b}_1\bar{q}^2\bar{x}_1\bar{z}^2 - \bar{b}_2\bar{q}^2\bar{x}_2\bar{z}^2 - \\ & - \bar{b}_3\bar{q}^2\bar{x}_3\bar{z}^2 - \bar{b}_2\bar{b}_3P_{12}\bar{x}_2\bar{x}_3 - \\ & - \bar{b}_2\bar{b}_3P_{13}\bar{x}_2\bar{x}_3 - \bar{b}_1\bar{b}_3P_{21}\bar{x}_1\bar{x}_3 - \bar{b}_1\bar{b}_3P_{23}\bar{x}_1\bar{x}_3 - \\ & - \bar{b}_1\bar{b}_2P_{31}\bar{x}_1\bar{x}_2 - \bar{b}_1\bar{b}_2P_{32}\bar{x}_1\bar{x}_2 - \bar{b}_2P_{12}\bar{q}\bar{x}_2\bar{z} - \\ & - \bar{b}_2P_{13}\bar{q}\bar{x}_2\bar{z} - \bar{b}_3P_{12}\bar{q}\bar{x}_3\bar{z} - \\ & - \bar{b}_3P_{13}\bar{q}\bar{x}_3\bar{z} - \bar{b}_1P_{21}\bar{q}\bar{x}_1\bar{z} - \bar{b}_1P_{23}\bar{q}\bar{x}_1\bar{z} - \bar{b}_3P_{21}\bar{q}\bar{x}_3\bar{z} - \bar{b}_3P_{23}\bar{q}\bar{x}_3\bar{z} - \bar{b}_1P_{31}\bar{q}\bar{x}_1\bar{z} - \\ & - \bar{b}_1P_{32}\bar{q}\bar{x}_1\bar{z} - \bar{b}_2P_{31}\bar{q}\bar{x}_2\bar{z} - \bar{b}_2P_{32}\bar{q}\bar{x}_2\bar{z} - \bar{b}_1\bar{b}_2\bar{b}_3\bar{x}_1\bar{x}_2\bar{x}_3 - \\ & - \bar{b}_1\bar{b}_2\bar{q}\bar{x}_1\bar{x}_2\bar{z} - \bar{b}_1\bar{b}_3\bar{q}\bar{x}_1\bar{x}_3\bar{z} - \bar{b}_2\bar{b}_3\bar{q}\bar{x}_2\bar{x}_3\bar{z} + 1. \end{aligned} \tag{3.56}$$

The Hurwitz matrix of $-J$ reads

$$H = \begin{bmatrix} a_1 & a_3 & 0 \\ 1 & a_2 & 0 \\ 0 & 1 & a_3 \end{bmatrix}$$

and the stability conditions are $a_1 > 0, a_1 a_2 - a_3 > 0, a_3 > 0, a_2 > 0$ (the last condition follows from the first three).

In the absence of switching, i.e. when $P_{ij} = 0$ for all $i \neq j$ the above conditions read:

$$\begin{aligned} a_3 &= -(\bar{b}_1\bar{x}_1 + \bar{q}\bar{z} - 1)(\bar{b}_2\bar{x}_2 + \bar{q}\bar{z} - 1)(\bar{b}_3\bar{x}_3 + \bar{q}\bar{z} - 1) > 0 && (3.57) \\ \frac{1}{3}a_1 &= 1 - \frac{1}{3}(\bar{b}_2\bar{x}_2 + \bar{b}_3\bar{x}_3 + \bar{b}_1\bar{x}_1) - \bar{q}\bar{z} > 0 && (3.58) \\ \frac{a_1 a_2 - a_3}{8} &= -\left[\frac{\bar{b}_1\bar{x}_1 + \bar{b}_2\bar{x}_2}{2} + \bar{q}\bar{z} - 1\right]\left[\frac{\bar{b}_1\bar{x}_1 + \bar{b}_3\bar{x}_3}{2} + \bar{q}\bar{z} - 1\right] \\ &\quad \left[\frac{\bar{b}_2\bar{x}_2 + \bar{b}_3\bar{x}_3}{2} + \bar{q}\bar{z} - 1\right] > 0 && (3.59) \end{aligned}$$

Conditions (3.57),(3.59),(3.58) are valid, and an infection peak can develop, if the cross-reactive and specific immune responses $\bar{z}$ and $\bar{x}_i$, $1 \leq i \leq 3$ are not strong. If these immune responses are too strong, a peak may not develop, and one must wait the time needed for these responses to decay (assuming that the memory of at least some immune response is finite).

Condition (3.57) means that the infection can develop if there are not enough specific and cross-reactive antibodies to prevent development of parasites of type 1, or 2, or 3, independently. Condition (3.59) means that the infection can develop if there are not enough antibodies to prevent development of parasites of any two types simultaneously. Finally, condition (3.58) means that the infection can develop if there are not enough antibodies to prevent development of parasites of the three types simultaneously.

Using (3.54) we find that with switching, the Condition (3.58) for developing three

variant peaks changes to

$$a_1(\bar{z},\bar{x}_1,\bar{x}_2,\bar{x}_3) = 1 - \frac{P_{12}+P_{13}+P_{21}+P_{23}+P_{31}+P_{32}}{3} - \frac{\bar{b}_2\bar{x}_2+\bar{b}_3\bar{x}_3+\bar{b}_1\bar{x}_1}{3} - \bar{q}\bar{z} > 0. \tag{3.60}$$

The two other expressions (3.55), (3.56) involved in the Routh-Hurwitz conditions are extremely intricate and can not be simplified even using state-of-the-art computer algebra packages. However, the investigation of Equation (3.54) suggests us a heuristic to simplify these expressions by substracting variants of (3.57) and (3.59), modified to include mean switching parameters, and simplifying the remaining expressions.

By using this method, we find that the Condition (3.57) for developing simple variant peaks is changed by the switching to

$$\begin{aligned} a_3(\bar{z},\bar{x}_1,\bar{x}_2,\bar{x}_3) = \quad & -(P_{12}+P_{13}+\bar{b}_1\bar{x}_1+\bar{q}\bar{z}-1) \\ & (P_{21}+P_{23}+\bar{b}_2\bar{x}_2+\bar{q}\bar{z}-1)(P_{31}+P_{32}+\bar{b}_3\bar{x}_3+\bar{q}\bar{z}-1)+ \\ & +\bar{b}_3\bar{x}_3P_{12}P_{21}+\bar{b}_2\bar{x}_2P_{13}P_{31}+\bar{b}_1\bar{x}_1P_{23}P_{32} \\ & +(\bar{q}\bar{z}-1)(P_{12}P_{21}+P_{13}P_{31}+P_{23}P_{32})+ \\ & +(P_{12}+P_{13})(P_{21}+P_{23})(P_{31}+P_{32}) > 0. \end{aligned} \tag{3.61}$$

Contrary to $a_1(\bar{z},\bar{x}_1,\bar{x}_2,\bar{x}_3)$ that is linear, $a_3(\bar{z},\bar{x}_1,\bar{x}_2,\bar{x}_3)$ is a cubic polynomial in $\bar{z}$. This leads to more intricate conditions for the development of an infection peak. Let $z_1 \leq z_2 \leq z_3$ be the ordered, possibly coinciding, real roots of a_3 considered as polynomial in $\bar{z}$. Because the coefficient of $\bar{z}^3$ is negative with and without switching, conditions (3.56), (3.61) for single variant peak development read

$$\bar{z} < z_1, \text{ or } z_2 < \bar{z} < z_3.$$

Finally, the condition (3.59) for developing double variants peaks is changed by the

switching to

$$\begin{aligned}\Delta(\bar{z},\bar{x}_1,\bar{x}_2,\bar{x}_3) = \frac{a_1a_2-a_3}{8} = &-\left[\frac{P_{12}+P_{13}+P_{21}+P_{23}}{2}+\frac{\bar{b}_1\bar{x}_1+\bar{b}_2\bar{x}_2}{2}+\bar{q}\bar{z}-1\right]\\ &\times\left[\frac{P_{12}+P_{13}+P_{31}+P_{32}}{2}+\frac{\bar{b}_1\bar{x}_1+\bar{b}_3\bar{x}_3}{2}+\bar{q}\bar{z}-1\right]\\ &\times\left[\frac{P_{21}+P_{23}+P_{31}+P_{32}}{2}+\frac{\bar{b}_2\bar{x}_2+\bar{b}_3\bar{x}_3}{2}+\bar{q}\bar{z}-1\right]\\ &+\frac{1}{8}\Big[\bar{b}_1\bar{x}_1(P_{12}P_{21}+P_{13}P_{31})\\ &+\bar{b}_2\bar{x}_2(P_{12}P_{21}+P_{23}P_{32})+\bar{b}_3\bar{x}_3(P_{13}P_{31}+P_{23}P_{32})+\\ &+(2(\bar{q}\bar{z}-1)+P_{12}+P_{13}+P_{21}+P_{23}+P_{31}+P_{32})\\ &(P_{12}P_{21}+P_{13}P_{31}+P_{23}P_{32})\\ &-P_{12}P_{21}P_{31}-P_{12}P_{21}P_{32}-\\ &P_{13}P_{21}P_{31}-P_{12}P_{23}P_{32}-P_{13}P_{23}P_{31}-\\ &-P_{13}P_{23}P_{32}-P_{12}P_{23}P_{31}-P_{13}P_{21}P_{32}\Big]>0 \qquad (3.62)\end{aligned}$$

Again, the condition involves Δ, a cubic polynomial in $\bar{z}$ and reads

$$\bar{z} < z_1, \text{ or } z_2 < \bar{z} < z_3,$$

where z_i, $1 \leq i \leq 3$ are the real roots of Δ considered as a polynomial in $\bar{z}$.

Eqs. 3.60,3.61,3.62 suggest that infection peaks are separated by larger periods in the presence of switching.

The Routh-Hurwitz approach can be utilized for models with arbitrary number of variants. The difficulty for larger numbers of variants comes from finding sets of solutions defined by conjunctions of high degree, multivariate polynomial constraints (semi-algebraic sets). If there are eigenvalues with zero real part, then further analysis is needed.

3.3 Stochastic Model with Switching and Constant Immune Response during Early Stages of Infection

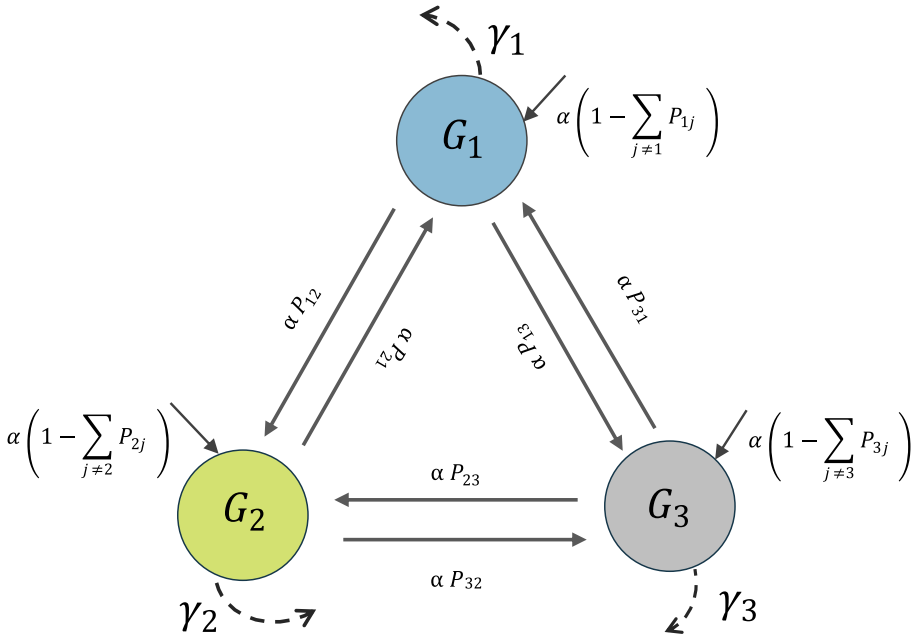

Figure 3.4: Model Schema for the three-state model for groups of variants. The parasites in each class can replicate without switching, at a rate $\alpha(1-\sum_{j\neq i} P_{ij})n_i$, where the second factor is the probability not to not switch to other states. A parasite in class i is removed (selected against) at a rate γ_i, and divides and transitions to a different state j with a propensity αP_{ij}.

The deterministic model introduced in the previous section provides conditions for the development of infection peaks presented as intervals on the values of the immune response. However, as we have already mentioned in the Section 3.1.2, the evolution of the parasitemia is governed by stochastic effects at low numbers of parasites. Therefore, a model that can cope accurately with both very low and high parasitemia and predict correctly peak development must be stochastic in nature. We therefore used a Markov jump process (Continuous-Time Markov chain) [Ethier and Kurtz, 2009; Crudu et al., 2012, 2009] to model the stochastic effects and the Gillespie Algorithm Gillespie [1977] to simulate this process. In order to reduce the complexity of the simulation, the number of variants was reduced by lumping several genes into M classes that are analogous to groups of variants with shared characteristics.

The state of the Markov jump process is defined by the numbers of parasites expressing genes from each class $(n_1, n_2, \ldots, n_M)$ and M =3 [Gillespie, 1977]. Each jump (also named elementary reaction) modifies the state of the process by changing the numbers of parasites in each class. Figure 3.4 shows the elementary reactions of the model. Each elementary reaction corresponds to one of the biological processes: proliferation without switching, proliferation with switching, or negative selection. The model is also characterized by the reaction propensities [Gillespie, 1977], defined as the mean number of reactions per unit time (see Table 3.1).

The stochastic model and the deterministic models introduced in the previous section are tightly related. Using the law of large numbers for Markov processes [Kurtz, 1970; RADULESCU et al., 2007; Crudu et al., 2009, 2012] one can show that solutions of the stochastic model converge to solutions of the ODEs (3.46) when the numbers of parasites are very big. In the paper of Kurtz [Kurtz, 1970], the convergence is in probability (weak law of large numbers). However, with some restrictions on the initial data, one can get the almost convergence (strong law of large numbers, see [Kotelenez, 1986]).

Note that in the stochastic model studied in this section the propensity coefficient γ_i of the negative selection is considered constant in time. This means that both the specific and cross-reactive immune responses are considered constant. This condition can be lifted by considering that $\gamma_i = px_i(t) - qz(t)$, where $x_i(t)$ and $z(t)$ are time-dependent specific and cross-reactive immune responses, respectively. As described in Nowak's model, $x_i(t)$ and $z(t)$ should follow ODEs. This more general model (not studied here) would be a piecewise-deterministic Markov process (PDMP) [Crudu et al., 2012, 2009; Davis, 1984]. For large parasites numbers, the PDMP solutions converge to solutions of the complete deterministic model of the previous section, namely Eqs. 3.46, 3.47,3.48.

Process	State$(t = t)$	State$(t = t + 1)$	Propensity
Proliferation without Switching	n_i, n_j	$n_i + 1, n_j$	$\alpha(1 - \sum_{j \neq i} P_{ij})n_i$
Negative selection	n_i, n_j	$n_i - 1, n_j$	$\gamma_i n_i$
Proliferation with Switching	n_i, n_j	$n_i, n_j + 1$	$\alpha P_{ij} n_i$

Table 3.1: Markov Jump Processes describing the stochastic antigenic variation model and Propensities for stochastic simulation.

Algorithm 1 Gillespie Algorithm for Stochastic Simulation

Define *state* and rate constants *c* for antigenic variants
Define stoichiometry matrix *smatrix*
Define maximum simulation time $t_{\max}$
Initialize time list *time* and append 0
Initialize empty lists: *waiting_times*, *state_trace*
Append initial *state* to *state_trace*
Set $t = 0$
while $t < t_{\max}$ **do**
    Generate two random numbers $r1, r2$ uniformly between 0 and 1
    Calculate propensities a with *propensities*$(c, state)$
    Calculate cumulative sum of a as a_{cum}
    Calculate total propensity $a_0 = a_{\text{cum}}[-1]$
    Set $t_{\text{old}} = t$
    Update time $t = t + (1/a_0) \times \log(1/r1)$
    Append t to *time*
    Append $t - t_{\text{old}}$ to *waiting_times*
    Determine which reaction will fire: use the index of the first element of a_{cum} larger than $r2 \times a_0$.
    Update *state* with the corresponding change from *smatrix*
    Append updated *state* to *state_trace*
end while
return *time*, *state_trace*

The Gillespie algorithm corresponding to the reactions described by Table 3.1 was simulated using the Algorithm 1. We considered three main groups of *var* variants that the parasites were partitioned into, and we used the set of parameters in the Table 3.2 for the model simulation.

Table 3.2: Simulation Parameters for each antigenic group

Parameter	Group 1	Group 2	Group 3
Growth Rate, α	8.5 per cycle	8.5 per cycle	8.5 per cycle
Removal rate, γ	7 per cycle	0.6 per cycle	0.6 per cycle

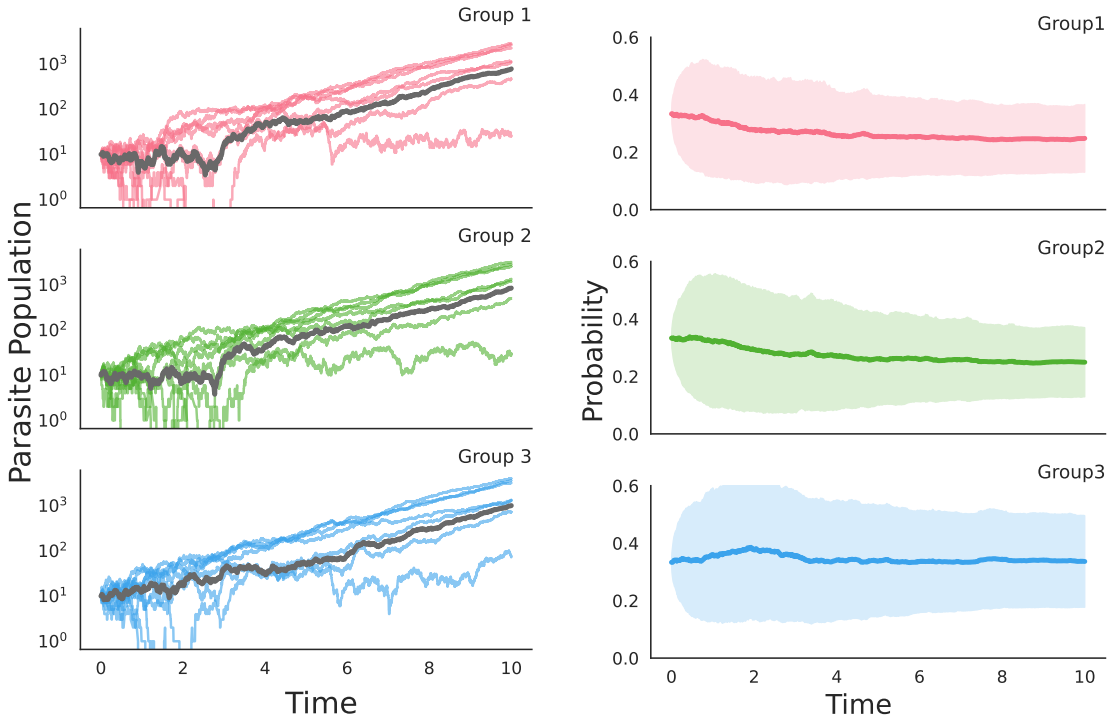

Figure 3.5: a) Stochastic realisations of the three-state model represented by figure 3.4. Parasitemia density time series are shown for early stages of infection using stochastic simulations: Groups G1 (pink), G2 (green) and G3 (blue) represent antigenic group variants and are proxies for parasite survival. Note: P_{ijs} correspond to transition rates arising from a generator matrix Q of the CTMC, which was simulated using a random-uniform distribution. b) The occupancy probabilities of parasites in the three antigenic groups across time. The shaded region represents the confidence interval of the occupancy probabilities, obtained from the variance.

Based on our simulations results shown in Figure 3.5, during early stages of the infection, the high growth rate and switching can sustain parasites in all groups, even if the removal rate is very high.

3.4 Random ODE Switching Model

In this subsection, instead of considering fixed switching parameters, we consider that they are elements of a random matrix. This allows us to study ensembles of parasites by taking into account the natural variability of intrinsic switching parameters. Furthermore, in order to simplify the model simulation, we consider that the parasite numbers are large enough and are limited by the availability of red blood cells in the body. Therefore the deterministic limit can be applied on the system for each set of parameters. According to the deterministic limit (law of large numbers for Markov jump processes, see Kurtz [1970]; Crudu et al. [2009, 2012]).

To understand the influence of various types of intrinsic transition properties on the system, we analysed the system with the following types of transition matrices satisfying the following properties:

1. Diagonal elements: The diagonal elements of the transition rate matrix are always negative and equal to the sum of the transition rates out of that state, i.e., $q_{ii} = -\sum_{j \neq i} q_{ij}$.

2. Off-diagonal elements: The off-diagonal elements of the transition rate matrix are always non-negative, i.e., $q_{ij} \geq 0$ for $i \neq j$.

3. Row sums: The row sums of the transition rate matrix are always zero, i.e., $\sum_j q_{ij} = 0$ for all i

3.4.1 Case I: Model Without Switching

We describe the case where we solve the system where there is no switching; in this case, the system becomes identical to the model of antigenic variation mentioned above. We retrieved the same system, introduced switching as mentioned above, and then proceeded to use a random-uniform switching scheme across all antigenic variants. The model in fig 3.6 was generated using the parameter values defined in table 3.3.

Algorithm 2 Continuous-Time Markov Chain based Switching Matrix to simulate for the model described in section3.2

Define the number of states n
Initialize transition rate matrix Q with zeros of size $n \times n$
for $i = 0$ to $n - 1$ **do**
  for $j = 0$ to $n - 1$ **do**
    if $i \neq j$ **then**
      Assign random value to $Q[i][j]$, scaled by 1×10^{-3}
    end if
  end for
end for
for $i = 0$ to $n - 1$ **do**
  $Q[i][i] = -\sum_{j \neq i} Q[i][j]$
end for
update parameters
Define time span t_{span}
Solve the initial value problem (IVP) Eqns3.46, 3.47,3.48

Parameter	Value	Description
$\beta_i = \beta$	1×10^{-4}	Selection by Specific Response
$\gamma_i = \gamma$	1×10^{-4}	Induction of Specific Response
μ	1×10^{-4}	Induction of cross-reactive response
q	1×10^{-4}	Selection by cross-reactive response
α	8.5	Intrinsic growth rate of parasites
p	0.1	Specific response decay
c	0.01	Cross-reactive response decay

Table 3.3: The parameters used to simulate the deterministic model described by Eqns 3.46, 3.47, 3.48

3.4.2 Case II: Uniform random transition matrix

1. The initial population parasite composition at time $t = 0$ is described by a random uniform distribution such that each v_i is equally likely to occur at the initial time, such that $v_i \in [100, 900]$, [Recker et al., 2004].

2. initial specific and cross-reactive responses are considered zero, i.e. there is no selection at the beginning.

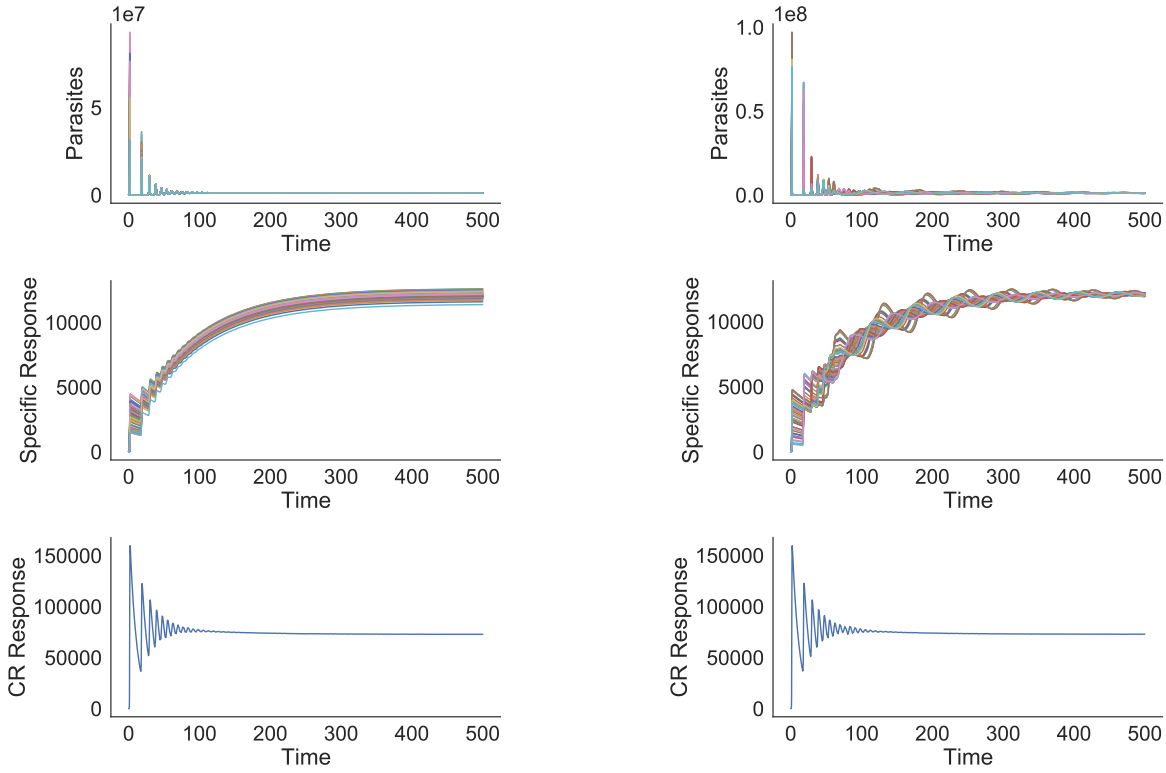

Figure 3.6: a) Variant specific parasitemia levels and specific immune response under random-uniform switching (top) and specific immune responses against (n=60) variants over time for the model described by Eqns 3.46, 3.47, and 3.48. Parameter values as described in table 3.3 and b)The time-series of different *var* variants in the population of parasites, initiated as a uniformly distributed population of all variants, subjected to specific and general immune responses without switching.

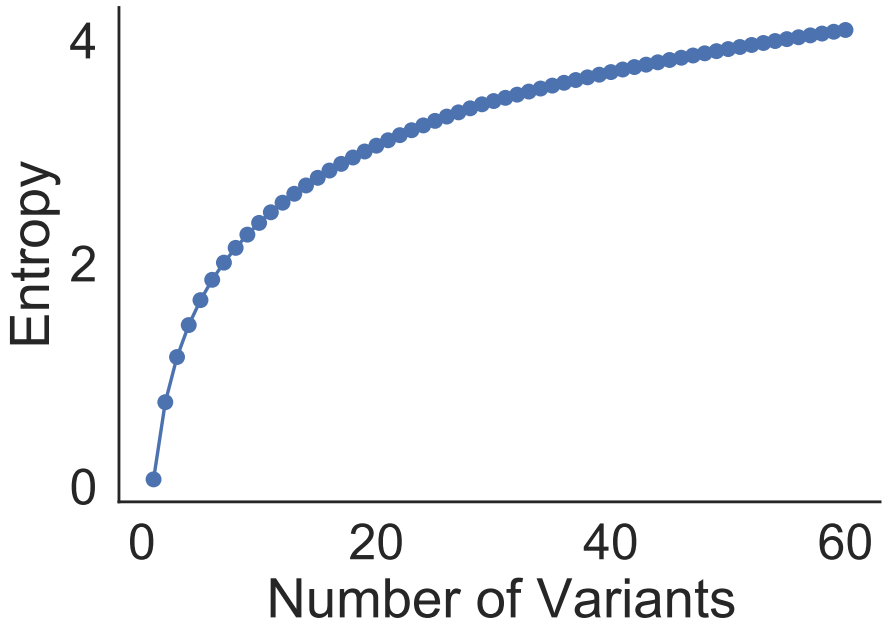

Figure 3.7: Entropy values from different simulated infections at the end of the infection. Infections simulated for the number of variants $N \in [1,60]$. All other parameter values are fixed as the table 3.3.

In the case when random switching is incorporated into the model, the peaks of parasitemia overlap across time, with multiple variants co-existing in the population at all times. Eventually, the antigenic variants exist at steady levels throughout the infection, without peak recurrence. This probably happens due to the continuous production of variants due to random switching across time Figure3.4.2. Random switching is also associated with entropy fixation that depends on the number of variants in the Figure3.7.

3.5 Discussion

Mathematical models of antigenic variation in malaria have provided thorough descriptions of parasite reproduction dynamics and immunological responses. To better understand the host's response, we considered a model which included both the variant specific and cross-reactive immune response mounted against parasites. Parasite dynamics with proliferation, negative selection, and *var* genes switching were modelled using both stochastic and deterministic approaches. The general structure

of the model proposed in this chapter can be implemented to a wide variety of settings. We incorporate antigenic variation exhibited by PfEMP1 in our hypotheses, however there exist other families of Variant Surface Antigens in *falciparum* that can be potentially responsible for shaping parasitemia dynamics as seen in asymptomatic infections from endemic regions. Based on our mathematical analyses, we were able to precisely quantify the periods between recrudescence associated with different PfEMP1 variants and characterise their amplitude, overlap with other variant peaks.

The theoretical results obtained in the section 3.1 are general, and can be implemented with modification to a variety of pathogens exhibiting antigenic variation within the host. On analysing the system described by the antigenic variation model, we find that the state trajectories can be completely described as a set of parabolas, similar to the SIR model for a constant population size. In the case of SIR models, the phase solutions characterise the peaks and troughs of individuals in susceptible and infected compartments, with implications in epidemiology. In our case, the solutions help in characterising the peaks of parasitemia in the chronic infections, for the first time.

We first characterised the system for a single antigenic variant v_i, whose population exhibited oscillations with dampening, but on the introduction of multiple variants in the parasite population, we observed infection prolongation, with multiple peaks of parasitemia. In the case of the cross-reactive response being more effective than the specific response, we proved that in the long-term, its only the specific response x_i that persists after the end of chronic infection. In the presence of the multiple variants subjected to the immune system, and the immune responses characterised by the variant and cross-reactive response shared across all antigenic variants, interestingly we found that the infection is ultimately cleared, but was the length of infection correlated linearly with the number of variants present in our system. The role of cross-reactive responses in maintaining long term infections has been highlighted in other studies [Recker et al., 2004; Childs and Buckee, 2015; Klein et al., 2014] with varying assumptions, but we are able to analyse infection dynamics with minimal assumptions about the host-parasite dynamics.

The implications of the cross-reactive response being effective in reducing infection length have been discussed in [Childs and Buckee, 2015], and the authors suggest

that there should be an ideal window for co-infection, because parasites expressing a large number of shared variants will be cleared by cross-reactive arm of the immune response, whereas distinct antigens will proliferate too soon and will elicit a strong specific response, affecting the duration of persistence of both types of variants. For multiple variants in a system, we are also able to define the inter-peak dynamics for the parasites expressing a variant i, the specific immune responses against the variants x_i, and the cross-reactive response z. In the case of the parasite sub-populations pertaining to variants, we find that the parasites are ultimately cleared before the next peak appears. Additionally, between two successive peaks, the cross-reactive responses also decline exponentially. Based on these properties, we established the condition for establishing a peak. Negative-selection eliminates variants and is therefore detrimental to the parasite survival, whereas intrinsic switching replaces one variant by another and maintains the expression diversity of the antigens, but at the same time increases repertoire exposure to the hosts' immune system. To address thee biological questions, we incorporated switching across variants in the model that we then analysed theoretically.

Switching was studied using three types of models: a stochastic model defined as a Markov jump process, a deterministic ODE model and a random ODE model. The deterministic ODE allowed us to obtain analytic conditions for the development of infection peaks. These conditions are presented as intervals in the levels of total (specific and cross-reactive) immune response. Because peaks develop starting with low parasitemia numbers, the peak developement is distributed stochastically within these deterministic bounds and the precise quantitative framework for the infection dynamics is provided by the stochastic model. The stochastic model was studied by numerical simulations using the Gillespie algorithm. These simulations allowed us to understand the dynamics of the system at the development of infection peaks, because this stage is characterised by initiation with a small number of molecules. We have considered a three-variant system, assuming that the three classes of parasites being simulated belonged to antigenic variants with shared properties (in this case, analogous to *var* groups). To reduce computational complexity, we assumed that the classes of parasites were under constant selection, and not a specific or cross-reactive response, analogous to an innate response. We found that the parasite populations in all groups were sustained at the end of ten cycles, and under slow switching rates, we

found that the parasite groups were equally likely to exist throughout the duration of infection. This theoretical setup is analogous to a CHMI challenge in individuals with low or no immunity against PfEMP1 antigens, where in a number of variants are initially present and continue to be expressed for the short duration the challenge lasts for.

Finally, we have used a random ODE model to look for robust properties of the deterministic dynamics. In the random ODE model, the dynamics is deterministic, but the switching rates are chosen randomly. This allows to test properties that are common to an ensemble of models, rather than testing individual models. We simulated the ODE model with switching deterministically, incorporating, cross-reactive and specific responses parasite antigens, for many random switching parameters. We found that if the switch rates are chosen from a random uniform distribution, the peaks of parasitemia are composed of many different variants. Our results indicated that, overall, the number and distribution of variants in the population eventually becomes stable over time. The entropy of this distribution, the number and diversity of variants, are reduced with respect to the initial values due to the immune response of the host.

CHAPTER 4

Conclusions and Perspectives

Our analyses based on CHMI data from The Gambia revealed that following infection challenge with sporozoites from NF54/3D7, individuals originating from the same geographical region could have diverse infection outcomes and *var* expression pattern during the CHMI. This distinct pattern of *var* gene expression was also highlighted in a previous study carried out in Gabon [Bachmann et al., 2019] where the *var* expression pattern with a limited number of *var* genes expressed later in the infection was associated with higher overall immune response, indicating the role of immune selection initially. Following a similar classification of individuals, we found that individuals that were classified as 'controllers' in both studies clustered together on performing hierarchical clustering on *var* gene expression data from RT-qPCR.

To quantify the heterogeneity, we exploited Shannon Entropy as a measure of the *var* parasite populations in each individual as a marker for parasite population diversity. We found considerable differences across sub-groups of individuals, indicating that the *var* expression diversity in infections with 3D7 is conserved, independent of geographical origin of the hosts, but is host immunity dependent [Warimwe et al., 2009, 2013; Bachmann et al., 2019].
Individuals classified as 'controllers' in the current study also presented longer

lasting infections, lower parasitemia before treatment and recognized a diverse range of PfEMP1 domains prior to infection challenge, indicating that pre-existing responses against PfEMP1 aid in controlling the infection in semi-immune individuals. It is remarkable that, although volunteers from Gabon and The Gambia had likely never been infected with a *P. falciparum* strain genetically similar to 3D7, the parasite exhibited a similar *var* gene expression pattern correlated with malaria immunity.

In addition to characterizing the *var* gene expression pattern in the CHMI participants, our goal was to analyze the turnover dynamics of expressed *var* genes. To achieve this, we exploited the limits of a theoretical model to compute the turnover probability for each gene in an individual, provided it was expressed initially. On comparing these *in vivo* turnover probabilities across different individuals, we found that the probabilities to switch away were extremely high, up to 100% in some genes expressed initially.
On analysing the data for change in *var* turnover in the CHMI volunteers, we found that the probability to transition away from the genes that were expressed initially increased rapidly with time. In the volunteer that was able to control the infection until the end of the CHMI without turning symptomatic, we found that the initial repertoire of *var* genes had completely transitioned away after three cycles post day 14, when the *var* expression was first recorded. Given the short interval between points in our time series, we suggest that the *var* turnover during an infection is much higher than reported previously [Peters et al., 2002].

Our estimates based on a two-state Markov model lead to transition probability estimates with group averages between 80% and 90% per day. To the best of our knowledge, this is the first study to quantify the probability in change of *var* expression in real time in a CHMI study. Additionally, we also found that group A *var* genes had the highest rates of transition *in vivo* , suggesting a strong influence of the immune system on the turnover during infection.
Since the changes in *var* expression are heavily influenced by the immune system *in vivo* , we wanted to get an accurate estimate of switching events and rates in the absence of immunity. Therefore, we measured the *var* transcripts coming from the CHMI volunteers *in vitro* for several cycles in culture, to explore the contrasts with *in*

vivo data. Our results showed that *var* expression profiles evolve towards a steady-state distribution characterized by significant entropy and many expressed *var* genes. In the *sero-low* group, the time to attain the steady state is reduced, and the final distribution displays diminished inter-individual variability. We also found that the steady state distribution in both sub-groups were comprised of the *var* groups B and C.

The parasite populations in the *sero-low* groups had reached the corresponding steady state relatively soon, in nearly 10 cycles. Moreover, our estimated *in vitro* transition rates are compatible with the frequencies of different *var* genes groups in the attractor (steady state). For *sero-high* individuals, the parasite cultures took longer to converge to the steady state and some samples still preserve the memory of the initial state after 50 days in culture. Given that the theoretical model was calibrated using the same switching rates for both subgroups, the differences in time to steady state are mainly explained by disparity in the initial expression profiles during the CHMI. Therefore, we hypothesize that epigenetic imprinting on the parasite populations coming from hosts with stronger immune responses favored a repertoire of *var* genes very different from the *in vitro* steady state. In *sero-high* hosts, only a few *var* genes survive the negative selection of the immune system and the multiplicity of steady state gene expression is difficult to recover. Therefore, we argue that in all *sero-low* individuals with multiple *var* genes expressed, the *var* distribution is very similar to the *in vitro* steady state. The parasite uses the diverse repertoire as 'bet-hedging' strategy in a hostile environment and then the distribution observed at later timepoints *in vivo* evolves by negative selection [Bachmann et al., 2019; Pickford et al., 2021]

Furthermore, to highlight the role of immune repertoire in shaping the *var* expression patterns, we analysed the immune responses against PfEMP1 from 3D7 as well as multiple other strains of *falciparum*. In this study, the antibody levels against PfEMP1 domains were significantly enriched in *sero-low* individuals following the expression of a diverse set of *var* variants. Additionally, we found that the presence of broad range of pre-existing anti-VSA antibodies is associated with a lower likelihood of reaching the treatment threshold for the infection caused by sporozoites from the NF54 isolate. The diversity in recognition, coupled with cross-reactivity against VSAs can be considered crucial to prevent symptomatic infections [Chan et al., 2019; Kimingi et al., 2022; Gupta et al., 1999] for controlling malaria infections.

Our results re-confirm that anti-PfEMP1 immunity is a marker for infection outcome

and severity of malaria infection Warimwe et al., 2009; Barry et al., 2011 and that certain PfEMP1 subsets have been linked to shield against severe symptoms of the disease [Tessema et al., 2019; Travassos et al., 2018; Avril et al., 2012; Nunes-Silva et al., 2015].
We also found that the specific PfEMP1 antibody levels were at least moderately negatively associated with the expression of *var* genes during the infection, and this stems from acquired immunity to previous malarial infections. The negative correlation was highest for group B and A PfEMP1, which are the *var* groups that constitute the repertoires of *var* genes in early stages of infection, indicating that the immune system may not be able to acquire antibodies to rarely expressed genes, for example group C genes.
On pooling the PfEMP1 domain data with the clinical data from the study, we also established correlation between the antibody levels and clinical outcomes of infection using machine learning. We showed the diversity and strength of antibody responses against domain sub-groups associated with severe outcomes (CIDR α1 domains that bind to EPCR-binding receptors) Kimingi et al., 2022; Tessema et al., 2019; Obeng-Adjei et al., 2020.

Previously, several studies have exploited 3D7 recombinant domains to assess the increase in antibody levels following a *falciparum* infection [Travassos et al., 2018], but our current study is the first to assess the 3D7 specific gain in anti-PfEMP1 antibodies because the CHMI was carried out with the same strain. Interestingly, the highest gain in antibodies was against the internal PfEMP1 domain ATS, indicating that this increase in antibody levels can be attributed to several domains being markers of exposure and not protection, as recently shown in [Kimingi et al., 2022]. In our data, gain in specific antibodies against PfEMP1 did not always correspond to their prior expression in the CHMI, which can be attributed to our lack of knowledge of the earliest expressed *var* genes, right after coming out of the liver. Alternatively, this may indicate cross-reactivity between different PfEMP1 antigens.

Despite finding a negative association between the intensity of existing specific immune response and *var* expression during the CHMI, we did not find a positive effect of *var* expression on specific anti-PfEMP1 responses. We found a lack of correlation between expression of *var* genes during the CHMI and the subsequent

increase in anti-PfEMP1 antibodies on day35, hinting that the expressed *var* genes did not trigger specific antibody production as opposed to ATS domains. Multiple hypotheses can explain why transcribed *var* genes do not elicit an antibody response 2 to 3 weeks later. First, we are making the assumption that the *var* transcript detected is systematically translated and exported to the infected red blood cell surface. Second, we assume that antibodies generated *in vivo* against PfEMP1 in its natural conformation will recognise the exact same epitopes from recombinant domains spotted on an array. These arrays have been previously validated with hundreds of plasma samples, mainly from Mali. However to the best of our knowledge this is their first use with CHMI-derived plasma, and, importantly, from volunteers infected with the same 3D7 strain that the arrays were based on. For our analyses, we excluded domains which were not detected by any volunteer in any sample. Thirdly, we are opening up a new hypothesis, that some PfEMP1 domains do not always elicit an antibody response despite their surface localisation. It is conceivable that evolution selects for PfEMP1 sequences that poorly immunogenic. This selective pressure only applies to surface exposed domains; this would explain why the intracellular ATS domain elicits such a strong antibody response, because there is no selection against it. To further test this hypothesis, future arrays should contain more polymorphic surface antigens (Surfins, EBA, RH, etc) to quantify immunogenicity level of each protein family. Another area to explore is predicting immunogenicity from peptite sequences, which is being developed from epitope databases using machine learning algorithm [Bravi et al., 2023]. As expected, we found that the antibody gain in PfEMP1 antibodies against ATS domains was strain transcendental immunological responses.

To better understand the host's response, we considered a mathematical model which included both the variant specific and cross-reactive immune response mounted against parasites. Parasite dynamics with proliferation, negative selection, and *var* genes switching were modelled using both stochastic and deterministic approaches.

Our theoretical results show that persistent infection with parasite recrudescence requires complex and dynamic interactions of the malaria parasite and the human immune system. In practice, our model can define when and how parasitemia peaks form in chronic malaria infections. *Var* gene switching creates phenotypic heterogeneity in the parasite population that the immune system responds to. Our

results showed that the switching patterns that sustain parasitemia are non-random, with variants being more heterogeneous early in the infection, then converging to fewer variants in long-term infection.
We suggest that the diversity in the antigenic pool explains this heterogeneity and chronic parasitaemia patterns and that extinction times depend on the number of antigenic choices available to the parasite. Furthermore, we show that the persistence time for each parasite population is a parameterised function of the specific and cross-reactive responses. Based on our analytical findings and simulation results, we proved that antigenic variation linearly depends on the number of variants present in a population and leads to extension of infection length. The stochastic implementation of our model shows that infections started with similar parasite and host attributes show diverse behaviour at the earliest stages, which is lost over time as the parasite population grows.

4.1 Future extensions

In the following sections, we also consider a few potential future extensions of this dissertation work, which can enhance the understanding of experimental data originating from malaria infections.

Turnover Rate Estimation

We make point estimates of turnover probabilities of *var* gene expression in *in vivo* and *in vitro* settings; however, to obtain summary statistics and infer more about that the parameters as shown in [Recker et al., 2011; Noble and Recker, 2012] with *in vitro* data, realistically we would need several more time points to compute statistics on *in vivo* transition parameters.

Model Validation

There are several future directions that can be adopted for the modelling approach described in this thesis. Our current approach has yet not been tested on data coming from patients, even though we qualitatively obtain results pertaining to parasite population dynamics that are known to occur in asymptomatic infections. To this end, there are no 'gold-standard' datasets to test our approach on. In literature, both

more and less complex models than ours that have been conceptualised and tested on the malariatherapy dataset analysed by [Collins and Jeffery, 1999].

A recent thorough review of these modelling approaches revealed that [Camponovo et al., 2021] that the malariatherapy dataset does not represent a typical chronic infection timeline because patients were likely malaria naive. The dataset does not include immune response data or information about parasite gene expression. In this regard, we might have be able to address some of these concerns as we now have *var* gene expression as well parasite kinetics from asymptomatic individuals sampled monthly in The Gambia [Collins et al., 2022] and in preparation.

Cross-Reactive Immune Response and *var* expression

An interesting extension of the work on immune responses against PfEMP1 domains is the identification of effect of cross-reactive responses in CHMI studies. Provided that some 3D7 PfEMP1 sequences are more similar than others, the variant level cross-reactive responses to PfEMP1 proteins that are sequentially similar should correlate. These antibodies should then be able to inhibit the expression of variants that are similar to each other.

Testing the hypothesis: weak immunogenicity

In our analyses of CHMI data, we found that the correlation between new antibodies formed against expressed *var* genes was poor for most expressed variants two-three weeks post-infection. Ideally, we expect hosts to acquired antibodies against variants that are expressed during an infection, to suppress the growth of parasites expressing these variants on re-encounter. Since this pattern was consistent in two groups of volunteers, we hypothesised that possibly PfEMP1 proteins are potentially weakly immunogenic and do not provoke specific immune responses as an additional mechanism of escape. As a potential follow up study, seroreactivity from the chronic infection cohort from The Gambia [Collins et al., 2022] can be checked, as the *var* gene transcription profile at monthly timepoint is already characterised in 10 individuals. However, each individual being infected with a different *P. falciparum* 'strain', it would require developing a specific array for each infection, with recombinant domains from all 60 unique *var* genes.

Bibliography

Mohamed T Abuelazm, Mohamed A Elzeftawy, Manar Ahmed Kamal, Helmy Badr, Mohamed Gamal, Mahmoud Aboulgheit, Basel Abdelazeem, Sherief Abd-elsalam, and Mohamed Abouzid. Protective efficacy and safety of radiation-attenuated and chemo-attenuated plasmodium falciparum sporozoite vaccines against controlled and natural malaria infection: a systematic review and meta-analysis of randomized controlled trials. *Infection*, pages 1–16, 2024.

Jane Achan, Isaie J Reuling, Xi Zen Yap, Edgard Dabira, Abdullahi Ahmad, Momodou Cox, Davis Nwakanma, Kevin Tetteh, Lindsey Wu, Guido JH Bastiaens, et al. Serologic markers of previous malaria exposure and functional antibodies inhibiting parasite growth are associated with parasite kinetics following a plasmodium falciparum controlled human infection. *Clinical infectious diseases*, 70(12):2544–2552, 2020.

Z Agur, D Abiri, and LH Van der Ploeg. Ordered appearance of antigenic variants of african trypanosomes explained in a mathematical model based on a stochastic switch process and immune-selection against putative switch intermediates. *Proceedings of the National Academy of Sciences*, 86(23):9626–9630, 1989.

MA Ahmed and Janet Cox-Singh. P lasmodium knowlesi–an emerging pathogen. *ISBT science series*, 10(S1):134–140, 2015.

Masamichi Aikawa. Human cerebral malaria. *The American journal of tropical medicine and hygiene*, 39(1):3–10, 1988.

Onome J Akpogheneta, Nancy O Duah, Kevin KA Tetteh, Samuel Dunyo, David E Lanar, Margaret Pinder, and David J Conway. Duration of naturally acquired antibody responses to blood-stage plasmodium falciparum is age dependent and antigen specific. *Infection and immunity*, 76(4):1748–1755, 2008.

RM Anderson, RM May, and S Gupta. Non-linear phenomena in host—parasite interactions. *Parasitology*, 99(S1):S59–S79, 1989.

Spinello Antinori, Laura Galimberti, Laura Milazzo, and Mario Corbellino. Biology of human malaria plasmodia including plasmodium knowlesi. *Mediterranean journal of hematology and infectious diseases*, 4(1), 2012.

John J Aponte, Clara Menendez, David Schellenberg, Elizeus Kahigwa, Hassan Mshinda, Penelope Vountasou, Marcel Tanner, and Pedro L Alonso. Age interactions

in the development of naturally acquired immunity to plasmodium falciparum and its clinical presentation. *PLoS medicine*, 4(7):e242, 2007.

Joan L Aron and Robert M May. The population dynamics of malaria. In *The population dynamics of infectious diseases: theory and applications*, pages 139–179. Springer, 1982.

Stephanie C Austin, Paul D Stolley, and Tamar Lasky. The history of malariotherapy for neurosyphilis: modern parallels. *Jama*, 268(4):516–519, 1992.

Marion Avril, Abhai K Tripathi, Andrew J Brazier, Cheryl Andisi, Joel H Janes, Vijaya L Soma, David J Sullivan Jr, Peter C Bull, Monique F Stins, and Joseph D Smith. A restricted subset of var genes mediates adherence of plasmodium falciparum-infected erythrocytes to brain endothelial cells. *Proceedings of the National Academy of Sciences*, 109(26):E1782–E1790, 2012.

Anna Bachmann, Michaela Petter, Ralf Krumkamp, Meral Esen, Jana Held, Judith AM Scholz, Tao Li, B Kim Lee Sim, Stephen L Hoffman, Peter G Kremsner, et al. Mosquito passage dramatically changes var gene expression in controlled human plasmodium falciparum infections. *PLoS pathogens*, 12(4):e1005538, 2016.

Anna Bachmann, Ellen Bruske, Ralf Krumkamp, Louise Turner, J Stephan Wichers, Michaela Petter, Jana Held, Michael F Duffy, B Kim Lee Sim, Stephen L Hoffman, et al. Controlled human malaria infection with plasmodium falciparum demonstrates impact of naturally acquired immunity on virulence gene expression. *PLoS pathogens*, 15(7):e1007906, 2019.

J Kevin Baird, Trevor R Jones, Emon W Danudirgo, Barry A Annis, Michael J Bangs, H Basri, Sofyan Masbar, et al. Age-dependent acquired protection against plasmodium falciparum in people having two years exposure to hyperendemic malaria. *The American journal of tropical medicine and hygiene*, 45(1):65–76, 1991.

Alan G Barbour and Blanca I Restrepo. Antigenic variation in vector-borne pathogens. *Emerging infectious diseases*, 6(5):449, 2000.

Alyssa Barry and Diana Hansen. Naturally acquired immunity to malaria. *Parasitology*, 143(2):125–128, 2016.

Alyssa E Barry, Angela Trieu, Freya JI Fowkes, Jozelyn Pablo, Mina Kalantari-Dehaghi, Algis Jasinskas, Xiaolin Tan, Matthew A Kayala, Livingstone Tavul, Peter M Siba, et al. The stability and complexity of antibody responses to the major surface antigen of plasmodium falciparum are associated with age in a malaria endemic area. *Molecular & Cellular Proteomics*, 10(11), 2011.

Alessandro Bartoloni and Lorenzo Zammarchi. Clinical aspects of uncomplicated and severe malaria. *Mediterranean journal of hematology and infectious diseases*, 4(1), 2012.

Priyanka Barua, James G Beeson, Kenneth Maleta, Per Ashorn, and Stephen J Rogerson. The impact of early life exposure to plasmodium falciparum on the development of naturally acquired immunity to malaria in young malawian children. *Malaria Journal*, 18:1–12, 2019.

Dror I Baruch, Britten L Pasloske, Hardeep B Singh, Xiahui Bi, Xin C Ma, Michael Feldman, Theodore F Taraschi, and Russell J Howard. Cloning the p. falciparum gene encoding pfemp1, a malarial variant antigen and adherence receptor on the surface of parasitized human erythrocytes. *Cell*, 82(1):77–87, 1995.

BioRender. Malaria transmission cycle. BioRender, n.d. URL `https://app.biorender.com/biorender-templates/figures/all/t-5e629fe09501410088a0182f-malaria-transmission-cycle-2`. [Figure].

Selina ER Bopp, Micah J Manary, A Taylor Bright, Geoffrey L Johnston, Neekesh V Dharia, Fabio L Luna, Susan McCormack, David Plouffe, Case W McNamara, John R Walker, et al. Mitotic evolution of plasmodium falciparum shows a stable core genome but recombination in antigen families. *PLoS genetics*, 9(2):e1003293, 2013.

JT Bousema, CJ Drakeley, and RW Sauerwein. Sexual-stage antibody responses to p. falciparum in endemic populations. *Current molecular medicine*, 6(2):223–229, 2006.

Fred Brauer. Compartmental models in epidemiology. In *Mathematical epidemiology*, pages 19–79. Springer, 2008.

Barbara Bravi, Andrea Di Gioacchino, Jorge Fernandez-de Cossio-Diaz, Aleksandra M Walczak, Thierry Mora, Simona Cocco, and Rémi Monasson. A transfer-learning approach to predict antigen immunogenicity and t-cell receptor specificity. *ELife*, 12: e85126, 2023.

KN Brown, IN Brown, World Health Organization, et al. Immunity to malaria: antigenic variation in chronic infections of plasmodium knowlesi. Technical report, World Health Organization, 1966.

Peter C Bull and Abdirahman I Abdi. The role of pfemp1 as targets of naturally acquired immunity to childhood malaria: prospects for a vaccine. *Parasitology*, 143(2):171–186, 2016.

Peter C Bull, Brett S Lowe, Moses Kortok, Catherine S Molyneux, Christopher I Newbold, and Kevin Marsh. Parasite antigens on the infected red cell surface are targets for naturally acquired immunity to malaria. *Nature medicine*, 4(3):358–360, 1998.

Noah S Butler, Tajie H Harris, and Ira J Blader. Regulation of immunopathogenesis during plasmodium and toxoplasma infections: more parallels than distinctions? *Trends in parasitology*, 29(12):593–602, 2013.

Flavia Camponovo, Tamsin E Lee, Jonathan R Russell, Lydia Burgert, Jaline Gerardin, and Melissa A Penny. Mechanistic within-host models of the asexual plasmodium falciparum infection: a review and analytical assessment. *Malaria journal*, 20(1):1–22, 2021.

Pedro Toniol Cardin and Marco Antonio Teixeira. Fenichel theory for multiple time scale singular perturbation problems. *SIAM Journal on Applied Dynamical Systems*, 16 (3):1425–1452, 2017.

Ilona Carneiro, Arantxa Roca-Feltrer, Jamie T Griffin, Lucy Smith, Marcel Tanner, Joanna Armstrong Schellenberg, Brian Greenwood, and David Schellenberg. Age-patterns of malaria vary with severity, transmission intensity and seasonality in sub-saharan africa: a systematic review and pooled analysis. *PloS one*, 5(2):e8988, 2010.

David R Cavanagh, Ibrahim M Elhassan, Cally Roper, V Jane Robinson, Haider Giha, Anthony A Holder, Lars Hviid, Thor G Theander, David E Arnot, and Jana S McBride. A longitudinal study of type-specific antibody responses to plasmodium falciparum merozoite surface protein-1 in an area of unstable malaria in sudan. *The Journal of Immunology*, 161(1):347–359, 1998.

David R Cavanagh, Daniel Dodoo, Lars Hviid, Jørgen AL Kurtzhals, Thor G Theander, Bartholomew D Akanmori, Spencer Polley, David J Conway, Kojo Koram, and Jana S McBride. Antibodies to the n-terminal block 2 of plasmodium falciparum merozoite surface protein 1 are associated with protection against clinical malaria. *Infection and immunity*, 72(11):6492–6502, 2004.

Joseph D Challenger, Katia Bruxvoort, Azra C Ghani, and Lucy C Okell. Assessing the impact of imperfect adherence to artemether-lumefantrine on malaria treatment outcomes using within-host modelling. *Nature communications*, 8(1):1373, 2017.

Jo-Anne Chan, Katherine B Howell, Linda Reiling, Ricardo Ataide, Claire L Mackintosh, Freya JI Fowkes, Michaela Petter, Joanne M Chesson, Christine Langer, George M Warimwe, et al. Targets of antibodies against plasmodium falciparum–infected erythrocytes in malaria immunity. *The Journal of clinical investigation*, 122 (9):3227–3238, 2012.

Jo-Anne Chan, Freya JI Fowkes, and James G Beeson. Surface antigens of plasmodium falciparum-infected erythrocytes as immune targets and malaria vaccine candidates. *Cellular and Molecular Life Sciences*, 71:3633–3657, 2014.

Jo-Anne Chan, Michelle J Boyle, Kerryn A Moore, Linda Reiling, Zaw Lin, Wina Hasang, Marion Avril, Laurens Manning, Ivo Mueller, Moses Laman, et al. Antibody targets on the surface of plasmodium falciparum–infected erythrocytes that are associated with immunity to severe malaria in young children. *The Journal of infectious diseases*, 219(5):819–828, 2019.

Rana Chattopadhyay, Amit Sharma, Vinod K Srivastava, Sudhanshu S Pati, SK Sharma, Bhabani S Das, and Chetan E Chitnis. Plasmodium falciparum infection elicits both variant-specific and cross-reactive antibodies against variant surface antigens. *Infection and immunity*, 71(2):597–604, 2003.

Qijun Chen, Victor Fernandez, Annika Sundström, Martha Schlichtherle, Santanu Datta, Per Hagblom, and Mats Wahlgren. Developmental selection of var gene expression in plasmodium falciparum. *Nature*, 394(6691):392–395, 1998.

Eli Chernin. The malariatherapy of neurosyphilis. *The Journal of parasitology*, 70(5): 611–617, 1984.

Lauren M Childs and Caroline O Buckee. Dissecting the determinants of malaria chronicity: why within-host models struggle to reproduce infection dynamics. *Journal of The Royal Society Interface*, 12(104):20141379, 2015.

Thanat Chookajorn, Ron Dzikowski, Matthias Frank, Felomena Li, Alisha Z Jiwani, Daniel L Hartl, and Kirk W Deitsch. Epigenetic memory at malaria virulence genes. *Proceedings of the National Academy of Sciences*, 104(3):899–902, 2007.

Kesinee Chotivanich, Rachanee Udomsangpetch, Julie A Simpson, Paul Newton, Sasithon Pukrittayakamee, Sornchai Looareesuwan, and Nicholas J White. Parasite multiplication potential and the severity of falciparum malaria. *The Journal of infectious diseases*, 181(3):1206–1209, 2000.

Marco Ciotti, Massimo Ciccozzi, Alessandro Terrinoni, Wen-Can Jiang, Cheng-Bin Wang, and Sergio Bernardini. The covid-19 pandemic. *Critical reviews in clinical laboratory sciences*, 57(6):365–388, 2020.

Stanca M Ciupe and Jane M Heffernan. In-host modeling. *Infectious Disease Modelling*, 2(2):188–202, 2017.

Antoine Claessens, Yvonne Adams, Ashfaq Ghumra, Gabriella Lindergard, Caitlin C Buchan, Cheryl Andisi, Peter C Bull, Sachel Mok, Archna P Gupta, Christian W Wang, et al. A subset of group a-like var genes encodes the malaria parasite ligands for binding to human brain endothelial cells. *Proceedings of the National Academy of Sciences*, 109(26):E1772–E1781, 2012.

S Cohen, IA McGregor, S Carrington, et al. Gamma-globulin and acquired immunity to human malaria. *Nature*, 192:733–7, 1961.

S Cohen, GA Butcher, and RB Crandall. Action of malarial antibody in vitro. *Nature*, 223(5204):368–371, 1969.

Katharine A Collins, Sukai Ceesay, Sainabou Drammeh, Fatou K Jaiteh, Marc Antoine Guery, Kjerstin Lanke, Lynn Grignard, Will Stone, David J Conway, Umberto D'alessandro, et al. A cohort study on the duration of plasmodium falciparum infections during the dry season in the gambia. *The Journal of infectious diseases*, 226 (1):128–137, 2022.

William E Collins and Geoffrey M Jeffery. A retrospective examination of sporozoite- and trophozoite-induced infections with plasmodium falciparum: development of parasitologic and clinical immunity during primary infection. *The American journal of tropical medicine and hygiene*, 61(1 Suppl):4–19, 1999.

Alan F Cowman, Julie Healer, Danushka Marapana, and Kevin Marsh. Malaria: biology and disease. *Cell*, 167(3):610–624, 2016.

Herbert W Cox. A study of relapse plasmodium berghei infections isolated from white mice. *The Journal of Immunology*, 82(3):209–214, 1959.

Janet Cox-Singh and Balbir Singh. Knowlesi malaria: newly emergent and of public health importance? *Trends in parasitology*, 24(9):406–410, 2008.

Alister G Craig, Georges E Grau, Chris Janse, James W Kazura, Dan Milner, John W Barnwell, Gareth Turner, Jean Langhorne, and participants of the Hinxton Retreat meeting on "Animal Models for Research on Severe Malaria". The role of animal models for research on severe malaria. *PLoS pathogens*, 8(2):e1002401, 2012.

Alina Crudu, Arnaud Debussche, and Ovidiu Radulescu. Hybrid stochastic simplifications for multiscale gene networks. *BMC Systems Biology*, 3:89, 2009.

Alina Crudu, Arnaud Debussche, Aurélie Muller, and Ovidiu Radulescu. Convergence of stochastic gene networks to hybrid piecewise deterministic processes. *Annals of Applied Probability*, 22(5):1822–1859, 2012.

Mark HA Davis. Piecewise-deterministic markov processes: A general class of non-diffusion stochastic models. *Journal of the Royal Statistical Society: Series B (Methodological)*, 46(3):353–376, 1984.

Kirk W Deitsch and Ron Dzikowski. Variant gene expression and antigenic variation by malaria parasites. *Annual review of microbiology*, 71:625–641, 2017.

Kirk W Deitsch and Lars Hviid. Variant surface antigens, virulence genes and the pathogenesis of malaria. *Trends in parasitology*, 20(12):562–566, 2004.

Kirk W Deitsch, Sheila A Lukehart, and James R Stringer. Common strategies for antigenic variation by bacterial, fungal and protozoan pathogens. *Nature Reviews Microbiology*, 7(7):493–503, 2009.

Edmund X DeJesus and Charles Kaufman. Routh-hurwitz criterion in the examination of eigenvalues of a system of nonlinear ordinary differential equations. *Physical Review A*, 35(12):5288, 1987.

Klaus Dietz, Gunter Raddatz, and Louis Molineaux. Mathematical model of the first wave of plasmodium falciparum asexual parasitemia in non-immune and vaccinated individuals. *The American journal of tropical medicine and hygiene*, 75(2 Suppl):46–55, 2006.

Daniel Dodoo, Trine Staalsoe, Haider Giha, Jørgen AL Kurtzhals, Bartholomew D Akanmori, Kojo Koram, Samuel Dunyo, Francis K Nkrumah, Lars Hviid, and Thor G Theander. Antibodies to variant antigens on the surfaces of infected erythrocytes are associated with protection from malaria in ghanaian children. *Infection and immunity*, 69(6):3713–3718, 2001.

E Dorman and C Shulman. Malaria in pregnancy. *Current Obstetrics and Gynaecology*, 10(4):183–189, 2000.

Alexander D Douglas, Nick J Edwards, Christopher JA Duncan, Fiona M Thompson, Susanne H Sheehy, Geraldine A O'Hara, Nicholas Anagnostou, Michael Walther, Daniel P Webster, Susanna J Dunachie, et al. Comparison of modeling methods to determine liver-to-blood inocula and parasite multiplication rates during controlled human malaria infection. *The Journal of infectious diseases*, 208(2):340–345, 2013.

Josefine Dunst, Faustin Kamena, and Kai Matuschewski. Cytokines and chemokines in cerebral malaria pathogenesis. *Frontiers in cellular and infection microbiology*, 7:324, 2017.

Ron Dzikowski, Matthias Frank, and Kirk Deitsch. Mutually exclusive expression of virulence genes by malaria parasites is regulated independently of antigen production. *PLoS pathogens*, 2(3):e22, 2006.

Philip A Eckhoff. Malaria parasite diversity and transmission intensity affect development of parasitological immunity in a mathematical model. *Malaria journal*, 11(1):1–14, 2012.

John D Enderle. Compartmental modeling. In *Introduction to Biomedical Engineering*, pages 359–445. Elsevier, 2012.

Stewart N Ethier and Thomas G Kurtz. *Markov processes: characterization and convergence*. John Wiley & Sons, 2009.

Chinonso Anthony Ezema, Innocent Uzochukwu Okagu, and Timothy Prince Chidike Ezeorba. Escaping the enemy's bullets: an update on how malaria parasites evade host immune response. *Parasitology Research*, pages 1–17, 2023.

Rick M Fairhurst and Thomas E Wellems. Modulation of malaria virulence by determinants of plasmodium falciparum erythrocyte membrane protein-1 display. *Current opinion in hematology*, 13(3):124–130, 2006.

Neil Fenichel. Geometric singular perturbation theory for ordinary differential equations. *Journal of differential equations*, 31(1):53–98, 1979.

Christian Flueck, Richard Bartfai, Jennifer Volz, Igor Niederwieser, Adriana M Salcedo-Amaya, Blaise TF Alako, Florian Ehlgen, Stuart A Ralph, Alan F Cowman, Zbynek Bozdech, et al. Plasmodium falciparum heterochromatin protein 1 marks genomic loci linked to phenotypic variation of exported virulence factors. *PLoS pathogens*, 5 (9):e1000569, 2009.

Matthias Frank, Ron Dzikowski, Borko Amulic, and Kirk Deitsch. Variable switching rates of malaria virulence genes are associated with chromosomal position. *Molecular microbiology*, 64(6):1486–1498, 2007.

Lúcio H Freitas-Junior, Emmanuel Bottius, Lindsay A Pirrit, Kirk W Deitsch, Christine Scheidig, Francoise Guinet, Ulf Nehrbass, Thomas E Wellems, and Artur Scherf. Frequent ectopic recombination of virulence factor genes in telomeric chromosome clusters of p. falciparum. *Nature*, 407(6807):1018–1022, 2000.

Beatriz Galatas, Quique Bassat, and Alfredo Mayor. Malaria parasites in the asymptomatic: looking for the hay in the haystack. *Trends in parasitology*, 32(4):296–308, 2016.

Beatriz Galatas, Helena Martí-Soler, Lidia Nhamussua, Pau Cisteró, Pedro Aide, Francisco Saute, Clara Menéndez, N Regina Rabinovich, Pedro L Alonso, Quique Bassat, et al. Dynamics of afebrile plasmodium falciparum infections in mozambican men. *Clinical Infectious Diseases*, 67(7):1045–1052, 2018.

Benoît Gamain, Arnaud Chêne, Nicola K Viebig, Nicaise Tuikue Ndam, and Morten A Nielsen. Progress and insights toward an effective placental malaria vaccine. *Frontiers in Immunology*, 12:634508, 2021.

Michelle L Gatton and Qin Cheng. Modeling the development of acquired clinical immunity to plasmodium falciparum malaria. *Infection and immunity*, 72(11):6538–6545, 2004.

Michelle L Gatton, Jennifer M Peters, Elizabeth V Fowler, and Qin Cheng. Switching rates of plasmodium falciparum var genes: faster than we thought? *Trends in Parasitology*, 19(5):202–208, 2003.

Athina Georgiadou, Hyun Jae Lee, Michael Walther, Anna E van Beek, Fadlila Fitriani, Diana Wouters, Taco W Kuijpers, Davis Nwakanma, Umberto D'Alessandro,

Eleanor M Riley, et al. Modelling pathogen load dynamics to elucidate mechanistic determinants of host–plasmodium falciparum interactions. *Nature microbiology*, 4(9): 1592–1602, 2019.

Daniel T Gillespie. Exact stochastic simulation of coupled chemical reactions. *The journal of physical chemistry*, 81(25):2340–2361, 1977.

E Gjini, DT Haydon, JD Barry, and CA Cobbold. Critical interplay between parasite differentiation, host immunity, and antigenic variation in trypanosome infections. *The American Naturalist*, 176(4):424–439, 2010.

Bénédicte Gnangnon, Manoj T Duraisingh, and Caroline O Buckee. Deconstructing the parasite multiplication rate of plasmodium falciparum. *Trends in Parasitology*, 37 (10):922–932, 2021.

Elena Gómez-Díaz, Rakiswendé S Yerbanga, Thierry Lefèvre, Anna Cohuet, M Jordan Rowley, Jean Bosco Ouedraogo, and Victor G Corces. Epigenetic regulation of plasmodium falciparum clonally variant gene expression during development in anopheles gambiae. *Scientific reports*, 7(1):40655, 2017.

S Jake Gonzales, Raphael A Reyes, Ashley E Braddom, Gayani Batugedara, Sebastiaan Bol, and Evelien M Bunnik. Naturally acquired humoral immunity against plasmodium falciparum malaria. *Frontiers in immunology*, 11:594653, 2020.

Weidong Gu and Robert J Novak. Habitat-based modeling of impacts of mosquito larval interventions on entomological inoculation rates, incidence, and prevalence of malaria. *The American journal of tropical medicine and hygiene*, 73(3):546–552, 2005.

Julien Guizetti and Artur Scherf. Silence, activate, poise and switch! mechanisms of antigenic variation in p lasmodium falciparum. *Cellular microbiology*, 15(5):718–726, 2013.

Sunetra Gupta, Robert W Snow, Christl A Donnelly, Kevin Marsh, and Chris Newbold. Immunity to non-cerebral severe malaria is acquired after one or two infections. *Nature medicine*, 5(3):340–343, 1999.

David Gurarie, Stephan Karl, Peter A Zimmerman, Charles H King, Timothy G St. Pierre, and Timothy ME Davis. Mathematical modeling of malaria infection with innate and adaptive immunity in individuals and agent-based communities. *PloS one*, 7(3):e34040, 2012.

Julius Clemence Hafalla, Olivier Silvie, and Kai Matuschewski. Cell biology and immunology of malaria. *Immunological reviews*, 240(1):297–316, 2011.

Mariah Hassert, Sahaana Arumugam, and John T Harty. Memory cd8+ t cell-mediated protection against liver-stage malaria. *Immunological reviews*, 2023.

Qixin He and Mercedes Pascual. An antigenic diversification threshold for falciparum malaria transmission at high endemicity. *PLOS Computational Biology*, 17(2): e1008729, 2021.

Carol A Holland and Frederick L Kiechle. Point-of-care molecular diagnostic systems—past, present and future. *Current opinion in microbiology*, 8(5):504–509, 2005.

Mark H Holmes. *Introduction to perturbation methods*, volume 20. Springer Science & Business Media, 2012.

Regina Hoo, Ellen Bruske, Sandra Dimonte, Lei Zhu, Benjamin Mordmüller, B Kim Lee Sim, Peter G Kremsner, Stephen L Hoffman, Zbynek Bozdech, Matthias Frank, et al. Transcriptome profiling reveals functional variation in plasmodium falciparum parasites from controlled human malaria infection studies. *EBioMedicine*, 48:442–452, 2019.

David Horn. Antigenic variation in african trypanosomes. *Molecular and biochemical parasitology*, 195(2):123–129, 2014.

Paul Horrocks, Robert Pinches, Zóe Christodoulou, Sue A Kyes, and Chris I Newbold. Variable var transition rates underlie antigenic variation in malaria. *Proceedings of the National Academy of Sciences*, 101(30):11129–11134, 2004.

Lars Hviid. Naturally acquired immunity to plasmodium falciparum malaria in africa. *Acta tropica*, 95(3):270–275, 2005.

Lars Hviid and Anja TR Jensen. Pfemp1–a parasite protein family of key importance in plasmodium falciparum malaria immunity and pathogenesis. *Advances in parasitology*, 88:51–84, 2015.

Peter Jahnmatz, Diana Nyabundi, Christopher Sundling, Linnea Widman, Jedidah Mwacharo, Jennifer Musyoki, Edward Otieno, Niklas Ahlborg, Philip Bejon, Francis M Ndungu, et al. Plasmodium falciparum-specific memory b-cell and antibody responses are associated with immunity in children living in an endemic area of kenya. *Frontiers in Immunology*, 13:799306, 2022.

Anja Ramstedt Jensen, Yvonne Adams, and Lars Hviid. Cerebral plasmodium falciparum malaria: The role of pfemp1 in its pathogenesis and immunity, and pfemp1-based vaccines to prevent it. *Immunological reviews*, 293(1):230–252, 2020.

Anja TR Jensen, Pamela Magistrado, Sarah Sharp, Louise Joergensen, Thomas Lavstsen, Antonella Chiucchiuini, Ali Salanti, Lasse S Vestergaard, John P Lusingu, Rob Hermsen, et al. Plasmodium falciparum associated with severe childhood malaria preferentially expresses pfemp1 encoded by group a var genes. *The Journal of experimental medicine*, 199(9):1179–1190, 2004.

Lubin Jiang, Jianbing Mu, Qingfeng Zhang, Ting Ni, Prakash Srinivasan, Kempaiah Rayavara, Wenjing Yang, Louise Turner, Thomas Lavstsen, Thor G Theander, et al. Pfsetvs methylation of histone h3k36 represses virulence genes in plasmodium falciparum. *Nature*, 499(7457):223–227, 2013.

William Ogilvy Kermack and Anderson G McKendrick. A contribution to the mathematical theory of epidemics. *Proceedings of the royal society of london. Series A, Containing papers of a mathematical and physical character*, 115(772):700–721, 1927.

Sammy Khagayi, Meghna Desai, Nyaguara Amek, Vincent Were, Eric Donald Onyango, Christopher Odero, Kephas Otieno, Godfrey Bigogo, Stephen Munga, Frank Odhiambo, et al. Modelling the relationship between malaria prevalence as a measure of transmission and mortality across age groups. *Malaria journal*, 18(1): 1–12, 2019.

David S Khoury, Rosemary Aogo, Georges Randriafanomezantsoa-Radohery, James M McCaw, Julie A Simpson, James S McCarthy, Ashraful Haque, Deborah Cromer, and Miles P Davenport. Within-host modeling of blood-stage malaria. *Immunological reviews*, 285(1):168–193, 2018.

Hannah W Kimingi, Ann W Kinyua, Nicole A Achieng, Kennedy M Wambui, Shaban Mwangi, Roselyne Nguti, Cheryl A Kivisi, Anja TR Jensen, Philip Bejon, Melisa C Kapulu, et al. Breadth of antibodies to plasmodium falciparum variant surface antigens is associated with immunity in a controlled human malaria infection study. *Frontiers in Immunology*, 13, 2022.

Hugh W Kingston, Aniruddha Ghose, Katherine Plewes, Haruhiko Ishioka, Stije J Leopold, Richard J Maude, Sanjib Paul, Benjamas Intharabut, Kamorat Silamut, Charles Woodrow, et al. Disease severity and effective parasite multiplication rate in falciparum malaria. In *Open forum infectious diseases*, volume 4, page ofx169. Oxford University Press US, 2017.

Samson M Kinyanjui, Tabitha Mwangi, Peter C Bull, Christopher I Newbold, and Kevin Marsh. Protection against clinical malaria by heterologous immunoglobulin g antibodies against malaria-infected erythrocyte variant surface antigens requires interaction with asymptomatic infections. *Journal of Infectious Diseases*, 190(9):1527–1533, 2004.

Eili Y Klein, Andrea L Graham, Manuel Llinás, and Simon Levin. Cross-reactive immune responses as primary drivers of malaria chronicity. *Infection and immunity*, 82(1):140–151, 2014.

Peter Kotelenez. Law of large numbers and central limit theorem for linear chemical reactions with diffusion. *The Annals of Probability*, pages 173–193, 1986.

Susan M Kraemer and Joseph D Smith. Evidence for the importance of genetic structuring to the structural and functional specialization of the plasmodium falciparum var gene family. *Molecular microbiology*, 50(5):1527–1538, 2003.

Susan M Kraemer and Joseph D Smith. A family affair: var genes, pfemp1 binding, and malaria disease. *Current opinion in microbiology*, 9(4):374–380, 2006.

Manisha A Kulkarni, Rachelle E Desrochers, and Jeremy T Kerr. High resolution niche models of malaria vectors in northern tanzania: a new capacity to predict malaria risk? *PLoS One*, 5(2):e9396, 2010.

Thomas G Kurtz. Solutions of ordinary differential equations as limits of pure jump markov processes. *Journal of applied Probability*, 7(1):49–58, 1970.

Sue Kyes, Paul Horrocks, and Chris Newbold. Antigenic variation at the infected red cell surface in malaria. *Annual Reviews in Microbiology*, 55(1):673–707, 2001.

Paco Axel Lagerstrom. *Matched asymptotic expansions: ideas and techniques*, volume 76. Springer Science & Business Media, 2013.

Daniel B Larremore, Sesh A Sundararaman, Weimin Liu, William R Proto, Aaron Clauset, Dorothy E Loy, Sheri Speede, Lindsey J Plenderleith, Paul M Sharp, Beatrice H Hahn, et al. Ape parasite origins of human malaria virulence genes. *Nature communications*, 6(1):8368, 2015.

Marc Lipsitch and Justin J O'Hagan. Patterns of antigenic diversity and the mechanisms that maintain them. *Journal of the Royal Society Interface*, 4(16):787–802, 2007.

Jose Juan Lopez-Rubio, Alisson M Gontijo, Marta C Nunes, Neha Issar, Rosaura Hernandez Rivas, and Artur Scherf. 5' flanking region of var genes nucleate histone modification patterns linked to phenotypic inheritance of virulence traits in malaria parasites. *Molecular microbiology*, 66(6):1296–1305, 2007.

Jose-Juan Lopez-Rubio, Liliana Mancio-Silva, and Artur Scherf. Genome-wide analysis of heterochromatin associates clonally variant gene regulation with perinuclear repressive centers in malaria parasites. *Cell host & microbe*, 5(2):179–190, 2009.

Katrina A Lythgoe, Liam J Morrison, Andrew F Read, and J David Barry. Parasite-intrinsic factors can explain ordered progression of trypanosome antigenic variation. *Proceedings of the National Academy of Sciences*, 104(19):8095–8100, 2007.

Gavin Mackenzie, Rasmus W Jensen, Thomas Lavstsen, and Thomas D Otto. Varia: a tool for prediction, analysis and visualisation of variable genes. *BMC bioinformatics*, 23(1):52, 2022.

GG MacPherson, MJ Warrell, NJ White, SORNCHAI Looareesuwan, and DA Warrell. Human cerebral malaria. a quantitative ultrastructural analysis of parasitized erythrocyte sequestration. *The American journal of pathology*, 119(3):385, 1985.

Almahamoudou Mahamar, Moussa Traore, Bruce Swihart, Oumar Attaher, Bacary Soumana Diarra, Gaoussou Santara, Djibrilla Issiaka, Amadou Barry, Youssoufa Sidibé, Yahia T Dicko, et al. Acquisition of antibodies that block plasmodium falciparum adhesion to placental receptor chondroitin sulfate a with increasing gravidity in malian women. *Frontiers in Immunology*, 14, 2023.

Alexander G Maier, Kai Matuschewski, Meng Zhang, and Melanie Rug. Plasmodium falciparum. *Trends in parasitology*, 35(6):481–482, 2019.

Sandip Mandal, Ram Rup Sarkar, and Somdatta Sinha. Mathematical models of malaria-a review. *Malaria journal*, 10(1):1–19, 2011.

Mayfong Mayxay, Sasithon Pukrittayakamee, Paul N Newton, and Nicholas J White. Mixed-species malaria infections in humans. *Trends in parasitology*, 20(5):233–240, 2004.

IA McGregor. Mechanisms of acquired immunity and epidemiological patterns of antibody responses in malaria in man. *Bulletin of the World Health Organization*, 50 (3-4):259, 1974.

F Ellis McKenzie and William H Bossert. An integrated model of plasmodium falciparum dynamics. *Journal of theoretical biology*, 232(3):411–426, 2005.

Philip G McQueen, Kim C Williamson, and F Ellis McKenzie. Host immune constraints on malaria transmission: insights from population biology of within-host parasites. *Malaria journal*, 12:1–18, 2013.

Elamaran Meibalan and Matthias Marti. Biology of malaria transmission. *Cold Spring Harbor Perspectives in Medicine*, 7(3):a025452, 2017.

Louis H Miller, Michael F Good, and Genevieve Milon. Malaria pathogenesis. *Science*, 264(5167):1878–1883, 1994.

Kathryn Milne, Alasdair Ivens, Adam J Reid, Magda E Lotkowska, Aine O'Toole, Geetha Sankaranarayanan, Diana Munoz Sandoval, Wiebke Nahrendorf, Clement Regnault, Nick J Edwards, et al. Mapping immune variation and var gene switching in naive hosts infected with plasmodium falciparum. *Elife*, 10:e62800, 2021.

L Molineaux, HH Diebner, M Eichner, WE Collins, GM Jeffery, and K Dietz. Plasmodium falciparum parasitaemia described by a new mathematical model. *Parasitology*, 122(4):379–391, 2001.

Elkhansaa Nassir, Abdel-Muhsin A Abdel-Muhsin, Suad Suliaman, Fiona Kenyon, Amani Kheir, Haider Geha, Heather M Ferguson, David Walliker, and Hamza A Babiker. Impact of genetic complexity on longevity and gametocytogenesis of plasmodium falciparum during the dry and transmission-free season of eastern sudan. *International journal for parasitology*, 35(1):49–55, 2005.

Francis Maina Ndungu, Ally Olotu, Jedidah Mwacharo, Mary Nyonda, Jordan Apfeld, Lazarus K Mramba, Gregory W Fegan, Philip Bejon, and Kevin Marsh. Memory b cells are a more reliable archive for historical antimalarial responses than plasma antibodies in no-longer exposed children. *Proceedings of the National Academy of Sciences*, 109(21):8247–8252, 2012.

Billy Ngasala, Marycelina Mubi, Marian Warsame, Max G Petzold, Amos Y Massele, Lars L Gustafsson, Goran Tomson, Zul Premji, and Anders Bjorkman. Impact of training in clinical and microscopy diagnosis of childhood malaria on antimalarial drug prescription and health outcome at primary health care level in tanzania: a randomized controlled trial. *Malaria Journal*, 7(1):1–11, 2008.

Mary Beth Nierengarten. Malariotherapy to treat hiv patients? *The Lancet Infectious Diseases*, 3(6):321, 2003.

Robert Noble and Mario Recker. A statistically rigorous method for determining antigenic switching networks. *PLoS One*, 7(6):e39335, 2012.

Robert Noble, Zóe Christodoulou, Sue Kyes, Robert Pinches, Chris I Newbold, and Mario Recker. The antigenic switching network of plasmodium falciparum and its implications for the immuno-epidemiology of malaria. *Elife*, 2:e01074, 2013.

Sarah I Nogaro, Julius C Hafalla, Brigitte Walther, Edmond J Remarque, Kevin KA Tetteh, David J Conway, Eleanor M Riley, and Michael Walther. The breadth, but not the magnitude, of circulating memory b cell responses to p. falciparum increases with age/exposure in an area of low transmission. *PloS one*, 6(10):e25582, 2011.

Martin Nowak and Robert M May. *Virus dynamics: mathematical principles of immunology and virology: mathematical principles of immunology and virology*. Oxford University Press, UK, 2000.

Sofia Nunes-Silva, Sébastien Dechavanne, Azizath Moussiliou, Natalia Pstrąg, Jean-Philippe Semblat, Stéphane Gangnard, Nicaise Tuikue-Ndam, Philippe Deloron, Arnaud Chêne, and Benoît Gamain. Beninese children with cerebral malaria do not develop humoral immunity against the it4-var19-dc8 pfemp1 variant linked to epcr and brain endothelial binding. *Malaria journal*, 14(1):1–15, 2015.

Prince B Nyarko and Antoine Claessens. Understanding host–pathogen–vector interactions with chronic asymptomatic malaria infections. *Trends in parasitology*, 37 (3):195–204, 2021.

Miranda S Oakley, Noel Gerald, Thomas F McCutchan, L Aravind, and Sanjai Kumar. Clinical and molecular aspects of malaria fever. *Trends in parasitology*, 27(10):442–449, 2011.

Nyamekye Obeng-Adjei, Daniel B Larremore, Louise Turner, Aissata Ongoiba, Shanping Li, Safiatou Doumbo, Takele B Yazew, Kassoum Kayentao, Louis H Miller, Boubacar Traore, et al. Longitudinal analysis of naturally acquired pfemp1 cidr domain variant antibodies identifies associations with malaria protection. *JCI insight*, 5(12), 2020.

Emelda A Okiro, Abdullah Al-Taiar, Hugh Reyburn, Richard Idro, James A Berkley, and Robert W Snow. Age patterns of severe paediatric malaria and their relationship to plasmodium falciparum transmission intensity. *Malaria journal*, 8:1–11, 2009.

Thomas D Otto, Sammy A Assefa, Ulrike Böhme, Mandy J Sanders, Dominic Kwiatkowski, Matt Berriman, Chris Newbold, et al. Evolutionary analysis of the most polymorphic gene family in falciparum malaria. *Wellcome Open Research*, 4, 2019.

S. Owusu-Agyei et al. Incidence of symptomatic and asymptomatic plasmodium falciparum infection following curative therapy in adult residents of northern ghana. *American Journal of Tropical Medicine and Hygiene*, 65(3):197–203, 2001.

S Paget-McNicol, M Gatton, Ian Hastings, and A Saul. The plasmodium falciparum var gene switching rate, switching mechanism and patterns of parasite recrudescence described by mathematical modelling. *Parasitology*, 124(3):225–235, 2002.

Brittan L Pasloske and Russell J Howard. Malaria, the red cell, and the endothelium. *Annual review of medicine*, 45(1):283–295, 1994.

REL Paul, F Ariey, and Vincent Robert. The evolutionary ecology of plasmodium. *Ecology Letters*, 6(9):866–880, 2003.

Alan S Perelson. Modelling viral and immune system dynamics. *Nature reviews immunology*, 2(1):28–36, 2002.

Jennifer Peters, Elizabeth Fowler, Michelle Gatton, Nanhua Chen, Allan Saul, and Qin Cheng. High diversity and rapid changeover of expressed var genes during the acute phase of plasmodium falciparum infections in human volunteers. *Proceedings of the National Academy of Sciences*, 99(16):10689–10694, 2002.

Jennifer M Peters, Elizabeth V Fowler, Darren R Krause, Qin Cheng, and Michelle L Gatton. Differential changes in plasmodium falciparum var transcription during adaptation to culture. *The Journal of infectious diseases*, 195(5):748–755, 2007.

Anastasia K Pickford, Lucas Michel-Todó, Florian Dupuy, Alfredo Mayor, Pedro L Alonso, Catherine Lavazec, and Alfred Cortés. Expression patterns of plasmodium falciparum clonally variant genes at the onset of a blood infection in malaria-naive humans. *Mbio*, 12(4):10–1128, 2021.

Shai Pilosof, Qixin He, Kathryn E Tiedje, Shazia Ruybal-Pesántez, Karen P Day, and Mercedes Pascual. Competition for hosts modulates vast antigenic diversity to generate persistent strain structure in plasmodium falciparum. *PLoS biology*, 17(6): e3000336, 2019.

Douglas G Postels and Gretchen L Birbeck. Cerebral malaria. *Handbook of clinical neurology*, 114:91–102, 2013.

Ovidiu RADULESCU, Aurélie MULLER, and Alina CRUDU. Théorèmes limites pour les processus de markov à sauts: Synthèse de résultats et applications en biologie moléculaire. *TSI. Technique et science informatiques*, 26(3-4):443–469, 2007.

Thomas S Rask, Daniel A Hansen, Thor G Theander, Anders Gorm Pedersen, and Thomas Lavstsen. Plasmodium falciparum erythrocyte membrane protein 1 diversity in seven genomes–divide and conquer. *PLoS computational biology*, 6(9): e1000933, 2010.

Mario Recker, Sean Nee, Peter C Bull, Sam Kinyanjui, Kevin Marsh, Chris Newbold, and Sunetra Gupta. Transient cross-reactive immune responses can orchestrate antigenic variation in malaria. *Nature*, 429(6991):555–558, 2004.

Mario Recker, Caroline O Buckee, Andrew Serazin, Sue Kyes, Robert Pinches, Zóe Christodoulou, Amy L Springer, Sunetra Gupta, and Chris I Newbold. Antigenic variation in plasmodium falciparum malaria involves a highly structured switching pattern. *PLoS Pathogens*, 7(3):e1001306, 2011.

John Rek, Sara Lynn Blanken, Joseph Okoth, Daniel Ayo, Ismail Onyige, Eric Musasizi, Jordache Ramjith, Chiara Andolina, Kjerstin Lanke, Emmanuel Arinaitwe, et al. Asymptomatic school-aged children are important drivers of malaria transmission in a high endemicity setting in uganda. *The Journal of infectious diseases*, 226(4):708–713, 2022.

David J Roberts, Craig, Anthony R Berendt, Robert Pinches, Gerard Nash, Kevin Marsh, and Christopher I Newbold. Rapid switching to multiple antigenic and adhesive phenotypes in malaria. *Nature*, 357(6380):689–692, 1992.

Josea Rono, Faith HA Osier, Daniel Olsson, Scott Montgomery, Leah Mhoja, Ingegerd Rooth, Kevin Marsh, and Anna Färnert. Breadth of anti-merozoite antibody responses is associated with the genetic diversity of asymptomatic plasmodium falciparum infections and protection against clinical malaria. *Clinical infectious diseases*, 57(10):1409–1416, 2013.

Fumiji Saito, Kouyuki Hirayasu, Takeshi Satoh, Christian W Wang, John Lusingu, Takao Arimori, Kyoko Shida, Nirianne Marie Q Palacpac, Sawako Itagaki, Shiroh Iwanaga, et al. Immune evasion of plasmodium falciparum by rifin via inhibitory receptors. *Nature*, 552(7683):101–105, 2017.

Jean Biram Sarr, Franck Remoue, Badara Samb, Ibrahima Dia, Sohibou Guindo, Cheikh Sow, Sophie Maiga, Seydou Tine, Cheikh Thiam, Anne-Marie Schacht, et al. Evaluation of antibody response to plasmodium falciparum in children according to exposure of anopheles gambiae sl or anopheles funestus vectors. *Malaria Journal*, 6: 1–9, 2007.

Lisa Sattenspiel. Modeling the spread of infectious disease in human populations. *American Journal of Physical Anthropology*, 33(S11):245–276, 1990.

Lisa Sattenspiel and Alun Lloyd. *The geographic spread of infectious diseases: models and applications*, volume 5. Princeton University Press, 2009.

A Saul. Models for the in-host dynamics of malaria revisited: errors in some basic models lead to large over-estimates of growth rates. *Parasitology*, 117(5):405–407, 1998.

A Scherf, R Hernandez-Rivas, P Buffet, E Bottius, C Benatar, B Pouvelle, J Gysin, and M Lanzer. Antigenic variation in malaria: in situ switching, relaxed and mutually exclusive transcription of var genes during intra-erythrocytic development in plasmodium falciparum. *The EMBO journal*, 1998.

Richard-Fabian Schumacher and Elena Spinelli. Malaria in children. *Mediterranean journal of hematology and infectious diseases*, 4(1), 2012.

Frederick L Schuster. Cultivation of plasmodium spp. *Clinical microbiology reviews*, 15 (3):355–364, 2002.

Lalita Sharma and Geeta Shukla. Placental malaria: a new insight into the pathophysiology. *Frontiers in medicine*, 4:117, 2017.

Irwin W Sherman, Shigetoshi Eda, and Enrique Winograd. Cytoadherence and sequestration in plasmodium falciparum: defining the ties that bind. *Microbes and infection*, 5(10):897–909, 2003.

Balbir Singh and Cyrus Daneshvar. Human infections and detection of plasmodium knowlesi. *Clinical microbiology reviews*, 26(2):165–184, 2013.

David L Smith, Katherine E Battle, Simon I Hay, Christopher M Barker, Thomas W Scott, and F Ellis McKenzie. Ross, macdonald, and a theory for the dynamics and control of mosquito-transmitted pathogens. *PLoS pathogens*, 8(4):e1002588, 2012.

David L Smith, Justin M Cohen, Christinah Chiyaka, Geoffrey Johnston, Peter W Gething, Roly Gosling, Caroline O Buckee, Ramanan Laxminarayan, Simon I Hay, and Andrew J Tatem. A sticky situation: the unexpected stability of malaria elimination. *Philosophical Transactions of the Royal Society B: Biological Sciences*, 368 (1623):20120145, 2013.

Neal R Smith, James M Trauer, Manoj Gambhir, Jack S Richards, Richard J Maude, Jonathan M Keith, and Jennifer A Flegg. Agent-based models of malaria transmission: a systematic review. *Malaria journal*, 17(1):1–16, 2018.

Georges Snounou and Jean-Louis Pérignon. Malariotherapy–insanity at the service of malariology. *Advances in parasitology*, 81:223–255, 2013.

Robert W Snow, Eline L Korenromp, and Eleanor Gouws. Pediatric mortality in africa: plasmodium falciparum malaria as a cause or risk? *The Intolerable Burden of Malaria II: What's New, What's Needed: Supplement to Volume 71 (2) of the American Journal of Tropical Medicine and Hygiene*, 2004.

Robert W Snow, Benn Sartorius, David Kyalo, Joseph Maina, Punam Amratia, Clara W Mundia, Philip Bejon, and Abdisalan M Noor. The prevalence of plasmodium falciparum in sub-saharan africa since 1900. *Nature*, 550(7677):515–518, 2017.

Trine Staalsoe, Rosette Megnekou, Nadine Fievét, Christina H Ricke, Hanne D Zornig, Rose Leke, Diane W Taylor, Philippe Deloron, and Lars Hviid. Acquisition and decay of antibodies to pregnancy-associated variant antigens on the surface of plasmodium falciparum-infected erythrocytes that protect against placental parasitemia. *The Journal of infectious diseases*, 184(5):618–626, 2001.

Trine Staalsoe, Caroline E Shulman, Judith N Bulmer, Ken Kawuondo, Kevin Marsh, and Lars Hviid. Variant surface antigen-specific igg and protection against clinical consequences of pregnancy-associated plasmodium falciparum malaria. *The Lancet*, 363(9405):283–289, 2004.

Will Stone, Bronner P Gonçalves, Teun Bousema, and Chris Drakeley. Assessing the infectious reservoir of falciparum malaria: past and future. *Trends in parasitology*, 31 (7):287–296, 2015.

Siske S Struik and Eleanor M Riley. Does malaria suffer from lack of memory? *Immunological reviews*, 201(1):268–290, 2004.

Jingyi Tang, Scott A Chisholm, Lee M Yeoh, Paul R Gilson, Anthony T Papenfuss, Karen P Day, Michaela Petter, and Michael F Duffy. Histone modifications associated with gene expression and genome accessibility are dynamically enriched at plasmodium falciparum regulatory sequences. *Epigenetics & chromatin*, 13:1–25, 2020.

Noppadon Tangpukdee, Chatnapa Duangdee, Polrat Wilairatana, and Srivicha Krudsood. Malaria diagnosis: a brief review. *The Korean journal of parasitology*, 47 (2):93, 2009.

Helen M Taylor, Susan A Kyes, Christopher I Newbold, et al. Var gene diversity in plasmodium falciparum is generated by frequent recombination events. *Molecular and biochemical parasitology*, 110(2):391–397, 2000.

Sofonias K Tessema, Rie Nakajima, Algis Jasinskas, Stephanie L Monk, Lea Lekieffre, Enmoore Lin, Benson Kiniboro, Carla Proietti, Peter Siba, Philip L Felgner, et al. Protective immunity against severe malaria in children is associated with a limited repertoire of antibodies to conserved pfemp1 variants. *Cell host & microbe*, 26(5): 579–590, 2019.

J Eric Tongren, Christopher J Drakeley, Suzanna LR McDonald, Hugh G Reyburn, Alphaxard Manjurano, Watoky MM Nkya, Martha M Lemnge, Channe D Gowda, Jim E Todd, Patrick H Corran, et al. Target antigen, age, and duration of antigen exposure independently regulate immunoglobulin g subclass switching in malaria. *Infection and immunity*, 74(1):257–264, 2006.

Mark A Travassos, Amadou Niangaly, Jason A Bailey, Amed Ouattara, Drissa Coulibaly, Kirsten E Lyke, Matthew B Laurens, Jozelyn Pablo, Algis Jasinskas, Rie Nakajima, et al. Children with cerebral malaria or severe malarial anaemia lack immunity to distinct variant surface antigen subsets. *Scientific reports*, 8(1):6281, 2018.

C Michael R Turner. The rate of antigenic variation in fly-transmitted and syringe-passaged infections of trypanosoma brucei. *FEMS microbiology letters*, 153(1):227–231, 1997.

Chigozie J Uneke. Impact of placental plasmodium falciparum malaria on pregnancy and perinatal outcome in sub-saharan africa: I: introduction to placental malaria. *The Yale journal of biology and medicine*, 80(2):39, 2007.

Britta C Urban and David J Roberts. Malaria, monocytes, macrophages and myeloid dendritic cells: sticking of infected erythrocytes switches off host cells. *Current opinion in immunology*, 14(4):458–465, 2002.

Marjan W Van Der Woude and Andreas J Bäumler. Phase and antigenic variation in bacteria. *Clinical microbiology reviews*, 17(3):581–611, 2004.

Mats Wahlgren, Suchi Goel, and Reetesh R Akhouri. Variant surface antigens of plasmodium falciparum and their roles in severe malaria. *Nature Reviews Microbiology*, 15(8):479–491, 2017.

Christian W Wang, Cornelus C Hermsen, Robert W Sauerwein, David E Arnot, Thor G Theander, and Thomas Lavstsen. The plasmodium falciparum var gene transcription strategy at the onset of blood stage infection in a human volunteer. *Parasitology international*, 58(4):478–480, 2009.

George M Warimwe, Thomas M Keane, Gregory Fegan, Jennifer N Musyoki, Charles RJC Newton, Arnab Pain, Matthew Berriman, Kevin Marsh, and Peter C Bull. Plasmodium falciparum var gene expression is modified by host immunity. *Proceedings of the National Academy of Sciences*, 106(51):21801–21806, 2009.

George M Warimwe, Mario Recker, Esther W Kiragu, Caroline O Buckee, Juliana Wambua, Jennifer N Musyoki, Kevin Marsh, and Peter C Bull. Plasmodium falciparum var gene expression homogeneity as a marker of the host-parasite relationship under different levels of naturally acquired immunity to malaria. *PLoS One*, 8(7):e70467, 2013.

Greta E Weiss, Boubacar Traore, Kassoum Kayentao, Aissata Ongoiba, Safiatou Doumbo, Didier Doumtabe, Younoussou Kone, Seydou Dia, Agnes Guindo, Abdramane Traore, et al. The plasmodium falciparum-specific human memory b cell compartment expands gradually with repeated malaria infections. *PLoS pathogens*, 6 (5):e1000912, 2010.

Nicholas J White, Sasithon Pukrittayakamee, Tran Tinh Hien, M Abul Faiz, Olugbenga A Mokuolu, and Arjen M Dondorp. Malaria. *Lancet (London, England)*, 383(9918):723–735, 2013.

Jan Stephan Wichers-Misterek, Ralf Krumkamp, Jana Held, Heidrun von Thien, Irene Wittmann, Yannick Daniel Höppner, Julia M Ruge, Kara Moser, Antoine Dara, Jan Strauss, et al. The exception that proves the rule: Virulence gene expression at the onset of plasmodium falciparum blood stage infections. *PLoS Pathogens*, 19(6): e1011468, 2023.

Jiraprapa Wipasa, Chaisuree Suphavilai, Lucy C Okell, Jackie Cook, Patrick H Corran, Kanitta Thaikla, Witaya Liewsaree, Eleanor M Riley, and Julius Clemence R Hafalla.

Long-lived antibody and b cell memory responses to the human malaria parasites, plasmodium falciparum and plasmodium vivax. *PLoS pathogens*, 6(2):e1000770, 2010.

Leesa F Wockner, Isabell Hoffmann, Lachlan Webb, Benjamin Mordmüller, Sean C Murphy, James G Kublin, Peter O'rourke, James S McCarthy, and Louise Marquart. Growth rate of plasmodium falciparum: analysis of parasite growth data from malaria volunteer infection studies. *The Journal of Infectious Diseases*, 221(6):963–972, 2020.

World Health Organization et al. World malaria report 2023. In *World Malaria Report 2023*. n.p., 2023. Accessed online.

Gigliola Zanghì, Shruthi S Vembar, Sebastian Baumgarten, Shuai Ding, Julien Guizetti, Jessica M Bryant, Denise Mattei, Anja TR Jensen, Laurent Rénia, Yun Shan Goh, et al. A specific pfemp1 is expressed in p. falciparum sporozoites and plays a role in hepatocyte infection. *Cell reports*, 22(11):2951–2963, 2018.

Xu Zhang, Francesca Florini, Joseph E Visone, Irina Lionardi, Mackensie R Gross, Valay Patel, and Kirk W Deitsch. A coordinated transcriptional switching network mediates antigenic variation of human malaria parasites. *Elife*, 11:e83840, 2022.